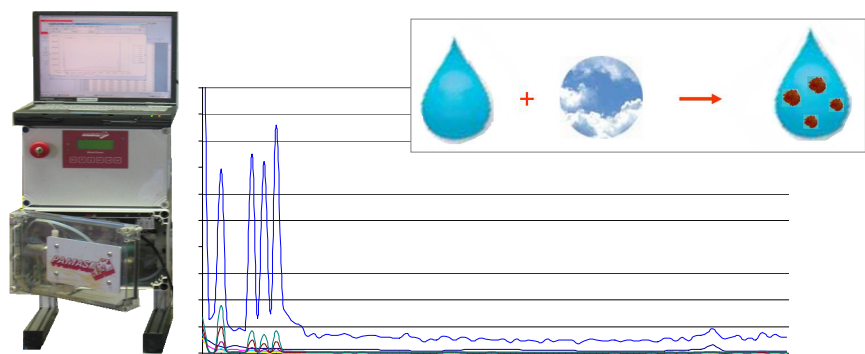


Iron removal at groundwater pumping station Harderbroek

May 2007

Karin Teunissen



Department of Water Management
Sanitary Engineering Section

Delft University of Technology

Faculty of Civil Engineering and Geosciences
Department of Water Management
Sanitary Engineering Section

Iron removal at groundwater pumping station Harderbroek

Master of Science thesis in Civil Engineering

Karin Teunissen

May 2007

Committee:

Prof. ir. J.C. van Dijk
Dr. ir. L.C. Rietveld
Dr. ir. A.J. Abrahamse
H. Leijssen
Prof. dr. ir. M.C.M. van Loosdrecht

Delft University of Technology
Delft University of Technology
Kiwa Water Research
Vitens N.V.
Delft University of Technology

We thought that we had the answers, it was the questions we had wrong.

Bono - U2 - 11 o'clock tick tock

Preface

The report you are reading now is the result of a research performed to finalise my study Civil Engineering at Delft University of Technology. The research is performed by Kiwa Water Research and is part of the joint research program (BTO) of the Dutch water companies. The research location was pumping station Harderbroek, operated by Vitens N.V.

At those three companies and institutes, Kiwa Water Research, Vitens N.V. and Delft University of Technology, I experienced enthusiasm for my research. It was a great opportunity to work on such an integrated project. I received a lot of support from all different kinds. I am thankful to everybody who had contributed anything to this research and to me as a researcher.

With this report as final piece of my study, I would like to take the opportunity to thank my whole family. All of you make me feel special and willing to use my talents. Special thanks to my parents who never doubted my capability. You never had too high expectations and gave me the time and the freedom to be a student. This unconditional support and trust in everything I did was valuable to me.

Besides my parents I would like to thank my boyfriend, Eric. Thanks for all the necessary pep talks during my study. You talked me through the first years and made me believe I could do it. This report proves that you were right. During my master study you showed a lot of interest and admiration.

To conclude, I would like to share with you a great experience I went through on 15 April 2007. About one month before my graduation I ran the marathon of Rotterdam, together with my professor Hans van Dijk. It was one of the greatest moments for me as a student and I will remember me our finish at the Coolsingel forever. Halfway, when we had to climb the Erasmus Bridge for the second time, somebody at the side held a board with the following text: *Pain is temporary, glory is forever*. This text is suitable for many situations, and I would like all of you to remember it when you are in a tough situation. Go for your own challenge!

Karin Teunissen,

Delft, May 2007.

Summary

Iron is the primary source for discolouration problems in the drinking water distribution system. The removal of iron from groundwater is a common treatment step in the production of drinking water. Even when clear water meets the drinking water standards, the water quality in the distribution system can deteriorate due to settling of iron (hydroxide) particles or post-treatment flocculation of dissolved iron. Therefore it is important to remove dissolved and particulate iron to very low levels.

The objective of this study was to reduce the particle load towards the distribution system and to improve the iron removal at the groundwater pumping station Harderbroek, consisting of aeration, rapid sand filtration and tower aeration. A maximum flow of 1800 m³/h can be treated and the average production is 800 m³/h. Although previous research showed the clear water meets the drinking water regulations, the drinking water company Vitens is not satisfied with the turbidity and iron concentration of the clear water. The mean iron concentration is 0.04 mg/l.

The research contains three parts: 1) a particle fingerprint of the treatment, resulting in the quantification of particles breaking through the rapid sand filtration. 2) small column experiments to study the oxidation and filterability of iron. 3) developing and optimising an iron removal model in the model environment Stimela.

1) A particle fingerprint for a drinking water treatment plant is meant to identify the presence of particles through the treatment plant. Besides, variation in particle size distribution, number and volume can be observed. In order to decrease the particle load towards the distribution system the presence and removal of particles in the treatment plant is measured at Harderbroek. A distinction is made between normal treatment and operational events. A particle size distribution is measured with particle counters. Particles are counted during a complete filter run (32 hours). The volume concentration during stable operation is compared with the volume concentration after an operational event. With this method it is possible to evaluate particle breakthrough of a rapid filter quantitatively.

2) With a four-column set-up research is executed, concerning the flock formation and oxidation of iron. The first part focussed on changing the pre-treatment of the filter influent water, in order to improve the iron(III) hydroxide flock formation and removal. Variation of mixing intensity, residence time, iron(II) concentration in the influent and the type of aeration were applied. The second part focussed on adjustments in the filtration process, in order to improve the oxidation and removal of iron in the filter. With caustic soda dosage and crushed limestone filtration the pH is increased.

3) In the Stimela environment an iron removal model is developed. This model is used to substantiate the relevant processes. The model includes oxidation from iron(II) to iron(III), iron(III) hydroxide flock removal and iron(II) adsorption.

The fingerprint showed that operational events have a significant impact on the volume concentration of particles breaking through the filter. Switching on/off of filters influences mainly the middle particle size ranges (2-7 μm). A backwash event mainly affects the larger particle size ranges. A backwash results in a peak in volume load for 4 hours. During this peak in 13% of the filter run time, 45% of the particle volume load is added to the effluent. The majority of this volume exists of the larger particles with good settling properties, which are undesirable in the distribution system. Recirculation of the filtrate during the first four hours can result in an improvement of the treatment at Harderbroek and a significant reduction of the volume load with 37% per filter run.

A comparison with other treatment plants suggests a reduction in ppb's leaving the treatment plant reduces the cleaning frequency of the distribution system.

An application for particle count data can be found in a norm value for average particle volume concentration in the clear water. For the moment companies should aim on an average particle volume concentration in the clear water below 1 ppb.

Column experiments showed that the aerated water mainly contained iron(II). pH measurements gave reason to assume a slow oxidation rate (pH = 7.5). After NaOH dosage, the oxidation and the subsequent removal by filtration of iron(II) increased. Thus for the flock filtration at Harderbroek the oxidation of iron(II) was found to be the rate determining step, limited by the pH.

Probably the iron removal at Harderbroek can be improved by caustic soda dosage or crushed limestone filtration. Both alternatives will result in a higher pH and therefore a better oxidation of iron. In addition crushed limestone filtration will increase the buffer capacity. These alternatives still need pilot research before conclusions can be drawn. An alternative without dosing a chemical could be to make tower aeration the first treatment step (instead of the last step). When tower aeration is applied on raw water, the pH of the aerated water will be higher than currently is the case with only cascade aeration, because tower aeration is a more intensive aeration method. It can be expected that fouling of the aeration tower can be controlled, because of the low iron content of the raw water.

The dataset obtained with the experiments is not complete enough to calibrate the model. In this study the model is mainly used to study the flock filtration iron removal. In the iron removal model adsorptive iron removal is included, but with the obtained data set, no conclusions could be drawn according this removal mechanism.

Further research should be focussed on optimising the oxidation of iron(II). A pilot study is recommended to investigate the alternatives as caustic soda dosage and crushed limestone filtration.

An extensive measurement program is necessary to calibrate the model parameters and make a clear distinction between the contributions of the different iron removal mechanisms on the total iron removal.

The knowledge gathered at Harderbroek is probably applicable at more pumping stations in the Netherlands.

Contents

1	Introduction	1
1.1	Pumping station Harderbroek	1
1.2	Problem definition	4
1.2.1	Conclusions from preceding research	5
1.2.2	Hypotheses	5
1.2.3	Research approach	6
1.2.4	Layout of the report	7
2	Theory of iron removal	9
2.1	Iron removal	9
2.1.1	Ferrous and ferric iron	9
2.1.2	Iron removal mechanisms in filters	9
2.1.3	Oxidation and hydrolysis of iron	10
2.1.4	Influence of pH	12
2.1.5	Flock filtration iron removal	13
2.1.6	Adsorptive iron removal	14
2.1.7	Biological iron removal	16
2.2	Aeration	18
2.2.1	Theory of gas transfer	18
2.2.2	Cascade aeration	21
2.2.3	Spray aeration	22
2.2.4	Tower aeration	23
2.3	Filtration	24
2.3.1	Filtration mechanisms	24
2.3.2	Modelling of filtration	25
2.3.3	Mathematical equations for filtration	25
2.3.4	Filter resistance	28
2.3.5	Backwashing	29
2.4	Adsorption	30
2.4.1	Theory of adsorption	30
2.4.2	Modeling of adsorption	31
3	Fingerprint	33
3.1	Introduction	33
3.2	Materials and methods	33
3.2.1	Particle counter	33
3.2.2	Analysis of particle counter data	34
3.2.3	Methods	36
3.3	Results	37
3.4	Discussion	40
3.4.1	Comparison of stable operation and operational events	41
3.4.2	Reduction measures	42
3.4.3	Frequency distribution	42
3.4.4	Comparison with other pumping stations	44
3.4.5	Application	46

4	Column experiments	49
4.1	Introduction	49
4.2	Methods	49
4.2.1	Equipment	49
4.2.2	Experimental set-up part 1	50
4.2.3	Experimental set-up part 2	51
4.2.4	Analyses	54
4.2.5	Measurement program	55
4.3	Results part 1	56
4.3.1	Observations	56
4.3.2	General results	57
4.4	Results part 2	57
4.4.1	Observations	57
4.4.2	Results	58
4.5	Discussion	60
4.6	Alternatives for Harderbroek	63
4.6.1	Tower aeration applied as a first treatment step	63
4.6.2	Caustic soda dosage	64
4.6.3	Crushed limestone filtration	64
5	Model	67
5.1	Method	67
5.1.1	Summary applied differential equations	67
5.1.2	Discretisation	67
5.1.3	Stimela	68
5.1.4	Simplifications and assumptions	69
5.1.5	Model structure	69
5.1.6	Parameters	70
5.1.7	Modelling approach	73
5.2	Model runs	74
5.2.1	Results for oxidation rate coefficient	74
5.2.2	Results for flock filtration iron removal	75
5.2.3	Results for Harderbroek filters	76
5.2.4	Results for adsorptive iron removal	79
5.3	Discussion	80
5.3.1	Reliability model results	80
5.3.2	Sensitivity of parameters	80
5.3.3	Simulation of alternatives	81
5.3.4	Proposal measurement program	84
6	Conclusions and recommendations	89
6.1	Conclusions	89
6.2	Recommendations	91
6.2.1	Treatment at Harderbroek	91
6.2.2	Further research	91
7	References	93

1 Introduction

Iron is removed during groundwater treatment. However, iron removal is usually incomplete. Iron particles in water supplies cause various aesthetic and operational problems including bad taste, discolouration, deposition and resuspension in distribution systems. Dissolved iron can cause post-treatment flocculation. Particulate and dissolved iron in the distribution system can cause incidences of high turbidity, in particular during periods of increased flow. In the Netherlands, the mandatory drinking water standard for iron is 0.2 mg/l. Verberk (2006a) showed that even with a clear water concentration of 0.01 mg Fe/l, post-flocculation of soluble iron can lead to a measurable increase of particulate iron. In order to avoid problems with iron particles and post-flocculation and subsequent sedimentation and resuspension of iron in the distribution network, companies should aim for very low iron concentrations in the clear water.

This research focuses on reducing total iron concentration in the clear water by reducing the dissolved iron and the particulate iron by optimising the removal of dissolved iron through the oxidation of dissolved iron(II) and the removal of the formed iron(III) hydroxide flocks.

The research is performed at groundwater pumping station Harderbroek, a plant in the Dutch province Flevoland.

1.1 Pumping station Harderbroek

Pumping station Harderbroek, Flevoland, is in operation since October 1997 and nowadays it is operated by Vitens N.V. The pumping station treats groundwater for drinking water production. Figure 1 shows the treatment scheme of Harderbroek. The yearly production in 2006 was 6 million m³ of water. A maximum flow of 1800 m³/h can be treated.

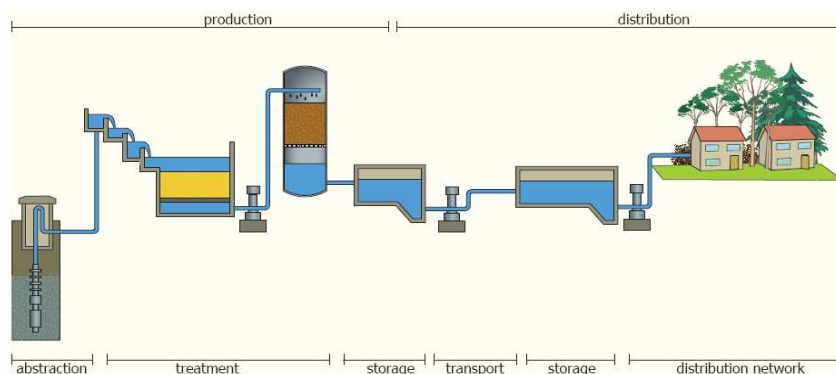


Figure 1: Treatment and distribution scheme Harderbroek.

Table 1: Average raw water composition at pumping station Harderbroek and (former) Vewin recommendation of maximum values in clear water (REWAB 2006).

Parameter	Unit	Raw water	(former) Vewin recommendation
Temperature	°C	12.9	25
Acidity	pH	7.47	7.8 < pH < 8.3
Saturation index	SI	-0.68	-0.2 < SI < 0.3
Conductivity	mS/m	16.4	80
Bicarbonate	mg/l	84.9	> 60
Chloride	mg/l	7.5	150
Sulphate	mg/l	8.44	150
Sodium	mg/l	6.39	120
Potassium	mg/l		12
Calcium	mg/l	25.8	150
Magnesium	mg/l	2.07	50
Total hardness	mmol/l	0.729	1.0 < TH < 2.5
Ammonium	mg/l	< 0.040	0.05
Nitrite	mg/l	< 0.0070	0.05
Nitrate	mg/l	< 0.50	25
Iron	mg/l	1.4	0.05
Manganese	mg/l	0.122	0.02

Abstraction

From 120 – 170 m below ground level, the groundwater is pumped up by 16 wells, each with a maximum capacity of 100 m³/h. There are 14 fixed pumps and two frequency-controlled pumps. These frequency-controlled pumps are used to control the desired flow for the treatment. This desired flow is determined from the level of the clear water storage and the actual water consumption. A carousel equally distributes the working hours of the pumps. The composition of the raw water is summarised in Table 1.

Cascade aeration

The raw water is divided over 4 cascades. Each cascade has a capacity of 500 m³/h. In the cascades the oxygen content of the water is increased while the concentration of carbon dioxide is decreased. One cascade consists of 6 cascade steps and a lower reservoir. From the lower reservoir the water enters a division gutter that feeds the filters.

For redundancy reasons the total flow is divided into two lanes. Each lane consists of two cascades. A glass wall is placed between the two streets. Both rooms have a separate blower to transport air with a capacity of 3600 Nm³/h, resulting in a RQ of 3.6.

Rapid sand filtration

Harderbroek has eight rapid sand filters, also split up in two lanes. Each filter has a filtration surface of 24 m². The filter material consists of sand, with a

particle size between 0.8 and 1.25 mm and a D10 of 0.9 mm. The maximum flow through one filter is 250 m³/h, so the maximum filtration rate is 10.4 m/h.

The bed height is 2.00 m and the supernatant water level is 0.05 mwc. This level is regulated by a supernatant water level measurement device and a regulator which operates the frequency-controlled filtrate pump.

The filter bottom contains 51 nozzles per square meter, which is 1224 nozzles per filter. A backwash cycle (Table 2) is started as soon as one of the following criteria is met:

- The filtrated volume exceeds 8,000 m³;
- The filter run time exceeds 60 hours;
- The pressure drop over the filter bed exceeds 17 kPa.

In practice a filter is backwashed after filtering 8,000 m³, which normally takes 32 filter run hours. A filter cycle takes 4 to 5 days, because during a filter run the filter is taken out of production every now and then. After backwashing the first filtrate of 300 m³ is drained and transported to an infiltration pond located just outside the building.

Table 2: Backwash program of the filters at Harderbroek.

Step		Time [s]	Q water [m ³ /h]	Q air [m ³ /h]
1	Run-up	30	0 – 600	
2	First wash	330	600	
3	Run-down	20	600 – 300	
4	Water and air	370	300	900
5	Release air	120	300	
6	Run-up	20	300 – 1000	
7	After wash	650	1000	
8	Run off	80	1000 – 0	

The backwash water is collected in two 400 m³ buffer tanks. Ferric chloride is dosed and mixed with the water to form flocks. The water flows to tilted plate settlers. The supernatant water from the tilted plate settlers flows to a backwash water pond. The sludge is collected in the sludge buffer tank (600 m³). Because of the long residence time in the sludge buffer tank, the sludge is thickened by gravity and the supernatant water is brought to the pond by a floating siphon construction, which ensures only clear supernatant water to be transported to the pond. From there the water is infiltrated into the soil.

Tower aeration

After the water is filtered, frequency-controlled filtrate pumps transport the water to three aeration towers. These towers have a surface of 6.06 m² and the packing material is 2 m high, type Pall 25 mm PP. If the water flow is below 320 m³/h, only one tower is in operation. When the flow exceeds 320 m³/h, a second tower switches on until 640 m³/h, above which the flow is divided over three towers. The air flow through each tower is 6000 m³/h and in counter-current direction. The RQ of the aeration towers is 18.

The towers are installed to remove carbon dioxide from the water, formed due to the oxidation of iron(II). This results in an increase in pH and SI. In addition, also the oxygen concentration increases.

Clear water reservoirs

The treated water enters 2 clear water reservoirs, which have a volume of 2,500 m³ each. Both lanes have their own reservoir. From there the water is transported in two directions; it can enter the transport pipeline to Almere, or the distribution pipeline for drinking water supply in Zeewolde. The water used for backwash purposes is also pumped from the clear water reservoirs. The clear water reservoirs function as storage to deal with variations in consumption.

1.2 Problem definition

Soon after the start-up of the plant (October 1997), it turned out that the clear water quality was not as good as expected. The filter run times also seemed to be shorter than expected. At December 1997 the turbidity and iron concentration of the effluent water were increased to about 0.7 FTU and > 0.1 mg Fe/l respectively. This high turbidity and the high iron concentration in the clear water are undesirable. The situation causes much customer complaints about coloured water. The measure taken now, cleaning the distribution system regularly, can be characterised on curing, not preventing the problem. The distribution system is cleaned once every three years, which costs 70,000 euros per cleaning. In addition to the operational costs, large administrative costs are made, in order to inform customers. The distrust of customers arising from these cleaning events is undesirable.

The objective of the project is to reduce the cleaning frequency of the transport and distribution system, by limiting the particulate and dissolved iron concentration in the clear water. Although the iron concentration in the clear water meets the drinking water regulations, the drinking water company Vitens N.V. is not satisfied with the present turbidity and iron concentration of the clear water. The mean iron concentration is 40 µg /l (see Figure 2). This value is far below the Dutch drinking water standard of 200 µg/l. It is even below the Vewin recommendation, 50 µg/l. But it is above the 10 µg/l leading to post-flocculation as measured by Verberk (2006a). The part of the project described in this report aims to reduce the particle load towards the distribution network and to reduce the clear water iron concentration.

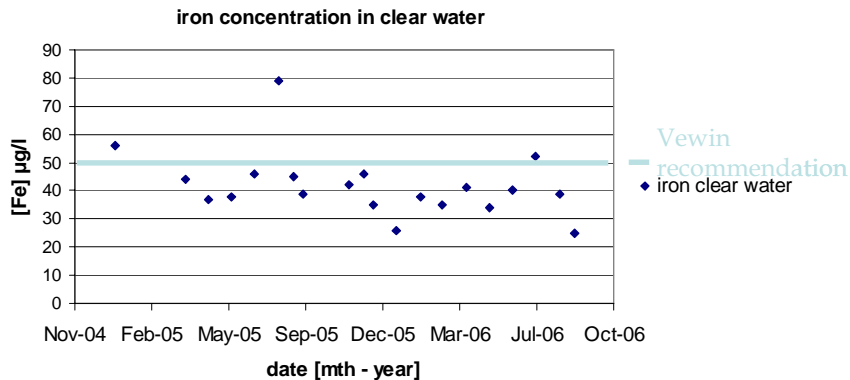


Figure 2: Total iron concentration in clear water at Harderbroek.

1.2.1 Conclusions from preceding research

Some research has already been carried out. Two main projects were executed:

- “Optimalisatie van de zuivering op pompstation Harderbroek. Projectnummer 16-9-60-000/01/03. J.A.M. van Paassen, June 2000”
- “Systeem en procesverbetering Harderbroek. Projectnummer HyAD: 211316. W.H. van der Pol, November 2005.”

Van Paassen stated that the residence time between aeration and filtration was of major influence on the iron removal process. In order to focus on adsorptive iron removal he recommended to raise the filter bed height and thereby decreasing the time between aeration and filtration. The bed height of all filters is increased from 2.00 to 2.20 m.

Van der Pol stated a small supernatant water layer caused short circuiting circumstances through the filter and disturbance of the top filter layer. He recommended to decrease the filter bed height. The supernatant water level and the time between aeration and filtration increased again. For some filters, filter 1 and 3 the bed height is decreased to 2.00 m.

1.2.2 Hypotheses

(1) Iron removal is not sufficient because the formed iron hydroxide flocks break down due to high turbulence in the cascade or filter inlet construction.

This hypothesis stems from the fact that groundwater pumping station Fledite produces water with a lower iron concentration (below 0.02 mg/l) from the same groundwater source. The treatment is comparable, with the exception of the aeration step. In Fledite spray aeration is used instead of cascade aeration

The main treatment scheme of Fledite exists of abstraction of groundwater, spray aeration, wet rapid sand filtration, tower aeration and finally the clear

water reservoirs. So, the major difference in treatment schemes is the first aeration step. The rapid sand filters are comparable. The design capacity of each filter is 250 m³/h, the surface 24 m² and therefore the filtration velocity is 10.4 m/h. These values are exactly the same as at Harderbroek. Also the number of filters is the same, at both locations eight filters are operated. Differences occur in supernatant water level, filter bed height, and the backwash program. The supernatant water level at Harderbroek varies between 1 and 5 cm. At Fledite this level is 10 cm. The filter bed height at Harderbroek ranges from 2.0 m till 2.2 m. At Fledite the average bed height is 2.35 m.

To test this hypothesis an experimental program was set-up, as described in the next paragraph. During the experiments the preliminary results changed the general ideas about the process at Harderbroek. Therefore another hypothesis was posed and another series of column experiments was carried out (part two, see paragraph 1.6). This hypothesis is formulated as:

(2) The oxidation of iron(II) to iron(III) does not perform well due to a too low pH of the cascade effluent.

A short explanation of the hypothesis: the major part of the iron in the filter influent is dissolved iron(II), instead of the expected hydrated iron(III). The dissolved iron(II) is removed by a different mechanism than the removal of suspended iron(III)hydroxide flocks. The treatment plant was designed for removal of iron according to the last mechanism.

1.2.3 *Research approach*

Fingerprint

At Harderbroek the presence and removal of particles in the treatment plant is measured, the so-called Fingerprint. A distinction is made between normal treatment and operational events. A particle size distribution is obtained by using particle counters. Particles are counted in the raw water, cascade effluent, the supernatant water, filter effluent, after tower aeration and in the clear water. In order to quantify the contribution of operational events on the total volume load, particle counts are converted to particle volumes in parts per billion (ppb).

For a complete description of this research the reader is referred to BTO report 2007.015 (Raffin and Teunissen, 2007). In this report only the measurements concerning the filtration step are discussed.

Column experiments

With column experiments the removal of iron is investigated. The experiments are split up in two parts. In part one hypothesis 1 is tested. These experiments were focussed on differences in pre-treatment of the water before filtration and emphasise the flock formation of iron(III). In part two hypothesis 2 is tested by two different experiments. These experiments emphasise the oxidation of iron(II).

The removal of iron is quantified by number of particles, turbidity and iron concentration. The particles were counted with particle counters and iron(II) and iron(III) concentrations were measured by chemical analysis. With this experiment the upper 25 cm of the filter bed is simulated. Only relative differences in removal of iron can be determined.

Thus, the experiments in part 1 are used to verify hypothesis (1) and give an idea for promising pre-treatment alternatives. Within part two the pH of the water is adjusted, as well as the filter material, in order to investigate the influence of a change in pH on the iron removal.

Model

In the Stimela environment an iron removal model is validated. The model includes oxidation from iron(II) to iron(III), iron(III) hydroxide flock removal and iron(II) adsorption. In addition, the influence of change in different parameters is simulated.

1.2.4 *Layout of the report*

The report starts with an introduction of the theory necessary for this thesis. After a description of the theory of iron removal and how the theory is linked with modelling, the parts as described in the previous paragraph are described in separate chapters. Chapter 3 discusses the particle fingerprint, Chapter 4 the column experiments and Chapter 5 the model. In each chapter the background, methods and results of that part of the research are given. In Chapter 6 general conclusions are drawn. Furthermore, recommendations for further research are stated.

2 Theory of iron removal

This chapter will briefly show the main theory concerning iron removal. It starts with the basics of iron removal. Afterwards the two techniques usually applied for iron removal, aeration and filtration, are described. The chapter finalises with a description of adsorption.

2.1 Iron removal

2.1.1 Ferrous and ferric iron

In water, iron mainly exist in two different forms: ferrous iron; iron(II) or Fe^{2+} and ferric iron; iron(III) or Fe^{3+} (Mayer and Jarrell, 2000). Ferrous iron can become ferric iron by oxidation. A commonly applied oxidiser in drinking water treatment is oxygen, mostly easily abstracted from air. Ferrous iron has a high solubility in water. Ferric iron has a low solubility product. The solubility product of iron(III) hydroxide at 25 °C is $2.0 \cdot 10^{-39}$ (Jones, 2000). So iron(III) easily forms iron hydroxide flocks. These flocks form particles and are visible in water.

Figure 3 shows the oxidation process between ferrous and ferric iron in water, under influence of oxygen.

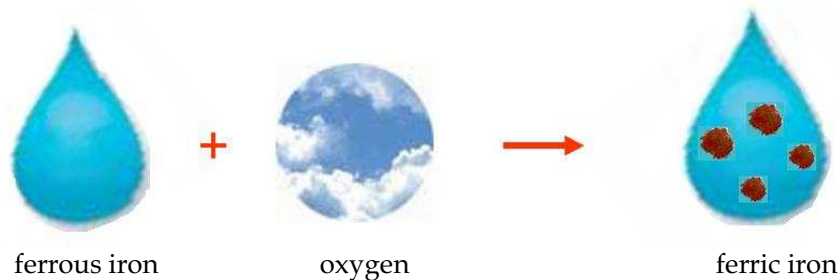
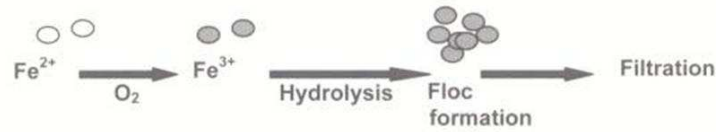


Figure 3: Oxidation of ferrous iron into ferric iron under influence of oxygen.

2.1.2 Iron removal mechanisms in filters

Iron present in groundwater will usually be dissolved iron(II), because of anaerobic conditions. Groundwater containing oxygen is mostly iron free. Aeration followed by rapid sand filtration is the most commonly used method for the removal of iron from groundwater (O'Connor, 1971; Salvato, 1992). There are several iron removal mechanisms which contribute to the iron removal in filters; flock filtration, adsorptive iron removal (Figure 4) and biological iron removal. In Dutch water treatment plants mainly flock filtration and adsorptive iron removal are applied. In practice often a combination of these two mechanisms occurs. Which mechanism is dominant depends on the groundwater quality and the process conditions (Lerk, 1965; Hatva, 1988).

Oxidation-floc formation mechanism



Adsorption-oxidation mechanism

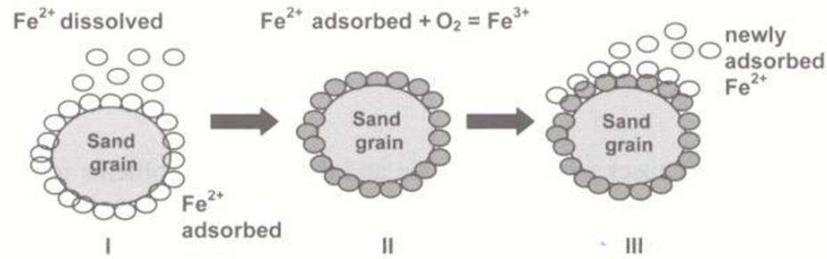


Figure 4: Flock filtration and adsorptive iron removal (Sharma 2001).

The next few paragraphs shortly describe the oxidation of iron, and the three mechanisms of iron removal: flock filtration, adsorptive removal and biological iron removal.

2.1.3 Oxidation and hydrolysis of iron

The transformation of iron takes place by means of two processes; oxidation and hydrolysis. In the presence of oxygen, iron(II) will be oxidised to iron(III) (Lerk, 1965). Because of the low solubility product of iron(III) hydroxide the iron(III) will quickly hydrolyse to form iron(III) hydroxide flocks. The oxidation and hydrolysis reaction are summarised in Box 1.

During the reaction H^+ is produced which will react with the HCO_3^- present in the water. CO_2 is produced resulting in a small decrease in pH. The reaction is self limiting because the oxidation velocity is pH dependent. In practice this phenomenon results in a pH drop over the filter bed height. From the reaction equations in Box 1 it follows that about 0.14 mg of oxygen is required for the oxidation of 1 mg of iron(II). The oxidation reaction is strongly pH dependent. A low pH will decrease the reaction rate, a high pH will increase the reaction rate. In case the pH of the groundwater is low, the pH has to be increased and an aeration step will be chosen that removes a lot of CO_2 . This will result in a higher pH and thus a higher oxidation rate. Figure 5 shows the influence of pH on the oxidation rate.

Box 1: Oxidation and hydrolysis of iron in water.

Oxidation (1) and hydrolysis (2) reaction (Lerk 1965)



General reaction equation becomes:



The equilibrium of oxidation of iron in water can be derived from the Nernst equation for the system $\text{Fe}^{2+}/\text{Fe}^{3+}$ E(1) and oxygen/water E(2):

Nernst:
$$E = E_0 + \frac{RT}{nF} \log \frac{\text{Ox}}{\text{Red}}$$

In which:

- E_0 = default potential redox couple, mV
- R = universal gas constant, 8.314570 J/K.mol
- T = absolute temperature, K
- n = number of electrons
- f = Faraday-constant, 96484.6 C/mol.

$$E(1) = 0.711 + 0.058 \log \frac{[\text{Fe}^{3+}]}{[\text{Fe}^{2+}]} \quad , \quad E(2) = 0.401 + \frac{0.058}{4} \log \frac{[\text{O}_2]}{[\text{OH}^-]^4}$$

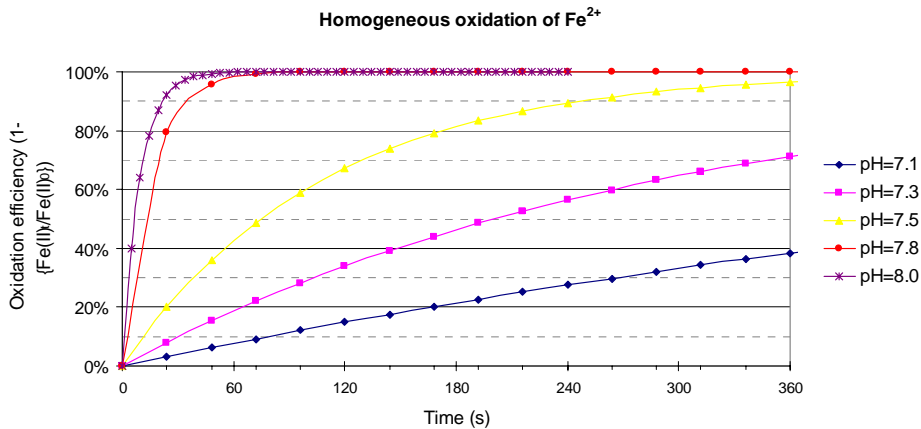


Figure 5: Oxidation efficiency of iron as a function of time at different pH values (de Vet, 2007).

The oxidation of iron(II) to iron(III) is described as (Lerk, 1965):

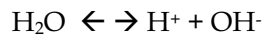
$$\frac{dFe^{3+}}{dt} = k \cdot [OH^-]^2 \cdot P_{O_2} \cdot [Fe^{2+}]^n$$

In which

k	=	oxidation rate coefficient	m ² / (s*atm)
P _{O₂}	=	partial oxygen tension	atm

2.1.4 Influence of pH

For the oxidation process and the flock formation, the pH is a very important parameter. One of the most important properties of water is the phenomenon that water is able to be an acid as well as a base, water is amphoteric. Because of its amphoteric properties water undergoes auto-ionisation thus,



The equilibrium constant for this reaction is

$$K = \frac{\{H^+\} \{OH^-\}}{\{H_2O\}}$$

K can be written as (with neglecting ionic strength (Snoeyink and Jenkins, 1980)):

$$K = [H^+] [OH^-]$$

The pH is defined as the negative logarithm of the concentration H⁺.

$$pH = - \log [H^+]$$

The most important acid-base reaction in water is the dissociation of carbon dioxide (see Box 2). The concentration bicarbonate determines the buffer capacity of the water. The buffer capacity (mmol/l/pH) is a value for the amount of acid or base that is necessary to obtain a change in pH. Figure 6 shows the relation between CO₂, HCO₃⁻ - CO₃²⁻ and pH.

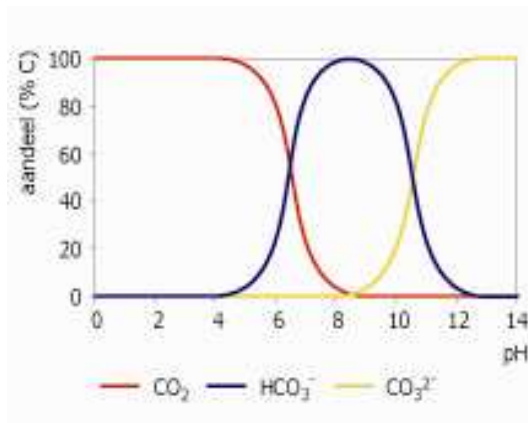


Figure 6: The relation between pH, CO₂, HCO₃⁻ and CO₃²⁻

Box 2: Dissociation of carbon dioxide (de Moel, 2006).

First CO₂ reacts with water:



The dissociation continues according the following equilibrium reaction:



$$K_1 = \frac{[\text{H}^+] \cdot [\text{HCO}_3^-]}{[\text{H}_2\text{CO}_3]} = \quad pK_1 = \text{pH} + \log \frac{[\text{H}_2\text{CO}_3]}{[\text{HCO}_3^-]} = 6.46 \quad \text{at } 10^\circ\text{C}$$



$$K_2 = \frac{[\text{H}^+] \cdot [\text{CO}_3^{2-}]}{[\text{HCO}_3^-]} = \quad pK_2 = \text{pH} + \log \frac{[\text{HCO}_3^-]}{[\text{CO}_3^{2-}]} = 10.49 \quad \text{at } 10^\circ\text{C}$$

Besides the dissociation of carbon dioxide phosphate can also function as a buffer. Phosphate is a trivalent buffer and depending on the pH it will form different buffer couples: O₄³⁻/HPO₄²⁻, HPO₄²⁻/H₂PO₄⁻ and H₂PO₄⁻/H₃PO₄. By a pH around 7.5 HPO₄²⁻/H₂PO₄⁻ will function as a buffer couple. Phosphate is usually present in significant concentrations in surface water. In groundwater the phosphate concentration is usually low. At Harderbroek the phosphate concentration at the abstraction pits is 0.05 mg/l.

2.1.5 Flock filtration iron removal

The suspended iron hydroxide flocks which are formed after oxidation and hydrolysis can be removed by a physical separation technique, in this case filtration. The total removal process (including oxidation and hydrolysis) consists of the following steps (Rott, 1973):

- Oxidation of Fe²⁺ to Fe³⁺ by means of aeration or by a chemical oxidant;
- Hydrolysis of Fe³⁺ to iron hydroxides;
- Flocculation/agglomeration of the hydroxide particles;
- Removal of flocks.

Rapid sand filtration is mostly applied to remove the iron hydroxide flocks. The filter material is (river) sand with a particle size between 0.6 and 3 mm. The bed height varies between 1 and 2 m, with a filtration velocity of 2 till 10 m/h. All these parameters depend on the water composition and the required effluent water quality.

To improve the filter effluent quality, finer sand may be chosen (0.5 – 0.8 mm). Operation in flock filtration mode with finer sand can improve the filtrate quality and results in much shorter ripening time of the filters. However, filter run times can become unacceptable short. The use of dual filter media (anthracite 0.8 – 1.2 mm and sand 0.5 – 0.8 mm) considerably prolongs the run time of the filter and gives good filtrate quality (Sharma, 2001b).

In addition to the conditions of the filter the performance of the agglomeration / flocculation step is of importance. For a proper iron removal by flock filtration large and stable flocks are required. Through oxidation of iron(II) small iron(III) pin flocks are formed, that will grow depending on residence time and G-values. Depending on the pH the formed colloids can become positively or negatively charged. Charged colloids do not flocculate very well. The DLVO-theory (Derjaguin, Landau, Verwey and Overbeek) describe the flock formation of colloidal particles. Between equal charged colloids repulsion occur due to equal charges. Between all particles attractions occur due to Van der Waals forces. The sum of these two energies determines the total interaction energy in order to result in adhesion. When the positive repulsion potential is zero, almost every incidental collision of two colloids result in the formation of a larger flock.

(Lerk, 1965; Moel et al., 2004; Sharma, 2001a, de Vet, 2007)

2.1.6 Adsorptive iron removal

During adsorptive filtration (Sharma, 2001) the iron(II) present in anoxic / anaerobic groundwater is adsorbed onto the surface of the filter media. Subsequently, in the presence of oxygen, the adsorbed iron(II) is oxidised forming a new surface for adsorption.

The adsorption-equilibrium can be described by the Freundlich isotherm. The Freundlich isotherm is the most widely used mathematical description of adsorption in aqueous systems. It is based on the assumption of heterogeneous adsorption surface comprising of different classes of adsorption sites and energies (Sharma, 2001):

$$q = K * C_e^n$$

In which

q	=	amount of solute absorbed per unit surface area of adsorbent	
C_e	=	equilibrium concentration dissolved substance	[g/m ³]
K and n	=	isotherm constants	[-]

Isotherm constant K is the measure of adsorption capacity and constant n is the measure of adsorption intensity. For the fixed values of C_e and n , the higher the value of K , the higher is the adsorption capacity. For the fixed values K and C_e , the lower the value n , the stronger is the adsorption bond. As n becomes very small, the capacity tends to be independent of C_e , and the isotherm plot approaches the horizontal. If the value of n is large, the adsorption bond is weak, and the value of q changes markedly with small changes in C_e (Snoeyink 1990).

The adsorption capacity for iron(II) depends on the surface conditions of the filter material and on the pH of the water. The capacity can be influenced by other substances present in the groundwater (Mn^{2+} , Ca^{2+} , NH_4^+ and NOM). The pH has a dominant influence on the surface charge. A high pH will result in a more negatively charged adsorption surface and therefore in a higher adsorption capacity of the cations.

Adsorption-oxidation is the dominant iron removal mechanism in dry filters and in sub-surface iron removal (van Beek, 1983; Rott, 1985; Braester and Martinell, 1988; Appelo et al., 1999). Adsorptive iron removal is also the dominant mechanism when pre-oxidation of iron(II) before filtration is minimal. This can be achieved by reducing the oxidant concentration or the time available for the oxidation reaction. With adsorptive iron removal mechanism only iron(II) is removed (Sharma, 2001a).

For a good adsorptive iron removal, the filter bed needs some time for ripening. During this ripening period, an iron oxide coating is created on the filter material. Many researchers studied the functioning of iron removal plants and observed that the iron oxide coating often plays an important role in the oxidation and removal of iron (Hauer, 1950; Cox, 1964; O'Connor, 1971; Anderson et al., 1973). After a coating has been developed on the filter media, improved iron removal occurs. Cox (1964) found that filters may serve as contact beds following aeration. The previously precipitated iron oxides will facilitate the oxidation reaction as some kind of "catalytic action." Ghosh et al. (1967) concluded from their studies on iron removal in filters that a fraction of the ferrous iron might have been adsorbed onto the ferric hydrate precipitates. O'Connor (1971) reported that precipitates of hydrous oxides of iron(III) formed after oxidation and deposited on the filter sand serve as adsorption media for iron still in solution. These hydroxides have high adsorption capacities for iron(II), and therefore account for the improved removal when filters are ripened and deposition of the precipitates have taken place.

When iron(II) enters a filter, it can be removed by adsorptive-oxidation, but it can also adsorb on iron hydroxide flocks. These flocks are commonly present in the filter through flock filtration. Sharma (2001) showed that this type of iron removal is not relevant. Sharma et al. (2001b) compared flock filtration and adsorptive filtration in a pilot study. In general, for single media fine

sand filters, the adsorptive mode gave a longer run time compared to the flock filtration mode.

2.1.7 Biological iron removal

In rapid sand filtration of groundwater biologically mediated oxidation and removal of iron has also been reported (Frischerz et al., 1985; Czekalla et al., 1985; Badjo and Mouchet, 1989; Hatva, 1989; Mouchet, 1992; Bourguine et al., 1994). Micro-organisms have the unique property of causing oxidation and precipitation of dissolved iron under pH, and redox potential (Eh) conditions that are between those of natural groundwater and those required for conventional (flock filtration) iron removal. Biological iron removal depends on the activities of micro organisms. Mouchet (1992) determined the conditions in which these bacteria are active (Figure 7). Biological oxidation of iron(II) gets a change when the chemical oxidation is not fast enough. The situation for Harderbroek is included in this figure by the horizontal and vertical lines. With the Nernst equations (see Box 1) the Eh [V] can be calculated. The applied setting and the calculation are summarised in Table 3:

Table 3: Calculation of the Nernst equation for the situation of Harderbroek.

Parameter	Concentration [mg/l]	Concentration in [mol/l]
Iron(II) concentration	1.25	2.232 e-5
Iron(III) concentration	0.12	2.143 e-6
Oxygen concentration	6	1.874 e-4
OH ⁻ concentration	pH=7.5, pOH = 6.5	3.16 e-7
E (1)		0.7119
E (2)		0.7240

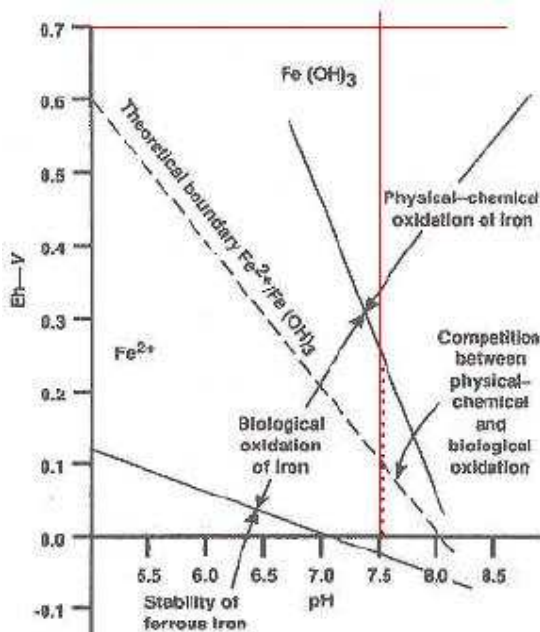


Figure 7: Conditions and oxidation mechanism (Mouchet, 1992) with Harderbroek situation included.

With an Eh of 0.72 and a pH of 7.5, the Harderbroek conditions are expected to be appropriate for the physical-chemical oxidation of iron more than biological iron oxidation.

There are several bacteria responsible for the biological iron removal; *Gallionella*, *Leptothrix*, *Crenothrix*, *Clonotrix*, *Siderocapsa*, *Sphaerotilus*, *Ferrobacillus* and *Sideromonas* (Degremont, 1991). These bacteria catalyze the exothermic oxidation of iron(II), due to oxidation reduction enzymes in the cell membrane; trivalent iron rendered insoluble in hydroxide form will participate in the mucilaginous secretions of those bacteria, like sheaths, stalks and capsules.

These iron oxidising bacteria are widespread and are prevalent in groundwater, ponds, hypolimnion of lakes or impoundments, sedimentary deposits and soil.

Mouchet (1992) reported improvement in performance when converting a conventional iron treatment plant to a biological one. Several of the main advantages of biological iron removal are: the high filtration rates (10-70 m/h), the high retention capacity (1-5 kg Fe/m²), the elimination of chemical reagents, the flexibility of operation and reduced capital and the operational costs. However, the rate of adsorption by the bacteria can be the limiting factor. High influent iron concentrations may cause breakthroughs. The main disadvantage of this process is the long maturation time before full efficiency is achieved. Stevenson (1997) reported 50-60 days of maturation for a new filter and 5 days after 2-months of shut down. The maturation can be speeded up by adding some sludge from an old treatment plant.

2.2 Aeration

Gas transfer is used in water treatment for two purposes; aeration (gas addition) and gas stripping (gas removal). In conventional groundwater treatment, usually aeration is the first treatment step. It aims to increase the oxygen concentration and to remove carbon dioxide, methane, hydrogen sulphide and other volatile organic compounds.

To remove iron, oxygen is required for the oxidation of iron(II) into iron(III), as explained before. Carbon dioxide removal results in a higher pH and in less aggressive water. For a proper oxidation and flock formation, a pH between 7.5 and 8.5 is required (van der Helm, 1998).

In the next paragraph (2.2.1) the theory of gas transfer is described in three different parts: The air water equilibrium, the kinetics and the mass balance. After that the different types of aeration are described which are applied in this thesis. Cascade aeration 2.2.2, spray aeration 2.2.3 and tower aeration 2.2.4.

2.2.1 Theory of gas transfer

Equilibrium

If water is exposed to air a continuous exchange of gas molecules will occur. The solubility of a gas in water depends on (van der Helm, 1998):

- The type of gas, expressed with a specific gas coefficient, the distribution coefficient k_H ;
- The concentration of a gas in the air, depending on the air temperature and the partial pressure of a gas in the air;
- The temperature of the water;
- Impurities in the water.

If the saturation concentration in the water is reached, the gas exchange in both directions is equal. The concentration of a volatile compound in the gas phase will be in equilibrium with the concentration in the water phase. The equilibrium can be described using Henry's law:

$$c_w = k_H * c_g$$

c_w	=	equilibrium concentration of a gas in water	[g/m ³]
k_H	=	Henry's constant, or the distribution constant	[-]
c_g	=	concentration of gas in air	[g/m ³]

For a water temperature of 10°C the distribution coefficient k_H for oxygen is 0.0398 and the coefficient for carbon dioxide is 1.23 (Pöpel, 1993).

The concentration of a gas in air, c_g , can be determined by using the universal gas law:

$$\frac{n}{V} = \frac{p}{RT}$$

In which:

p	=	partial pressure of a gas in gas-phase	[Pa]
V	=	total gas volume	[m ³]
n	=	amount of substances of gas	[mol]
R	=	universal gas constant, 8.3142	[J/(K.mol)]
T	=	temperature of gas	[K]

The gas concentration can then be calculated:

$$c_w = \frac{p}{RT} \cdot MW = \frac{n}{V} \cdot MW$$

MW	=	molecular weight of a gas	[g/mol]
----	---	---------------------------	---------

Gas transport

For the transport of compounds 4 mechanisms are distinguished:

- Convection, transport of a substance by a flow
- Dispersion, transport as a result of velocity differences over a cross section
- Turbulent diffusion, transport as a result of turbulence
- Molecular diffusion, transport as a result of the Brownian motion of the molecules.

The responsible mechanism for the gas transport between air and water is diffusion. This type of transport can be described by Ficks law:

$$\phi_d'' = -D \cdot \frac{\partial c}{\partial y}$$

ϕ_d''	=	the diffusion flux	[g/(m ² /s)]
D	=	diffusion coefficient	[m ² /s]
c	=	concentration of the gas	[g/m ³]

Kinetics

The kinetics describe the gas transport rate. As soon as water and air are in contact, gas molecules will continuously be exchanged. This transport depends on the gas concentration in the water and the equilibrium concentration.

Figure 8 shows the gas transport from air to water. When the volume of air is large (or the air is constantly renewed) the concentration of the gas in the air does not change significantly. Therefore this concentration is shown as a horizontal line. The concentration of the gas in water changes over the course of time. This is represented in Figure 8 by different lines at different times. Finally, at t=infinite, the gas concentration in water equals the equilibrium concentration, represented by a horizontal line.

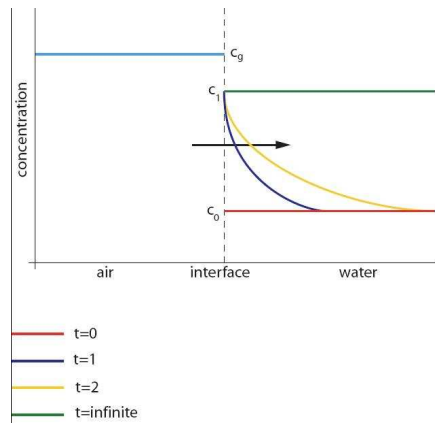


Figure 8: Gas transport from air to water.

The gas transfer rate can be described by a kinetic equation:

$$\frac{dc_w}{dt} = k_2 \cdot (c_s - c_w)$$

In which:

$$\begin{aligned} c_w &= \text{concentration of gas in water} && [\text{g/m}^3] \\ k_2 &= \text{gas transfer coefficient} && [\text{s}^{-1}] \end{aligned}$$

In this formula the time-dependency of the gas concentration in water, as shown in Figure 8, is represented by $\frac{dc_w}{dt}$.

k_2 in this equation is the gas transfer coefficient.

$$k_2 = k_L \cdot a \quad \text{and} \quad a = \frac{A}{V_w}$$

In which

$$\begin{aligned} k_L &= \text{partial transfer coefficient for water} && [\text{m/s}] \\ a &= \text{specific surface} && [\text{m}^{-1}] \\ A &= \text{contact surface} && [\text{m}^2] \\ V_w &= \text{water volume} && [\text{m}^3] \end{aligned}$$

k_2 is proportional with the diffusion coefficients D in water. Therefore a relation can be made between k_2 values for different gasses (van der Helm, 1998)

$$k_{2,O_2} = k_{2,CH_4} \cdot \left(\frac{D_{O_2}}{D_{CH_4}} \right)^n = k_{2,CH_4} \cdot \left(\frac{1.39}{1.16} \right)^n$$

$$k_{2,CO_2} = k_{2,CH_4} \cdot \left(\frac{D_{CO_2}}{D_{CH_4}} \right)^n = k_{2,CH_4} \cdot \left(\frac{1.30}{1.16} \right)^n$$

n is the power of the diffusion coefficient and depends on the diffusion theory.

Mass balance

When the gas concentration in air changes in time significantly, a mass balance needs to be formulated. A mass balance is schematically represented in Figure 9.

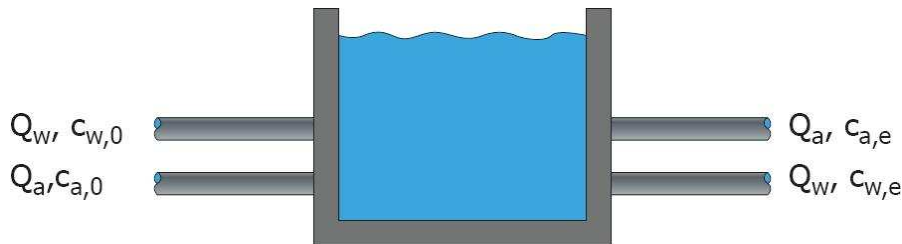


Figure 9: Mass balance of a gas in water.

The mass balance can be represented by (with neglecting conversion / use of oxygen):

$$Q_w \cdot c_{w,0} + Q_a \cdot c_{a,0} = Q_w \cdot c_{w,e} + Q_a \cdot c_{a,e}$$

This results in the air water ratio RQ:

$$RQ = \frac{Q_a}{Q_w} = \frac{c_{w,e} - c_{w,0}}{c_{a,0} - c_{a,e}}$$

In which

RQ	=	air-water ratio	[-]
Q _a	=	air flow	[m ³ /s]
Q _w	=	water flow	[m ³ /s]

With the three equations derived for gas transfer systems: equilibrium equation; kinetic equation and mass balance, it is possible to calculate the changes in the gas concentration in water and air.

2.2.2 Cascade aeration

In cascade aeration, the available fall height is subdivided into several steps. During each step the water falls over a weir into the next step. When water passes over the weir, an interface between air and water is created, where gas transfer can take place. More relevant in cascade aeration is the entrained air. The falling water jet enters the water body in the lower cascade chamber and

air is entrained in the form of bubbles. Due to turbulence during entraining, a mixture of air and water is provided, in which gas transfer will occur. The amount of air that can be entrained by the falling water jet is limited and therefore the RQ is also limited. According to practical measurements and model investigations the RQ of a cascade is approximately 0.4.

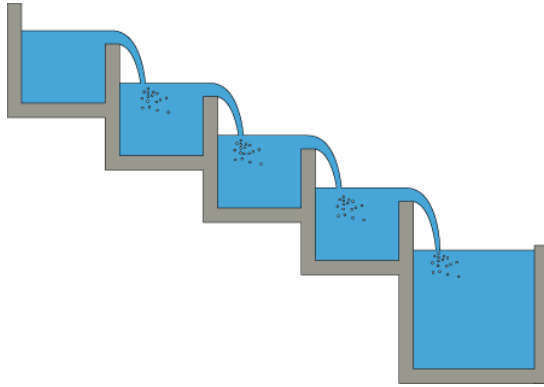


Figure 10: Falling water jets entrain air in the water.

An estimation of the efficiency of cascades can be made, assuming that there is a relationship between the measured fall height and the efficiency. The efficiency of a cascade depends also on the number of steps:

$$K = \frac{c_{w,e} - c_{w,0}}{c_s - c_{w,0}} = 1 - (1 - k)^n$$

K	=	efficiency of each step	[-]
n	=	number of steps	[-]

2.2.3 Spray aeration

Spray aerators divide the water into small droplets. Thus a large air-water interface is created. An advantage of spray aerators is the ease to incorporate them in existing installations. They do not require much space and can easily be placed above existing filters. A disadvantage is their high sensitivity to clogging.

The efficiency of the spray aeration depends on the fall height of the water droplet. After a certain fall height the efficiency remains constant. A spray aerator produces small droplets and the interface between air and water is not renewed. After some time this interface is saturated and the gas transfer stops. In case of bigger droplets internal forces are able to renew the air water equilibrium, but small droplets have a higher contact surface and are preferred. The efficiency of a spray aerator can be described as:

$$K = 1 - e^{(-k_2 \cdot t)} = 1 - e^{(-k_2 \cdot \sqrt{\frac{2h}{g}})}$$

In which:

K	=	efficiency	[-]
k_2	=	gas transfer coefficient	[s ⁻¹]
h	=	fall height	[m]
g	=	gravitational acceleration	[9.81 m/s ²]
t	=	time	[s]

2.2.4 Tower aeration

A tower aerator is a reactor filled with a packing medium. Packing media can be stacked slats or tubes, or specially designed packing material such as Pall-rings. The water enters the tower at the top of the reactor and is divided over the material. A large contact surface between air and water arises from the flow of the water over the medium surface. In addition the air water interface is renewed continuously: at every fall from a water droplet.

The air in the tower is normally renewed by a ventilator, preferably in counter-current flow direction in relation to the water flow.

A tower aerator is very efficient for CO₂-removal and can reach an efficiency of 95%. The efficiency of an aeration tower is somewhat independent of the surface loading. So an increase in water flow through the tower does not significantly influence the efficiency. This can be explained by the residence time in the tower. The retention time does not depend on the flow, but mainly on the fall height.



Figure 11: Tower aeration packing media Pall 25 PE, which is the packing media for the tower aerators at Harderbroek.

(de Moel et al, 2006)

2.3 Filtration

In water treatment, filtration is a purification process, in which water flows through a granular material. In the process, suspended solids are retained, substances are biochemically decomposed and pathogenic micro-organisms are removed.

Due to the accumulation of suspended solids in the filter bed, the hydraulic resistance increases. To reduce this resistance and to prevent a breakthrough of suspended solids, filters need to be cleaned regularly.

Next to the removal of suspended solids, the filter can also function as a biological or chemical reactor. Especially during groundwater treatment, this is of importance. Iron, manganese and ammonium are oxidised before or in the filter bed. The removal of micro-organisms is of importance during surface water treatment. Groundwater is generally free of pathogenic micro-organisms.

Rapid sand filtration is the most common application of filtration in water treatment. Rapid sand filtration consists of a filter bed with coarse granular medium, 0.8 – 1.2 mm, mostly sand. On top of the filter bed a layer of supernatant water exists. The filtration velocity of rapid sand filtration is between 5 and 20 m/h.

Clogging occurs due to the accumulation of suspended solids and colloidal material and to the biological and chemical processes. The filter is cleaned by backwashing. During backwashing the water flows in the opposite direction and the filter bed is expanded.

This paragraph begins by mentioning the different mechanism in filtration, 2.3.1. Then modelling of filtration 2.3.2. The mathematical description of filtration in 2.3.3. The paragraph ends with the increasing resistance in a filter due to clogging 2.3.4 and backwashing 2.3.5.

2.3.1 Filtration mechanisms

When the water passes through the filter, suspended and colloidal particles are retained. Not only the particles that are larger than the pore size are removed, but also smaller particles. Several filtration mechanisms contribute to the removal of particles (from left to right in Figure 12).

- Sedimentation
- Inertia
- Diffusion
- Interception
- Turbulence

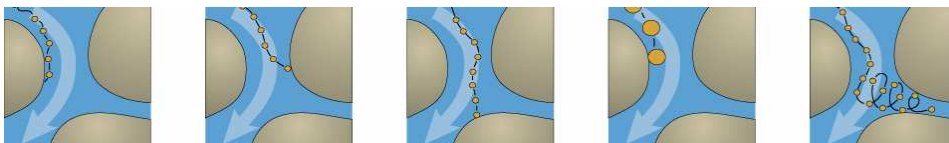


Figure 12: Filtration mechanisms.

The particles follow a trajectory when flowing through the filter bed. When this trajectory approaches the filter grains, particles can be intercepted. Heavy particles are subjected to sedimentation, lighter particles to diffusion. In a curvature of a trajectory, a heavy particle can be transported towards the filter material due to inertia. Due to these mechanisms and to turbulence, the particle can switch to other trajectories that flow nearer to a grain or they can collide directly with a grain. In the filter bed, the suspended or colloidal particles can attach to the grains.

2.3.2 *Modelling of filtration*

Continuous model evaluation of different operational scenarios will lead to improved operation that will vary over the course of time. Therefore, phenomenological models are used that are based on the numerical integration of partial differential equations which describe the process and dynamic behaviour of the process.

Water quality models attempt to simulate changes in the concentration of pollutants as they move through the environment or a reactor. (In this research the filter bed). Most of the reactions are multiphase reactions; they occur in more than one single phase. Filters are one of the characteristic water treatment processes. They operate continuously, because of the large volumes of water to be processed (Rietveld, 2005).

The removal processes in water treatment can be divided into two main groups:

- Mass transport processes
The pollutants are only transported, their concentration can be regarded as unchanging. Examples of these physical transport processes are advection and dispersion.
- Kinetic processes
Physical, chemical and biological processes, superimposed upon the mass transport processes mentioned above. These processes cause changes in the concentration of the pollutants.

What finally happens to the pollutants is a result of interaction between mass transfer and kinetic processes (James, 1993).

2.3.3 *Mathematical equations for filtration*

Due to the accumulation of suspended and colloidal solids in the filter bed, the pore volume will be reduced over the course of time (Figure 13). In addition, the grain size of the filter medium will increase in time. When a constant filtration rate is applied, the pore velocity will increase as a filter clogs. These processes can be described by the formulas for momentum and continuity.

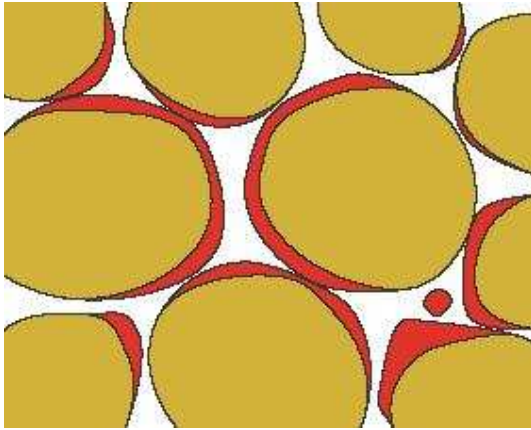


Figure 13: Decrease in pore size by accumulation of solids.

For a concentration c of impurities carried by the water, it may be assumed that the decrease of c is proportional to the concentration still present (Fick's law). This gives the basis for the equation of motion:

$$-\frac{\partial c}{\partial y} = \lambda c$$

in which

y	=	depth of filter bed	[m]
λ	=	filtration coefficient	[m ⁻¹]

A mass balance, in = out + storage + deposition, can be set up for the particle concentration (see also Figure 14):

$$V \cdot c \cdot dt = v(c + \frac{\partial c}{\partial y} dy)dt + p \frac{\partial c}{\partial t} dt \cdot dy + \frac{\partial \sigma}{\partial t} dt \cdot dy$$

$$\frac{\partial \sigma}{\partial t} = -v \frac{\partial c}{\partial y} - p \frac{\partial c}{\partial t}$$

in which:

v	=	filtration rate	[m/s]
p	=	porosity	[%]
σ	=	deposits in pores	[g/m ³]
c	=	concentration of suspended and colloidal solids in the water	[g/m ³]

The change of concentration due to the filtration process strongly depends on the filter bed depth, but less on time. The latter formula can therefore be simplified into:

$$\frac{\partial \sigma}{\partial t} = -v \frac{\partial c}{\partial y}$$

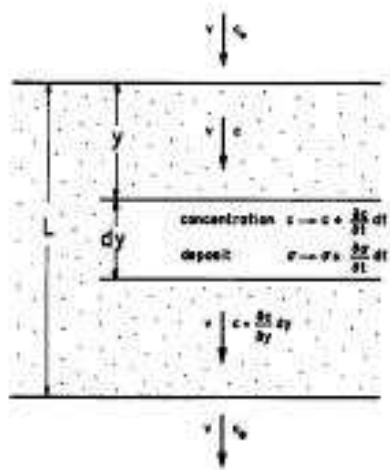


Figure 14: Continuity during filtration.

To solve this set of equations, λ must be known. λ depends on different parameters, such as filtration velocity, viscosity, grain size, the quality of the raw water, and the clogging of the bed.

λ has to be deduced from column experiments. From the start the filtration coefficient will increase initially. This is related to the ripening of the filter bed. Due to pore clogging, the pore velocity increases and less solids accumulate, resulting in lower filtration coefficient. When the top layer of the filter bed is saturated, particles need to be captured in the lower layers until the filter is completely saturated and particles start to break through.

The relation between the clean bed filtration coefficient, λ_0 , the filtration coefficient λ and the amount of accumulated solids, σ , has to be determined in practice. Generally, this relation has the shape of the graph in Figure 15.

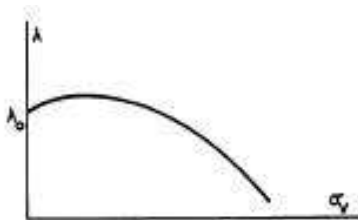


Figure 15: Change of filtration coefficient λ during operation (Huisman, 1984).

More than 50 researchers proposed empirical relationships for the filtration coefficient, mainly in relation to iron removal. The relations proposed by Lerk and Maroudas are widely applied:

Maroudas: $\lambda = \lambda_0 \left(1 - k_3 \frac{\sigma_v}{p_0}\right)$

Lerk: $\lambda = \lambda_0 \cdot \left(1 - \frac{\sigma_v}{n \cdot p_0}\right)$

With, according to Lerk $\lambda_0 = \frac{k_1}{\nu \cdot \nu \cdot d^3}$

$$\sigma_v = \frac{\sigma}{\rho_{solids}}$$

in which:

λ_0	=	initial filtration coefficient	[m ⁻¹]
k_3, k_1	=	experimental coefficients	[-]
σ_v	=	deposits in pores	[m ³ /m ³]
n	=	experimental exponent	[-]
ν	=	dynamic viscosity	[m ² /s]

2.3.4 Filter resistance

The pore size of the filter material decreases as a result of the accumulation of solids. During filtration the pore clogging increases and, therefore, the resistance in the filter bed. After a certain time the filter reaches a maximum head loss.

A maximum head loss of a filter is chosen to avoid negative pressures in the filter bed. The maximum available head loss is the difference between the supernatant water level and the pressure head in the effluent water, minus the clean bed resistance H_0 and the head loss caused by filter bottoms, pipes and valves. The clean bed resistance is described by the Carman-Kozeny equation. This equation is only valid when the Reynolds number is below 5.

$$I_0 = \frac{H_0}{L} = 180 \frac{\nu}{g} \frac{(1 - p_0)^2}{p_0^3} \frac{\nu}{d_\lambda^2}$$

In which

I_0 = initial resistance gradient [-]

When clogging occurs, the equation that describes the filter bed resistance changes into:

$$I = I_0 \left(\frac{p_0}{p_0 - \sigma_v} \right)^2$$

The filter resistance over the filter bed (in time) can graphically be represented by the Lindquist diagram (Figure 16).

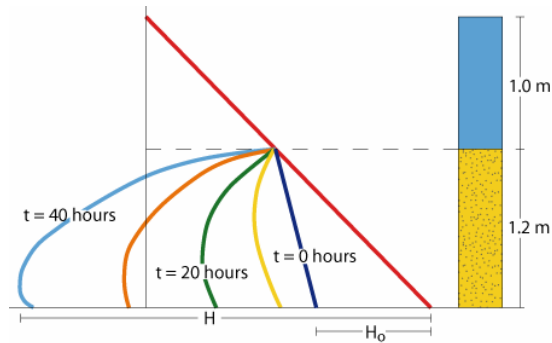


Figure 16: Lindquist diagram.

The pressure in the filter bed is build up by the hydrostatic pressure and the pressure loss due to the resistance in the filter bed. The straight (most right) line in the diagram represents the hydrostatic pressure. At the beginning of a filter run the pressure loss by the filter bed is only the initial filter resistance H_0 . The total pressure in the bed at $t=0$ is represented by the $t=0$ hours line. During the filter run the filter resistance increases, represented by the other lines.

If the pressure line crosses the vertical $H=0$ line, negative pressures in the filter occur. Before this point in time, the filter needs to be backwashed.

2.3.5 Backwashing

When the filter bed resistance has increased to a maximum acceptable level, the filters will be backwashed. Rapid filters are normally cleaned with filter effluent water, which flows in the opposite direction when compared to filtration. So the water flows in upwards direction through the filter. The water scours the filter grains and the accumulated solids re-suspend and are transported towards backwash troughs. Normally a combination of water and air is used to scour the filter material.

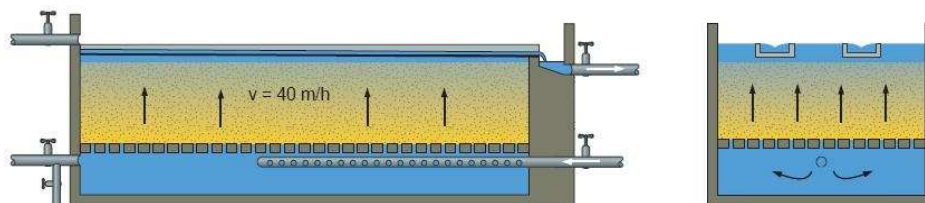


Figure 17: Schematic representation of a backwash process.

(Moel et al. 2006, Huisman 1993)

2.4 Adsorption

Adsorption is based on the principle that different particles will attract each other because of the surface forces, such as van der Waals force and surface tension.

This paragraph shortly describes the theory of adsorption (2.4.1) and how the adsorption process can be modelled (2.4.2).

2.4.1 Theory of adsorption

Equilibrium

During adsorption an equilibrium is established. The maximum loading capacity depends on the concentration of absorbable matter in the water. The higher this concentration, the higher is the loading capacity. The relation between the concentration of absorbable matter and the loading capacity can be described by the Freundlich isotherm:

$$q = K * C_e^n$$

In which

q	=	amount of solute absorbed per unit surface area of adsorbent	[g/m ²]
C _e	=	equilibrium concentration dissolved substance	[g/m ³]
K and n	=	isotherm constants	[-]

Kinetics

The kinetics equation for adsorption describes a change in concentration by a transport and a removal term:

$$\frac{dc}{dt} = -v \frac{dc}{dy} - M(c - c_e)$$

In which

v	=	pore velocity of the water	[m/s]
M	=	mass transfer coefficient	[s ⁻¹]
c	=	initial concentration compound	[mg/l]
c _e	=	equilibrium concentration compound	[mg/l]

The driving force for adsorption is the difference between the prevailing concentration and the equilibrium concentration. This equilibrium concentration depends on the loading capacity determined by the Freundlich isotherm. Therefore c_e is determined:

$$c_e = \sqrt[n]{\frac{q}{K}}$$

In the beginning of the filtration process the loading of the filter material is low. This results in a low equilibrium concentration and therefore in a high mass transfer rate.

2.4.2 Modeling of adsorption

Adsorption can be modelled as a combination of film diffusion and adsorption (Figure 18). The water with the iron(II) flows through the filter bed. The iron(II) needs to diffuse into the diffusion layer, represented in Figure 18 by arrow A. The thickness of this layer is depending on the turbulence, by the Reynolds number. From this diffusion layer the iron(II) can be adsorbed on the grain, depending to the Freundlich isotherm, arrow B.

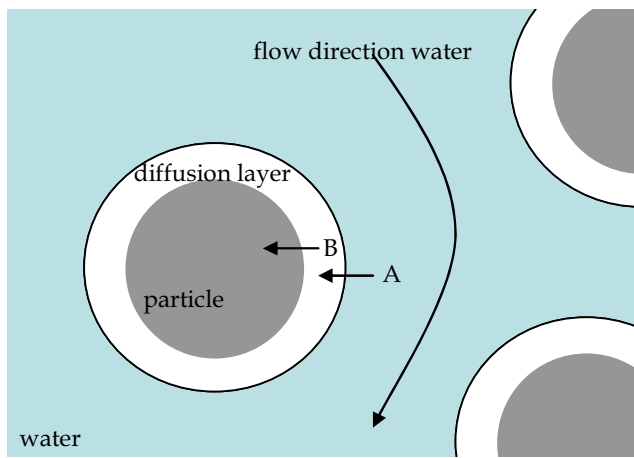


Figure 18: Adsorption modelled as adsorption, arrow B, subsequent to film diffusion, arrow A.

The kinetic constant for adsorption (for process A) is the mass transfer coefficient for the film diffusion theory. The mass transfer follows from the film diffusion coefficient, which can be calculated by the equations from Sherwood and Schmidt. (van der Meer, 2003, Schagen, 2007, Sharma, 2000):

$$Sh_x = \frac{k_x d_h}{D_x} = a Re^b Sc_x^c$$

a , b and c are constants which have to be determined by experiments. Wilson and Geankopolis (1966) proposed for fixed beds of spherical particles with bed porosity between 0.35 and 0.75:

$$Sh = \frac{1.09}{p} Sc^{1/3}$$

for $0.0016 < Re < 55$ and $165 < Sc < 70600$

$$Sc_x = \frac{\eta}{\rho D_x}$$

$$\text{Re} = \frac{\rho v d_h}{\eta} \text{ and for fixed bed } \text{Re}_h = \frac{2}{3} \frac{\rho v d_h}{\eta}$$

$$k_x = \frac{Sh \cdot D_x}{d_h}$$

From the film diffusion coefficient the mass transport rate can be calculated:

$$M = \frac{6}{d_h} \cdot (1-p) \cdot k_x$$

In which

Sh_x	=	Sherwood number	[-]
k_x	=	film diffusion coefficient	[m/s]
d_h	=	diameter filter bed grain, 0.001	[m]
D_x	=	diffusion coefficient	[m ² /s]
Re	=	Reynolds number	[-]
Sc	=	Schmidt number	[-]
η	=	dynamic viscosity, 0.001 for water	[Pa s], [kg/m s]
ρ	=	density of water, 1000	[kg/m ³]
v	=	(local) velocity	[m/s]
p	=	bed porosity, 0.4	[-]
M	=	kinetic constant adsorption or mass transfer rate	[1/s]

3 Fingerprint

This chapter presents the fingerprint method. It starts with an explanation of the calculations performed with the particle counter data. Afterwards the sampling point is illustrated and the operational events that are taken into account are explained. At the end the results are given and discussed.

3.1 Introduction

A particle fingerprint for a drinking water treatment plant is meant to identify the presence of particles through the treatment plant. Besides, variation in particle size distribution, number and volume can be observed. In between every treatment step particles are counted, to be able to quantify the contribution of a specific step to the formation or removal of particles. At Harderbroek the presence of particles through the treatment plant is identified (Raffin and Teunissen, 2007). A distinction is made between normal treatment and operational events. The numbers and sizes of particles are determined with particle counters in raw water, cascade effluent, the supernatant water, filter effluent, after tower aeration and in the clear water. This report focuses on the measurements performed on the filters. During one complete filter runtime (32h) particle counters were applied in the filter effluent.

Vreeburg (2007) reported a high contribution of operational events to the total particle volume concentration leaving the treatment plant and entering the distribution system. In order to quantify the contribution of particles in the water during operational events on the total volume load of particles in the distributed water, particle counts (#/ml) are converted to particle volume from particle volume in $(\mu\text{m})^3/\text{ml}$, which can also be expressed as volume parts per billion (ppb). The volume concentration during stable operation can be compared with the volume concentration after an operational event. With this method it is possible to evaluate particle breakthrough of a rapid filter quantitatively.

For a complete description of this research and the fingerprint of Harderbroek the reader is referred to BTO report 2007.015 (Raffin and Teunissen, 2007). In this report only the measurements concerning the filtration step are discussed.

3.2 Materials and methods

3.2.1 Particle counter

The particle counter used for these experiments is from PAMAS, type WaterViewer. This particle counter has eight channels allowing counting the particles between 1 to 100 μm . One is able to choose the range of each channel. The chosen channel range depends on the experiment and the expected particle sizes. The particle counter is equipped with a pump which maintains a flow of 25 ml/min. The chosen sampling time is 2 minutes. After

every 2 minutes the particle counter gives an average number of particles for each channel measured in 50 ml of water.

The sampled water is pumped through the sensor. The sensor consists of a transmitter of a light probe and a detector, where the water flows in between. If there are particles in the water they will block the transmitted light which is sent to the detector. The detector measures a difference in current. The current difference is linked to a specific particle size by a calibration performed by PAMAS. By measuring the current on the detector the number and size of the particles are known (Figure 19).

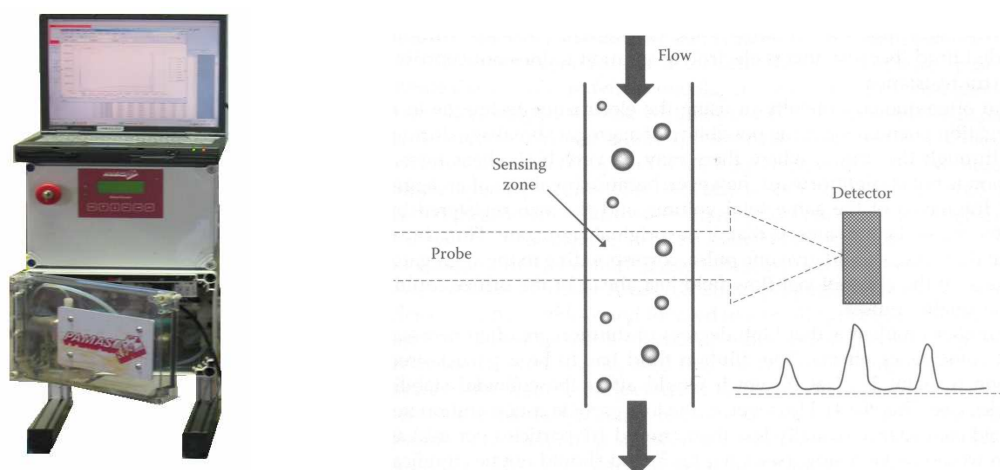


Figure 19: a) The particle counter equipment and b) schematic representation of the sensor (Gregory, 2006)

3.2.2 Analysis of particle counter data

A particle counter produces a huge amount of data. These data should be converted into practical information. Data reduction on particle counting is required to smooth the counts (Ceronio and Haarhoff, 2002). The particle counter is quite sensitive and needs some time to stabilise. Therefore, first it should be studied what the useful and representative parts of the data are. Which data is representative depends also on the research question. Measuring an average particle concentration during stable treatment needs other parts of the data when measuring peaks. After the representative data are chosen, the calculations can be started. In this report the number of particles are presented, as well as the volume of particles.

Number of particles

Number of particles are actually measured as the mean or average concentration of particles. The particle counter gives an amount of particles every 2 minutes. This number is a concentration of particles per ml water. For stable parts the average over a longer period can be calculated. An example is given in Figure 20. In this graph all measured data are plotted, when measuring during stable operation. The representative data is the part of the graph between the two vertical red lines. The first peak is caused by the particle counter itself, which needs some time to stabilise. The peak at the end is caused by an operational event, but within this measurement one was only

interested in stable operation. From these data, it is possible to calculate one average number, without a big standard deviation, or losing important information.

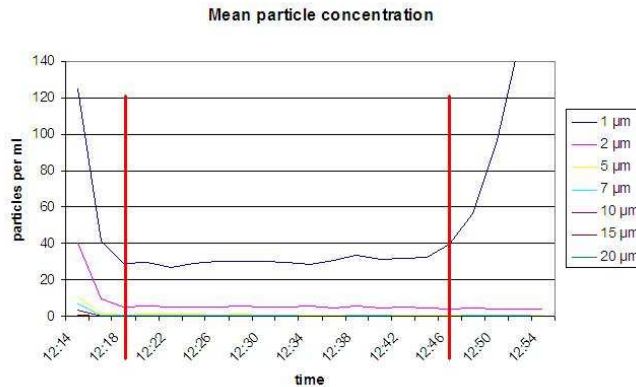


Figure 20: Example of graph with representative and less representative data, depending on the research question.

Volume distribution

Numbers of particles provide a lot of information. But the ultimate aim of this study is to reduce the particle load in the distributed water. When discussing problems in the distribution network, volume (or mass) of iron is of much more importance than number of (iron) particles. Therefore already in this stage of the study, the volume of particles is calculated. The volume concentration of particles in each size range is estimated by multiplying the number of particles detected in that channel by the volume of the average diameter of particles (d_g) in each channel. This geometric mean size is used in the volume calculation. Using the geometric mean has its origin in sieve analysis where the geometric mean size is used as an approximation of the average particle size between two sieves. In particle counting, the thresholds or “bin boundaries” act as the sieves. The geometric mean size of a bin is calculated as shown below and is used when plotting the incremental and normalised counts as these counts do not relate to one specific threshold, but rather to a count between thresholds (Ceronio and Haarhoff, 2001).

$$d_g = \sqrt{d_i \cdot d_j}$$

Where d_i and d_j denote the upper and lower thresholds of a bin.

When d_g is known, the average volume of a particle in a specific bin can be estimated:

$$Volume = \frac{1}{6} \pi d_g^3$$

An example calculation is given in Box 3.

When the volume of particles is calculated, particles are assumed to be spherical. In practice this is not the case. Particles have mostly a flock shape and they contain a lot of water. Especially calculated volumes in the bigger particle size ranges (above 20 μm) need to be taken with care.

Box 3: Example volume calculation.

Size range / bin:	5 – 7 μm
Detected number of particles N:	0.721 per ml
$d_i = 5 \mu\text{m}$	
$d_j = 7 \mu\text{m}$	
$d_g = \sqrt{d_i \cdot d_j} = \sqrt{5 \cdot 7} = 5.916 \mu\text{m}$	
Volume of an average particle, V_p in the bin can be estimated by using d_g	
$\text{Volume} = \frac{1}{6} \pi d_g^3 = \frac{1}{6} \pi \cdot 5.916^3 = 108.41$	
The total volume of particles detected in the bin:	
$V = N * V_p = 0.721 * 108.41 = 78.17 \mu\text{m}^3/\text{ml}$	

In order to calculate the mass of iron, the volume should also be corrected for the density of the flocks. Verberk (2007a) proposed a density of $\rho = 1.972 \text{ kg/m}^3$ for small iron hydroxide flocks ($1 \mu\text{m}$) and $\rho = 1.061 \text{ kg/m}^3$ for the bigger particles ($10 \mu\text{m}$). But these measurements were performed on a specific location and mainly valid for the tested water type.

Therefore, within this report, it is chosen to present the data as volume per volume (more specifically parts per billion (ppb)) and not as the mass per volume as this cannot be derived from the data. 1 ppb means one volume of particle in 1,000,000,000 volume parts of water. Because the density of one ppb is almost the same as water, the volume concentration will be in the same order of magnitude as mass concentration. In Box 4 the transfer from volume in [$\mu\text{m}^3/\text{ml}$] to volume in [ppb] is shown.

Box 4: transfer from $\mu\text{m}^3/\text{ml}$ to ppb.

$1 (\mu\text{m})^3 / \text{ml}$	=	$10^{-18} \text{ m}^3 / \text{ml}$
	=	$10^{-18} \text{ m}^3 / 10^{-6} \text{ m}^3$
	=	$10^{-12} \text{ m}^3 / \text{m}^3$
1 ppb	=	$10^{-9} \text{ m}^3 / \text{m}^3$
1 ppb	=	$1000 (\mu\text{m})^3 / \text{ml}$

3.2.3 Methods

A particle counter was installed in the filter effluent, after the filtrate pump (see Figure 21a). It was not allowed to measure before the pump during the night.

The particle counter was installed at the dead end of a pipeline which collects the filter effluent water for all filters. But because of the dead end, the sampled water is assumed to originate only from filter 1 or 2 (Figure 21b).

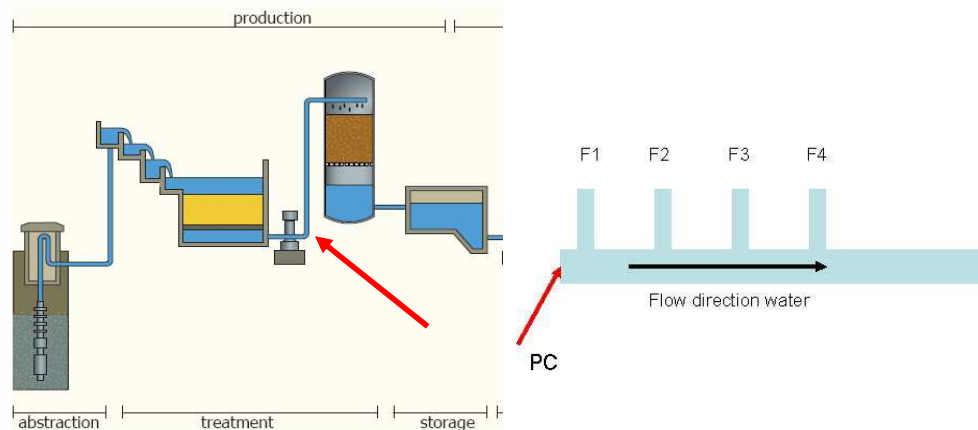


Figure 21: Measurement location particle counter a) in treatment and b) in effluent pipeline.

Two operational events are taken into consideration:

- A filter switch
- A backwash event

During the filter switch experiment at the start filter 2 was switched on and filter 1 was switched of. When the particle counter was stabilised filter 2 is switched off and filter 1 switched on.

For the backwash event a complete filter run was measured. Filter 6 was backwashed during the night before the experiment and the first filtrate of 300 m³ was filtered and drained. This is a standard procedure for Harderbroek. At 9:00h the filter was switched on for 32 hours, until 17:00h the next day. In the mean time the process was not interrupted.

3.3 Results

The number of particles and volume concentrations in the filter effluent, after the two operational events are shown in Figures 22a,b and 23a,b. The number of particles are plotted on a logarithmic scale.

In addition, the results are summarised in Table 4. In this table the particle size ranges are subdivided in three classes. The class 'smaller particles' contains the size range 1-2 μm . The class 'middle particles' contains the size ranges 2-5 μm , 5-7 μm and 7-10 μm . The class 'larger particles' contains the size ranges 10-15 μm , 15-20 μm and >20 μm .

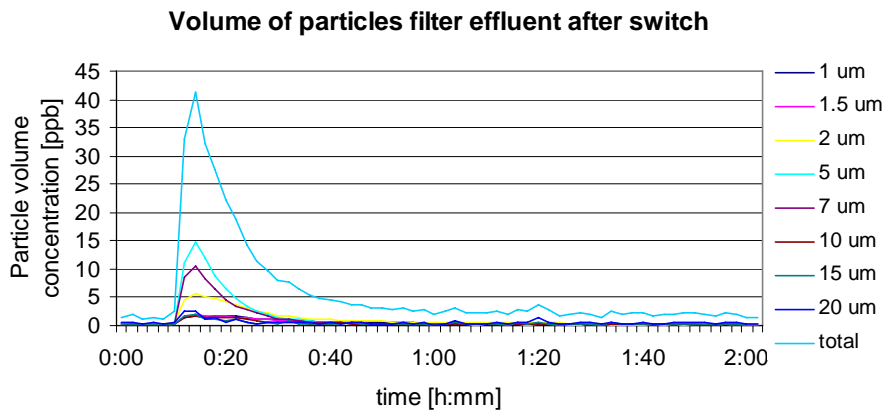
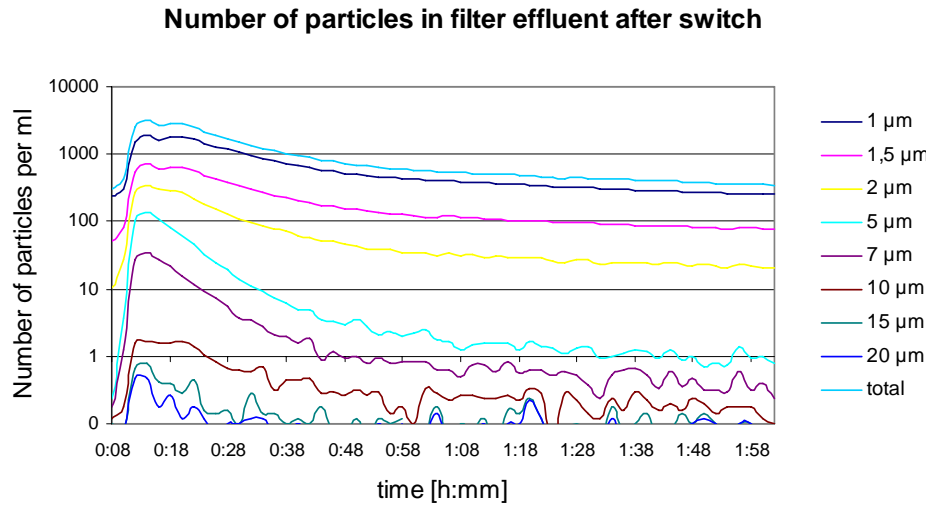


Figure 22: Results measurements during filter switch a) particle number and b) particle volume.

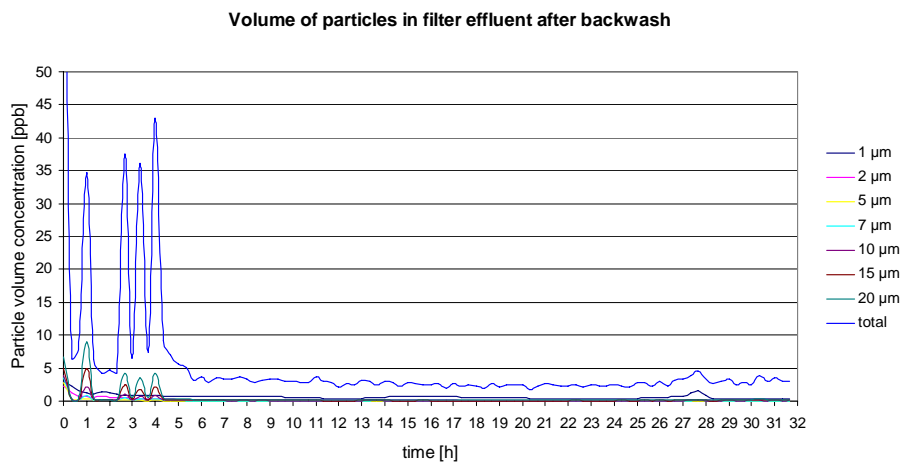
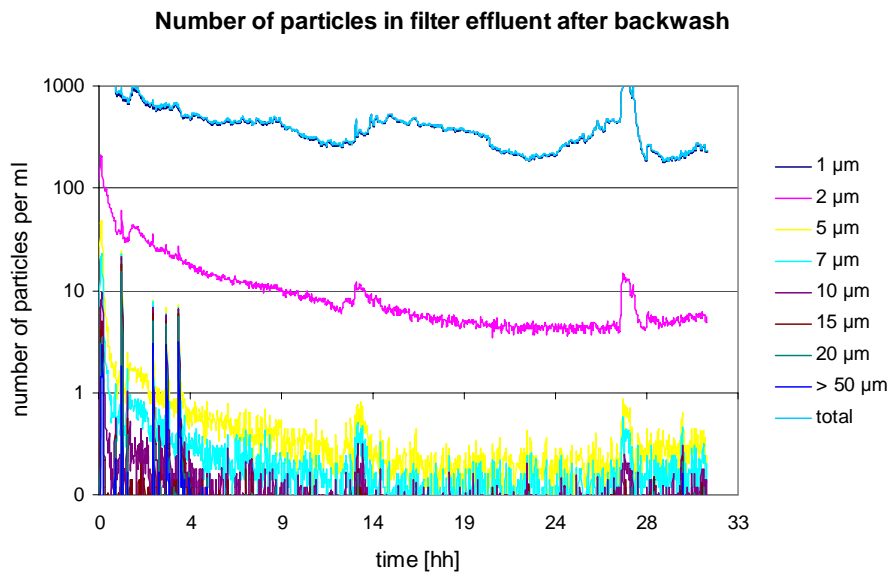


Figure 23: Results measurements after filter backwash a) particle number and b) particle volume.

Table 4: Volume during stable operation and during peaks.

Average Volume [ppb]	3.05
Smaller particles	0.62
Middle particles	0.60
Larger particles	1.83
Volume 0.5h after switch [ppb]	19.40
Smaller particles	2.72
Middle particles	13.56
Larger particles	3.12
Volume 4h after backwash [ppb]	19.90
Smaller particles	1.36
Middle particles	1.72
Larger particles	16.82

Filter switch

After the particle counter showed stable counts filter 2 was switched off and filter 1 switched on. The number of particles detected by the particle counter in the filter effluent immediately increased. The volume of particles in the filter effluent is influenced too. Until 0:30h the volume is significantly augmented. Half an hour after the filter switch the volume seems to stabilise again. Table 4 shows the average particle volume in the three classes and the volume after the switch. Especially the volume in the class middle particles increased during the first half hour after the filter switch.

Backwash

For the backwash experiment a complete filter run is recorded. At the start of the filtration the number of particles are higher as expected compared to stable operation. The number decreases during the filter run. The increase of number of particles on 21-02 at 14:00h is probably due to an increase of flow, which was registered at this time.

The graph with the volume of particles shows a clear picture on the duration of the influence of the backwash event. After 4 hours the volume of particles in the filter effluent is suddenly stable. Table 4 shows a major increase in volume in the class larger particles.

3.4 Discussion

A volume graph is preferred over the graph displaying the actual measured numbers of particles. The volume graph gives a clear view on the duration of a disturbance, caused by an operational event. Besides, finally in the distribution system, mass of iron is of most importance. Through the density (which is unknown) the volume concentration is related to mass. A third advantage of the volume concentration graph is the preservation of the information on bigger particles.

3.4.1 Comparison of stable operation and operational events

To evaluate the influence of a peak caused by an operational event, the volume load during the peak is compared with the volume load during stable operation. The particle volume load for a certain time period can be calculated from the volume concentration and the flow (Box 5). During the experiment with the filter switch the flow through the filter was 250 m³/h. The volume concentrations during the peak (0.5h) and during stable operation (23.5h) are summarised in Table 5 below. With this information and the formula in Box 5 the volume load can be calculated. The volume obtained by this calculation is a volume in m³, which can be converted to a volume load in ml (factor 10⁶).

The particle volume load during the peak after a filter switch, which lasts for 30 min, was 2.4 ml. During stable operation, lasting for 24 h, the particle volume load was 15.7 ml. During this operational event in only 2 % of the time more than 15% of the particle volume breaks through the filter.

For a backwash event the load from the peak is compared to the load of the total filter run (32h). The load during the first 4h is 18.7 ml, while the load during the stable part of the filter run is slightly higher, 22.6 ml. In 13% of the time, 45% of the particle volume load is added to the filter effluent.

Box 5: Calculation volume load.

Volume load = $C \cdot Q \cdot 10^{-9} \cdot t$			
VL	=	volume load	[m ³ particles]
C	=	volume concentration	[ppb], [m ³ particles / 10 ⁹ m ³ water]
Q	=	flow	[m ³ water/h]
t	=	time	[h]
VL [ml] = VL[m ³] * 10 ⁶			

Table 5: Volume load during peak and stable situation after operational event.

	Backwash	Switch
Total time [h]	32	24
Peak	4	0.5
Stable	28	23.5
Average concentration [ppb]		
Peak	19.9	19.4
Stable	3.44	2.62
Flow rate [m ³ /h]	235	250
Volume load [ml]		
Peak	18.70	2.42
Stable	22.66	15.70

Volume concentration expressed in parts per billion is closely related to the mass of particles in water. One could defend that 1 ml of particle volume corresponds with 1 g. In order to prevent discussion, all values are presented

in volumes. Expressing volume load in ppb's give a measure to evaluate the breakthrough of particles quantitatively.

3.4.2 Reduction measures

In order to reduce the total particle volume load towards the distribution system, Harderbroek can take some measures. Because operational events showed to have a significant contribution to the daily amount of particles, it is advised to apply a smooth treatment operation. A reduction of the number of filter switches by two switches a day will result in a reduction of the particle volume load of 21%.

Besides it is advised to Harderbroek to recirculate the first filtrate water, in order to eliminate the particle breakthrough after a backwash event. A first filtrate of 300m³ is nowadays drained and transported to an infiltration pond, which means a loss in production and it is not very effective. The peak last for 4 hours by a flow of 230 m³/h. Draining this amount of water would be a spill. But this water can also be recirculated to the filter influent. If the peak of 4 hours is eliminated, the particle volume load during one filter run time (32 h) is reduced by 37%.

Table 6 shows the influence of recirculating the first filtrate for several hours.

Table 6: Volume load particles after discharging first filtrate.

Discharge time		-	1h	2h	3h	4h
Duration peak	h	4	3	2	1	0
Stable period	h	28	28	28	28	28
Filter run time	h	32	31	30	29	28
Discharged water	m ³	300	535	770	1005	1240
Volume load peak	ml	18.7	11.1	7.5	3.9	-
Total volume load	ml	41.7	33.9	30.2	26.6	22.7
Time	%	12.5	9.7	6.7	3.5	0
Volume load	%	45	33	25	15	0

3.4.3 Frequency distribution

A frequency curve is plotted, for the different size ranges of particles (Figure 24). A steep S-curve indicates for that particle size range a uniform concentration during the measured time interval. An S-curve which is more stretched out indicates some variation in the measured volume concentrations during the measured time interval.

In addition Tables 7 and 8 show the 50%-, 90%- and 99.9%-percentile. For example the concentration mentioned in the 90%-percentile is 90% of the time below this value and exceeded in 10% of the measured time.

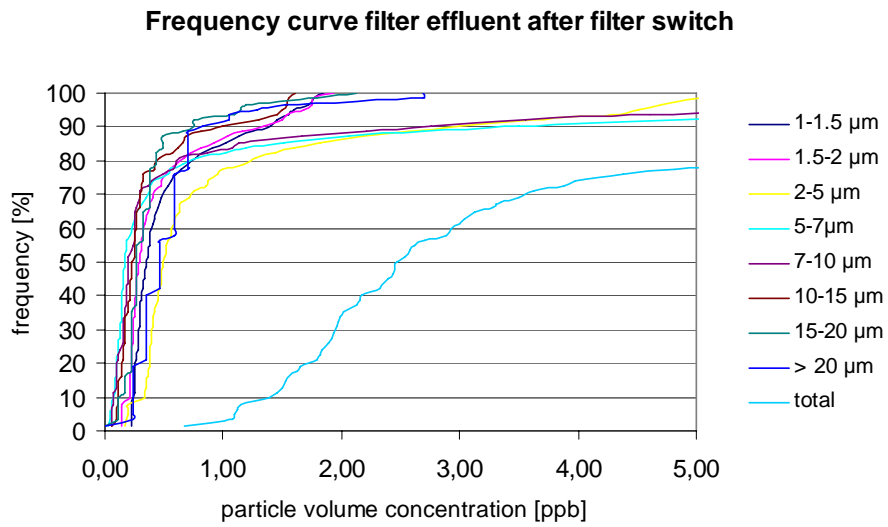


Figure 24a: Frequency curve of different particle size ranges in the filter effluent during a filter switch.

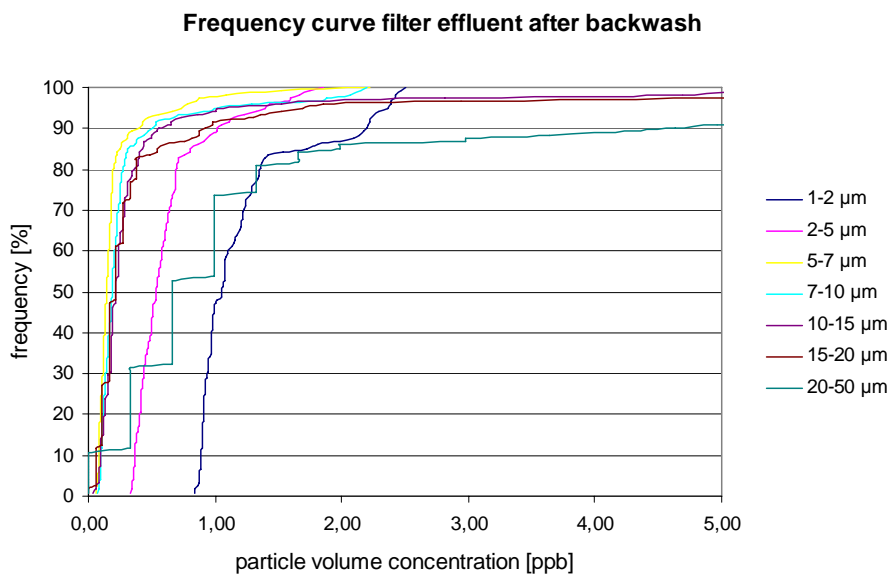


Figure 24b: Frequency curve of different particle size ranges in the filter effluent after a backwash event.

Table 7: Volume in 50%-, 90%- and 99.9%-percentile after a filter switch.

		Volume 50%	Volume 90%	Volume 99.9%
Smaller particles	< 2	0.64	2.74	3.78
Middle particles	2 - 10 μm	0.86	9.26	31.09
Larger particles	> 10 μm	0.97	2.58	6.43
Total particles		2.47	14.57	41.31

Table 8: Volume in 50%-, 90%- and 99.9%-percentile after a backwash.

		Volume 50%	Volume 90%	Volume 99.9%
Smaller particles	< 2	0.67	1.40	7.39
Middle particles	2 - 10 μm	0.16	0.45	21.08
Larger particles	> 10 μm	1.74	5.27	263.99
Total particles		2.97	7.22	341.42

In Figure 24a the C-curve for a filter switch is plotted. The curve of the size ranges 1 and 1.5 and 10, 15 and 20 show a steep S-shape. These particles occur in a constant volume over the measured time interval. But the size ranges 2, 5 and 7 μm show a less steep S-curve. The smaller particles (1 and 1.5) are worst removed by filtration, so an event does not significantly influence the filterability of these particles. The bigger particles (10, 15 and 20 μm) have such a high filterability that they are always well removed, also during an event. The particles in the middle size ranges (2, 5 and 7 μm) are significantly influenced by the event. Table 7 shows the 50%-percentile (median), the 90%-percentile and the 99.9%-percentile. The same phenomenon is noticeable. Over the different percentiles the volume of the middle particles increases and varies most.

In Figure 24b the frequency curves for the complete filter run are plotted. In this graph the curves for the size ranges 10-15 and 15-20 show more variation in volume concentration. Also Table 8 shows a major variation in the larger particles. After a backwash event mainly the larger particle break through during the peak. This can be explained by the settling properties of particles. Larger particles have better settling properties and may therefore be more difficult to be removed by backwashing. If so, these particles stay behind in the filter bed and break through when the filtration is started. These larger particles with good settling properties are undesired in the distribution system.

3.4.4 Comparison with other pumping stations

Verberk (2007b) applied on-line turbidity meters and particle counters at six different treatment locations in the Netherlands. From the particle counter data he determined the particulate volume load fed to and in a distribution system. In Table 9 the main characteristics of the different drinking water treatment plants and the successive distribution systems are summarised. Table 10 shows the measured particle volume concentration in the water leaving the treatment plant, for the particle size ranges from 2 μm till > 15 μm .

Table 9: Characteristics of the six water treatment plants and distribution systems of this comparison (Kivit, 2004, van der Meulen, 2004, Verberk et al., 2006b).

ID	Source water	Treatment processes	Type of network
UF	sw ¹	Artificial infiltration in dunes, recharge, aeration, rapid sand filtration, activated carbon filtration, ultra filtration	Asbestos cement transport main, cast iron reticulation pipes
SSF	sw	Artificial infiltration, recharge, powdered activated carbon filtration, softening, aeration, rapid sand filtration, slow sand filtration	Concrete and cast iron transport main, cast iron reticulation system
GW	gw ²	Aeration, rapid sand filtration	PVC and asbestos cement transport main, PVC reticulation pipes
BF	sw & gw	Bank filtration, aeration, rapid sand filtration	PVC and asbestos cement transport main
AL	sw	Artificial infiltration, recharge, aeration, rapid sand filtration, ozonation, softening, activated carbon filtration, slow sand filtration	Asbestos cement transportation system
AW	sw	Reservoir, rapid sand filtration, ozonation, softening, activated carbon filtration, slow sand filtration	Asbestos cement transportation system
Additional treatment plants			
RF	gw	Aeration, rapid sand filtration, softening, rapid sand filtration	
RF UF	gw	Aeration, rapid sand filtration, softening, rapid sand filtration, ultra filtration	

¹ sw means source is surface water

² gw means source is ground water

Table 10: Average particle volume in the clear water at 6 different plants in the Netherlands.

Location	Average particle volume concentration [$\mu\text{m}^3/\text{ml}$]	Average particle volume [ppb]
UF	478	< 1
SSF	295	< 1
GW	5,332	5
BF	24,863	25
AL	605	< 1
AW	12,413	12
Additional treatment plants		
RF		15
RFUF		< 1

Verberk (2007b) concluded that the treatment plants UF, SSF and AL have a pvc lower than 1 ppb. These treatment plants make use of slow sand filtration or ultra filtration as the final treatment step. (However, the AW treatment plant also has slow sand filtration as a final treatment step). The treatment plants having rapid sand filtration as a final treatment step have much higher particle volume concentration values.

Vreeburg (2007) performed particle measurements at location RF. In addition he treated the water from location RF with an ultra filtration step. This water was fed to an isolated and previously cleaned distribution network. After the UF step lower particle volume loads (from 15 ppb to < 1 ppb) were found in the distribution system. In addition he expected the cleaning frequency of the distribution system to decrease from once every year to about once every 10 or 12 years. For location RF the present cleaning frequency is once every year, while the particle volume load in the clear water is 15 ppb. For location GW (Harderbroek) the present cleaning frequency is once every 3 years, with an average particle volume load in the clear water of 5 ppb. This suggests a reduction in particle volume load will reduce the necessary cleaning frequency of the distribution system.

3.4.5 Application

Volume of particles expressed in parts per billion can be used to evaluate the operation of a treatment plant and to quantify discontinuities in operation. If particle counts are used to evaluate a pumping station, long term measurements are preferred above grab sampling measurements.

The installation of a particle counter in the clear water gives information about the average water quality leaving the treatment. It supplies information about the load for the distribution system. But individual information about the origin of particles gets lost.

The installation of a particle counter in the filter effluent is more convenient when judging the filtration step. Information is gathered about one filter only,

but there is no information loss. The measurements can be used for optimisation purposes.

Finally an application could be found in applying a norm value for ppb leaving a treatment plant, for example on average per day. Based on the measurements at Harderbroek and the experience on other treatment plants, companies should aim on an average particle volume load below 1 ppb. In addition they should aim to keep the 90%-percentile particle volume load below 2 ppb.

4 Column experiments

In this chapter the column experiments are presented. After a short introduction the method is explained, including the set-up and analyses applied. Afterwards the results are given and discussed. In the last paragraph of this chapter some alternatives for the treatment at Harderbroek are proposed.

4.1 Introduction

In this chapter column experiments are described which are used to study the removal of iron from the water. The results of the experiments to test hypothesis 1 (see Paragraph 1.2.2) gave reason to change the hypothesis. Therefore, an extra set of experiments was carried out to test the new hypothesis 2. The column experiments are therefore presented in two parts; part 1 is focussed on changing the pre-treatment of the filter influent water, in order to improve the iron(II) hydroxide flock formation and removal. Part 2 is focussed on adjustments in the filtration process, in order to improve the oxidation and removal of iron in the filter.

The column experiments are executed at location Harderbroek.

4.2 Methods

4.2.1 Equipment

With a four-column set-up research is executed, concerning the removal of iron. The columns have a diameter of 9 cm and are flow controlled with four separate flow controllers. The applied flow was 60 l/h per column, which corresponds to a filtration velocity of 10 m/h. They are operated by hand and filled with ripened filter material from the Harderbroek filters. The filter gravel is taken from the full scale filters with buckets and put into the columns. The available filter bed height was approximately 25 cm in the columns. This simulates the uppermost layer of the filter bed in Harderbroek. In this uppermost layer the main iron removal was expected.

Before starting the experiments the columns were flushed for 8 hours with clear water to wash out most dirt.

The filterability is determined from turbidity measurements, iron concentration (iron(II) and total iron separately) and particles are measured. Samples were taken 1 hour and 4 hours after the start-up of the filtration experiment. After an experiment the filters were backwashed. The backwash was performed with drinking water. The applied backwash flow was 350 l/h (55 m/h) for 10 minutes. The expansion during a backwash event was between 20 and 28%.

For the experiments of part 1 the four columns had the same materials and were fed from the same water source. The columns showed to have reproducible and comparable effluent values. Therefore in part 2 only two columns with the same material are applied, in order to be able to compare alternatives and have a reference at the same time.

4.2.2 Experimental set-up part 1

During the first part of the column experiments the influent water was treated in four different ways, see Figure 25. The four treatment methods are described in more detail below. Influent 1 and 2 are used to verify the hypothesis (1), that the formed iron hydroxide flocks will break down due to high turbulence in the filter inlet construction. The experiments with influent 3 and 4 are a quick scan for possible alternatives. Each different treatment method is done twice, during which the major parameter for that treatment method is varied.

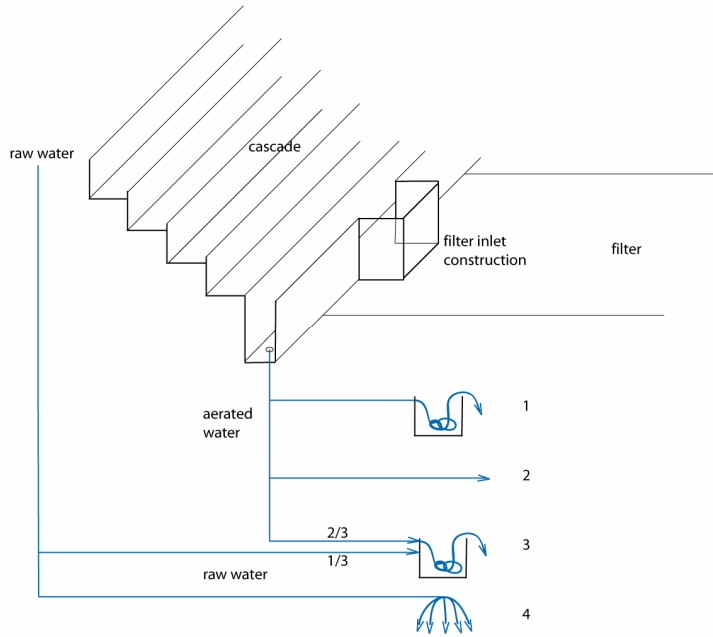


Figure 25: Four different pre-treatments to produce water for the column experiments.

Influent 1

Influent 1 functions as a reference experiment. It simulates the situation at the filters in Harderbroek. In the treatment plant the water passes a filter inlet construction between the cascade and the filters. It is expected that during the passage of this inlet construction the water experiences a high turbulence, energy loss and therefore G-value.

The G-value is a measure for the amount of power added to a specific volume of water and can be calculated by the following formula:

$$G = \sqrt{\frac{P}{\mu V}}$$

In which

P	=	inserted power	[W]
μ	=	dynamic viscosity	[Ns/m]
V	=	Volume of vessel	[m ³]

The effect of turbulence on the filterability is tested within this experiment. A mixing device is added to the basic set-up. By applying different mixing intensities different G-values can be achieved.

The applied mixer had a full power of 72 Watt. The mixing intensity was 500 rpm for experiment 1.1 and 900 rpm for experiment 1.2, resulting in G-values of 1000 s^{-1} and 1800 s^{-1} .

The applied stirrer was a one blade paddle stirrer, with a blade diameter of 70 mm and a blade height of 70 mm.



Influent 2

Influent 2 was taken directly from the cascade. The difference in filterability between influent 1 and influent 2 gives the influence of the filter inlet construction. The major parameter for influent 2 is the residence time. In experiment 2.1 the residence time was 2 min, in experiment 2.2 it was 7 min.

Influent 3

For influent 3 two water sources are mixed. $\frac{2}{3}$ of the water was taken directly from the cascade. $\frac{1}{3}$ of the water was raw water, un-aerated. Perhaps the dissolved iron(II) from the raw water will oxidise to iron(III) when it comes in contact with air. Colloidal iron is expected to be in the cascade effluent. The iron(II) might function as a flocculent aid for flocculation of the broken colloids, resulting in larger flocks. Generally larger flocks have a better filterability.

The ratio of cascade effluent and raw water is the major process parameter. In experiment 3.1 this was 2:1 and in experiment 3.2 1:1.

Influent 4

Influent 4 was raw water, aerated by a different aeration system existing of an air pump for bubble aeration and a shower for spray aeration. Not only the change in aeration system is important, but also the difference in residence time between aeration and filtration. To compare influent 1 and 4, the residence time should be identical for at least one experiment. The RQ is the main parameter of interest. In this research only the air flow was changed to change the RQ. In experiment 4.1 the water flow was 240 l/h and the air flow 200 l/h. ($RQ = 0.8$), while in experiment 4.2 the air flow was 400 l/h ($RQ = 1.6$). Considering the residence time, experiment 4.2 is comparable with experiment 1.2.

4.2.3 Experimental set-up part 2

During the second part of the column experiments the pH was adjusted, in order to investigate the kinetics of the iron oxidation processes at Harderbroek. From the four columns available in the set-up, two were used as a reference and fed with cascade effluent. In the other two columns different conditions were applied:

Two alternatives are elaborated; a change in pH by the dosage of caustic soda (NaOH) and the application of crushed limestone filtration. The increase of

the pH until a value of 8.0 should result in faster oxidation of iron. A solution for Harderbroek could be crushed limestone filtration. Oomen et al. (1983) reported crushed limestone filtration as a convenient process for the treatment of iron containing aggressive groundwater. With crushed limestone filtration calcium carbonate will dissolve. This reaction results in a decrease of the CO₂ concentration and therefore in a higher pH. In addition the HCO₃⁻ concentration is increased, resulting in a higher buffering capacity of the water. A third effect is the increase of the Ca²⁺ concentration and thus the total hardness of the water.

Here, the calculation is shown to obtain a pH value of 8 in the cascade effluent by dosing caustic soda:

The CO₂ concentration in the cascade effluent water is 5.5 mg/l, which is equivalent to 0.125 mmol/l. This amount of CO₂ has to react to achieve an increase in pH.

The increase of the pH until a value of 8.0 should result in a fast oxidation of iron. The dominant iron removal process in that case should be flock filtration.

The pH depends on the carbonic acid equilibrium, see Box 2, Chapter 2.

At a temperature of 10 °C, pK₁ is 6.46. This means that, with a pH of 6.46 the ratio of [CO₂] and [HCO₃⁻] = 1 : 1. Carbon dioxide and bicarbonate concentrations are related with equation K₁.

Because of the logarithmic relation between pH and the concentration H⁺, an increase of 1 in pH result in a difference of the [CO₂] : [HCO₃⁻] ratio of 10. So at a pH of 7.4, the ratio [CO₂] : [HCO₃⁻] = 1 : 10. And at a pH of 8.4 this ratio is [CO₂] : [HCO₃⁻] = 1 : 100. To achieve a pH of 8.0 as desired within the experiment, the ratio should be 1 : 50. The cascade effluent values at Harderbroek are measured by van der Pol (2005):

$$\begin{array}{lcl} [\text{CO}_2] & = & 0.125 \text{ mmol/l} \\ [\text{HCO}_3^-] & = & 1.34 \text{ mmol/l} \end{array}$$

This ratio is about 1 : 10, which complies with the measured pH of 7.5. But because of the low bicarbonate concentration almost all carbon dioxide must be removed.

Caustic soda dosage

Caustic soda dissolves in a water environment:



An increase of OH⁻ concentration results in an increase of pH. The applied solution of caustic soda was 0.01 M, in a vessel of 20 litres. In order to remove 0.125 mmol/l CO₂ in 120 l/h of water (the flow through two columns), 0.125*120 = 15 mmol/h NaOH needs to be dosed. With a solution of the caustic soda of 0.01 M, the expected flow was 1.5 l/h.

With a membrane pump the caustic soda is dosed in one of the two influent pipe lines, feeding column 1 and 2. The dosing point was situated 2 meter before the columns.

In a preliminary experiment the flow of the pump was calibrated as well as the necessary dosage to achieve a pH of 8.0. The necessary flow rate was 2.2 l/h (60%) to achieve a pH of 8.0 in the column influent. With a flow of 2.2 l/h, 22 mmol/h caustic soda is dosed. This is somewhat higher as expected from theory. Perhaps the CO₂ concentration of the water was somewhat higher, or the low phosphate concentration functioned as a buffer. Figure 26 shows a picture from the dosing pump.



Figure 26: Experiment with caustic soda dosage to column 1 and 2.

Crushed limestone filtration

Within crushed limestone filtration calcium carbonate will dissolve and form calcium ions and bicarbonate acid. This reaction results in a decrease of the CO₂ concentration and therefore in a higher pH.



From two columns the filter material is removed and replaced by crushed limestone. The applied medium is Jura Perle grains, in the size range of 1.1 – 1.8 mm. The two other columns with default filter material are used as a reference.

Figure 27 shows a picture from the column set-up during crushed limestone filtration.



Figure 27: Experiment with crushed limestone filtration in column 1 and 2.

4.2.4 Analyses

Turbidity

Turbidity is measured with a turbidity meter from Dr Lange (Nephla type nr LPG 2309) at Harderbroek. This portable turbidity meter is tested at the Kiwa Water Research Laboratory first in order to verify the values of the portable meter. Some samples from Harderbroek and some calibration fluids are measured with the Dr Lange turbidity meter and the turbidity meter from the Laboratory at Kiwa Water Research. The results from the two turbidity meters were comparable and the Dr de Lange meter is used at Harderbroek.

Head loss

To determine the accumulation of solids in the filter bed, the head loss over the columns is measured. Therefore a pressure differential meter is used. First the pressure in the system is measured, by opening three valves. One valve above the column, one below the column and a system valve. After closing the system valve the pressure between these two valves is measured. The applied pressure difference meter was from the brand Endress + Hauser, type Deltabar.

Iron concentration

Because iron is the main issue in the situation of Harderbroek, the removal of iron is measured by taking iron samples. These samples are analysed at the laboratory of Vitens (total iron) and Kiwa Water Research (Fe(II)).

Iron(II)

Samples are taken in 100 ml PE bottles and conserved with 2 ml 1 M HCl. HCl is used because it does not oxidise Fe(II). The HCl results in a very low pH which stops the oxidation of iron(II) into iron (III).

The analysis method applied is a spectrophotometric method: Dissolved Fe(II) forms a purple complex with the reagent ferrozine; (3-(2-pyridyl)-5,6-diphenyl-1,2,4-triazine 4,4'-disulfonacid disodium salt. xH₂O). Fe(III) does not form complexes with this reagent.

Total iron

Samples were taken in 100 ml PE bottles and conserved by adding 2 ml HNO₃. The concentration is determined with ICP-MS, in accordance to ISO 17294-2.

Iron(III)

The iron(III) concentration is calculated from the total iron concentration and the iron(II) concentration.

HCO₃⁻, pH, Ca²⁺ and EGV

During part two of the column experiments, the analyses were extended with bicarbonate and calcium concentrations, the conductivity and the pH of the water. These values are relevant when the pH is adjusted.

All these analyses were performed at the laboratory of Vitens. The samples for pH and bicarbonate were taken in 'air removal bottles'. The pH is analysed according to NEN 6411, HCO₃⁻ is determined by titration with hydrochloric acid. The calcium concentration is determined with ICP-MS.

4.2.5 Measurement program

Each experiment ran during four hours. The total experimental program took two weeks. Table 11 summarizes the experiments performed. Table 12 shows the measurements performed during each experiment. In the effluent tubing of the columns a sample point is installed. Before a sample was taken, the tap is opened en flushed for a few minutes to flush out settled particles.

Table 11: Scheme experiments.

Part	exp. no.	variation	device	Settings		
1	2a	cascade	-	t = 2 min		
	2b	cascade	tank	t = 7 min	V tank = 20 l	
	1a	cascade	tank, stirrer	rpm = 500	G= 1000 s ⁻¹	
	1b	cascade	tank, stirrer	rpm = 900	G= 1800 s ⁻¹	
	3a	raw and cascade	flow meters	ratio = 2c, 1r		
	3b	raw and cascade	flow meters	ratio = 1c, 1r		
	4a	raw	tank, pump	RQ = 0.5	Qa = 200	
	4b	raw	tank, pump	RQ = 1.0	Qa = 400	
	2	5a	NaOH	Pump	pH = 8.0	
		6a	Crushed limestone	Juraperle	t = 1 min	

Table 12: Measurements during each experiment.

Parameter	time	Sampling point
bed height	t = 0h	Over columns
turbidity	t = 0,1,2,3,4h	influent / effluent
Pressure difference	t = 0,1,2,3,4h	Over columns
Samples for chemical analysis	t = 1,4h	influent / effluent
Particle counters	during 4 hours	influent / effluent

4.3 Results part 1

4.3.1 Observations

During all experiments the influent water as well as the effluent water look clear to the naked eye. After a day of experiments, and in the morning before new experiments, the filters were backwashed separately. The expansion of the bed was measured at every backwash event. The average expansion was in the order of 25%. Figure 28 shows the expansion during the backwash of column 2. Especially during the experiments with influent 1 and 2, a front of dirt came out the filter bed, which was observed in the backwash water.



Figure 28: Expansion of the filter bed when backwashing filter 2.

4.3.2 General results

In the first part of the experiments, the different influent water types, did not result in significant differences in the effluent. Later on it was concluded that the pH was too low and was the limiting factor in the iron removal process. Therefore no significant differences, caused by variation of G-value and residence time, were measured during part 1 of the experiments. Because the pH was limiting, it is not possible to draw conclusions from the results of part 1, according to residence time and G-value. The results from the measurements are summarized in Annex I.

As explained above, no differences between the influent water types were measured. However, the iron in the cascade effluent water consisted, in all experiments, mainly of iron(II) (Figure 29), while after aeration iron(III) is expected. The oxidation has not been successfully. pH measurements gave reason to assume a slow oxidation rate.

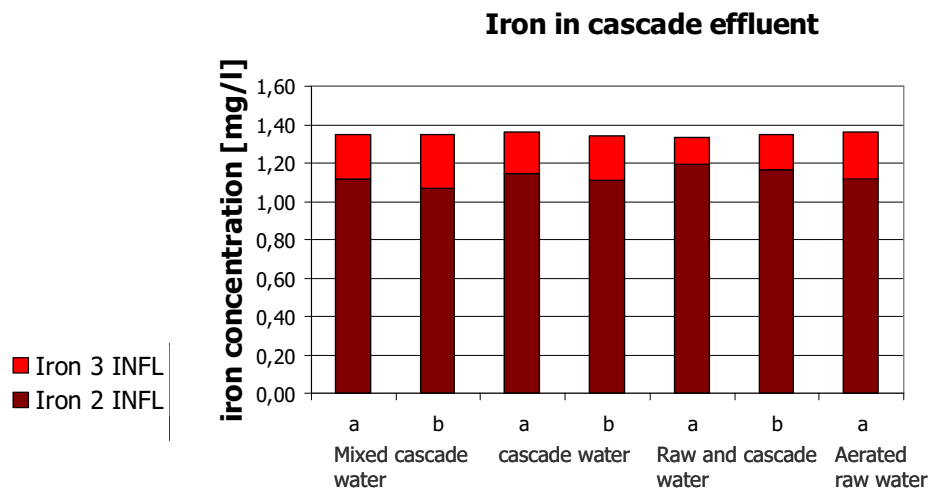


Figure 29: Iron(II) and iron(III) concentration in cascade effluent water (=column influent water) for the 4 experiments, version a and b (see Table 11).

4.4 Results part 2

4.4.1 Observations

While backwashing after the caustic soda dosage experiment, the backwash water showed a brownish red colour. This colour indicates iron hydroxide flocks.

During the crushed limestone filtration this colour was not observed. An explanation can be that the crushed limestone filtration increases the pH during filtration, while caustic soda dosing already increased the pH in the influent. The iron(III) hydroxide flocks may be formed deeper in the filter bed and may be harder to remove by backwashing.

On other explanation can be found in the white limestone particles to mask the colour of the iron(III) hydroxide flocks.

4.4.2 Results

The iron(II) concentrations and pH values are plotted in Figure 30 and 31. The pH in the influent of the columns after dosing NaOH is 7.9/8.0. The iron(II) concentration in the influent water is decreased compared to the reference, from 1.2 mg/l to 0.8 mg/l (the influent sampling point was 2 m downstream from the dosing point). The iron(II) concentration in the effluent is decreased from 0.4 mg/l to less than 0.1 mg/l.

The crushed limestone filtration increases the pH in the effluent water slightly when compared to the effluent of the reference columns: from 7.5 to 7.65. The contact time between the water and the crushed limestone was too short for the required pH increase. But still a slight improvement in iron removal is noticed. The iron(II) concentration in the effluent is decreased from 0.4 mg/l in the reference columns to 0.2 mg/l. The measured iron(II) concentration in column 4 is however doubtful, because during all other reference experiments, the iron(II) concentration in the effluent is 0.40 mg/l.

It should be noted that during the column experiments part one, the influent iron(II) concentration was 1.2 mg/l and the effluent iron(II) concentration 0.4 mg/l. Similar values were found in the reference experiments during column experiments part two.¹

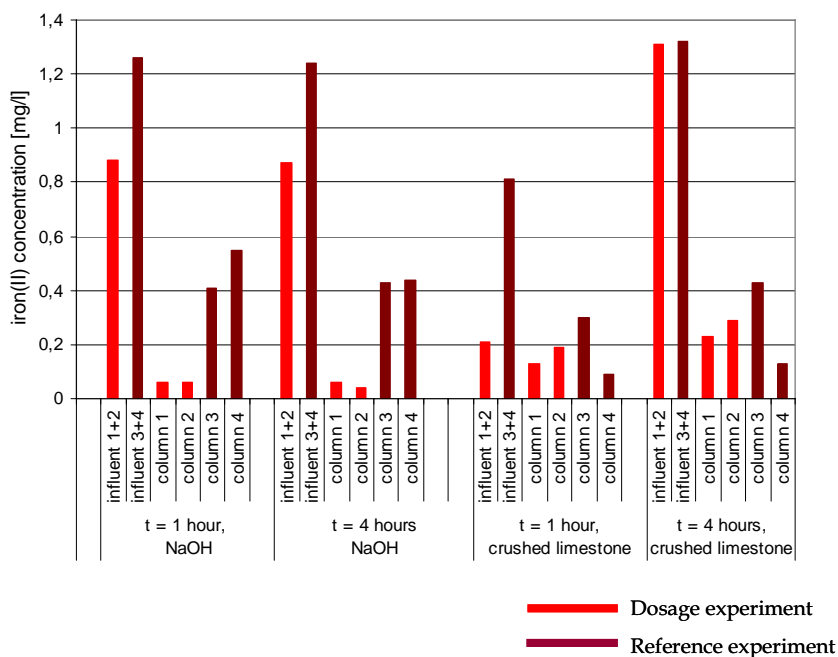


Figure 30: Iron(II) concentrations after 1 and 4 hours during the column experiments part 2. Columns 1 and 2 are the dosed columns, columns 3 and 4 are the reference columns.

¹ Two applicon iron analysers, installed at Harderbroek after this research measured in cascade effluent water (column influent) iron(II) as 1.20 mg/l and iron(III) as 0.25 mg/l.

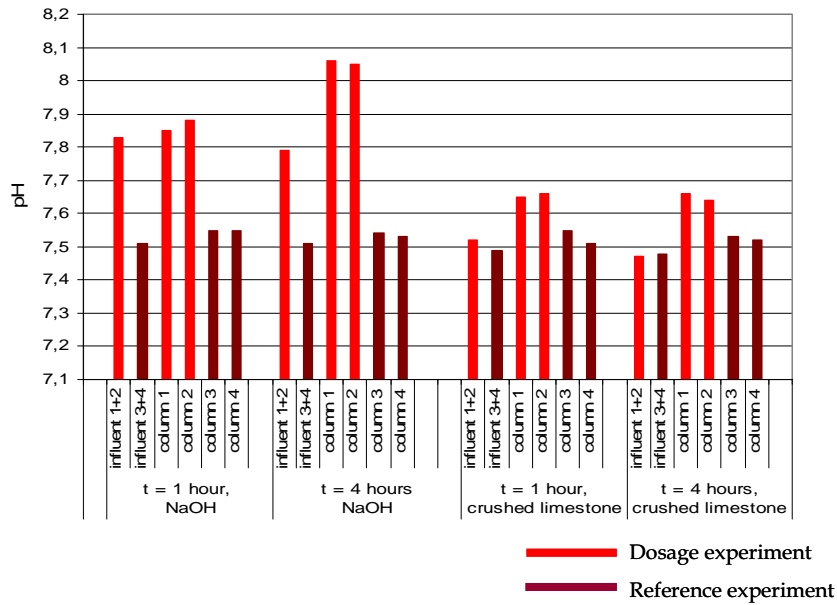


Figure 31: pH values measured after 1 and 4 hours during the column experiments part 2. Columns 1 and 2 are the dosed columns, columns 3 and 4 are the reference columns.

Iron(II) and iron(III) concentrations are presented in Figure 32. The red bars indicate iron(II), the blue bars iron(III). A dark tint is used for the reference columns, a light colour for the adjusted columns.

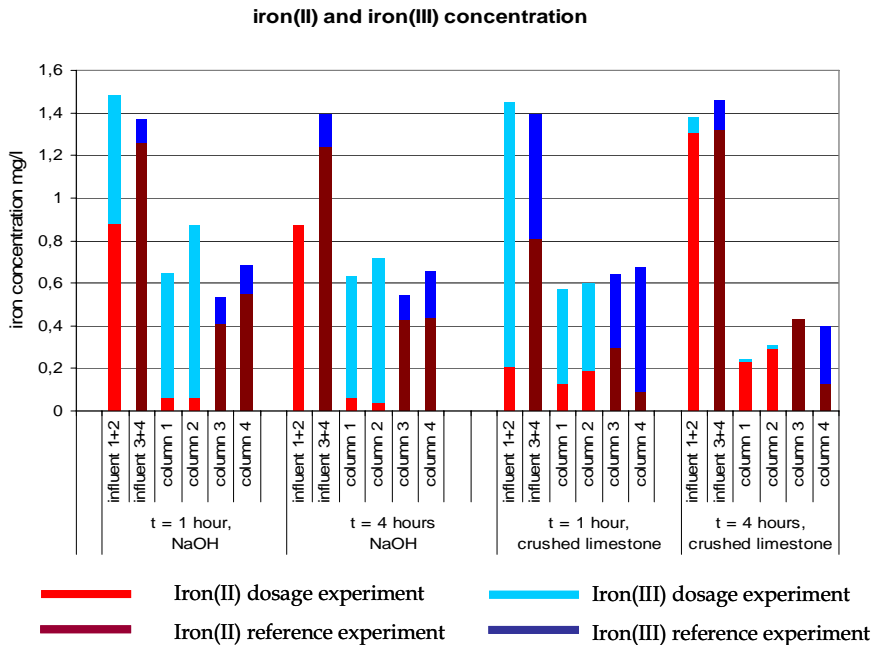


Figure 32: Iron(II) and iron(III) concentrations after 1 and 4 hours during the column experiments part 2. Columns 1 and 2 are the dosed columns, columns 3 and 4 are the reference columns.

The bicarbonate and calcium measurements did not show any unexpected or striking phenomena. The values are summarized in Annex II.

4.5 Discussion

From the column experiments part one it became clear that the majority of iron after aeration is iron(II). This was unexpected as the treatment plant was designed for flock filtration. The total iron concentration in the clear water at Harderbroek is 0.04 mg/l on average. In the cascade effluent, which is filter influent the total iron concentration is 1.4 mg/l. The removal is probably a combination of flock filtration and adsorptive iron removal. For the moment one can only guess which process is dominant. When the dominant iron removal process is known, alternative treatments to improve the iron removal can be considered. To get more insight, it is recommended to measure iron(II) and iron(III) in the filter effluent. But in order to draw conclusions concerning adsorptive iron removal, long term experiments need to be performed. Sharma (2001) noticed an improvement of iron(II) removal by adsorption even after a few years. This improvement can probably be attributed to biological iron removal. This process sometimes needs a long term to get going.

The results obtained during part 2 of the column experiments indicate that increasing the pH improves the iron(II) removal. In Figure 33 the measured iron(II) concentrations are plotted against the pH, on a logarithmic scale. The figure shows a strong dependency of iron(II) concentration on pH. The straight line in a graph with logarithmic scales shows an exponential relation between iron(II) concentration and pH.

In this figure, the results from the different experiments show to group together, indicated with the three red ellipsis.

The measurements with varying pH can be calibrated with Lerk's theory.

$$\frac{dFe^{3+}}{dt} = k \cdot [OH^-]^2 \cdot P_{O_2} \cdot [Fe^{2+}]^n \quad [4.1]$$

Equation [4.1] can be converted into:

$$\frac{dFe^{3+}}{dt} = k \cdot [H^+]^{-2} \cdot [O_2] \cdot [Fe^{2+}]^n \quad [4.2]$$

De Vet mentioned for k 4.17e11 m²/s atm. This value corresponds with the k in equation [4.1] and is converted to a k corresponding with equation [4.2], calculated as 2.4e-14 m²/s. Stuyfzand (2007) mentioned k to be 3*10⁻¹²* 0.0464 e^{0.1535 T}. With a water temperature of 12 degrees Celsius, k is calculated as 8.7e-13. The measurements are calibrated with the theory. The results are shown in Figure 34. The oxygen concentration is chosen in such a way that it are not limiting. The oxygen concentration is 10 mg/l. The time in the calculation is

280 seconds, this is the total residence time in the cascade (10 s), dividing cutter (20 s), tubing to the columns (120 s), columns supernatant water (80 s) and column filter bed (50 s). The slope of the graph is determined by n. n is proposed by Lerk and Stuyzand as 2 (second order reaction). There is a deviation in slope noticeable between the measured values and the theory. The value of n determines the slope.

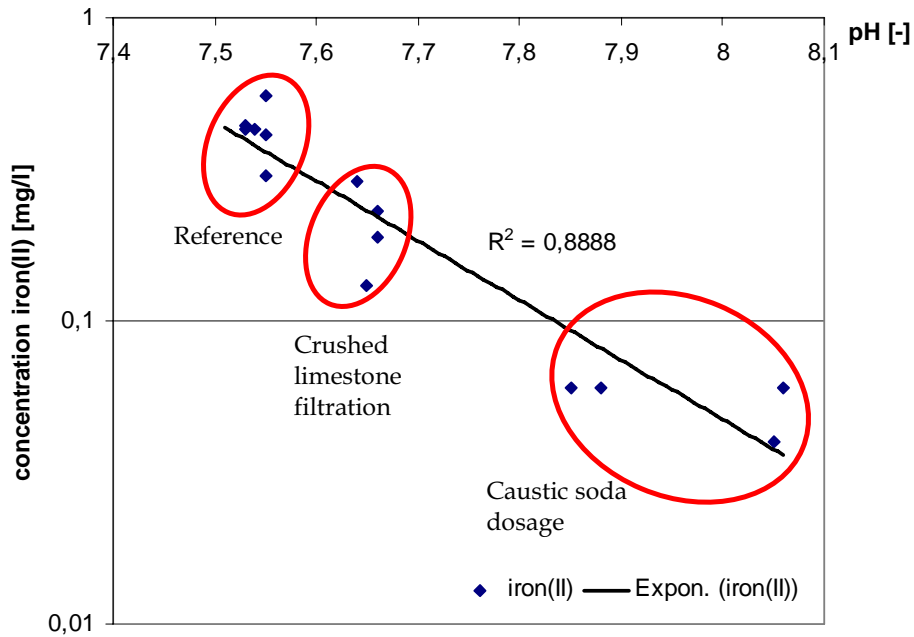


Figure 33: Relation iron(II) concentration and pH.

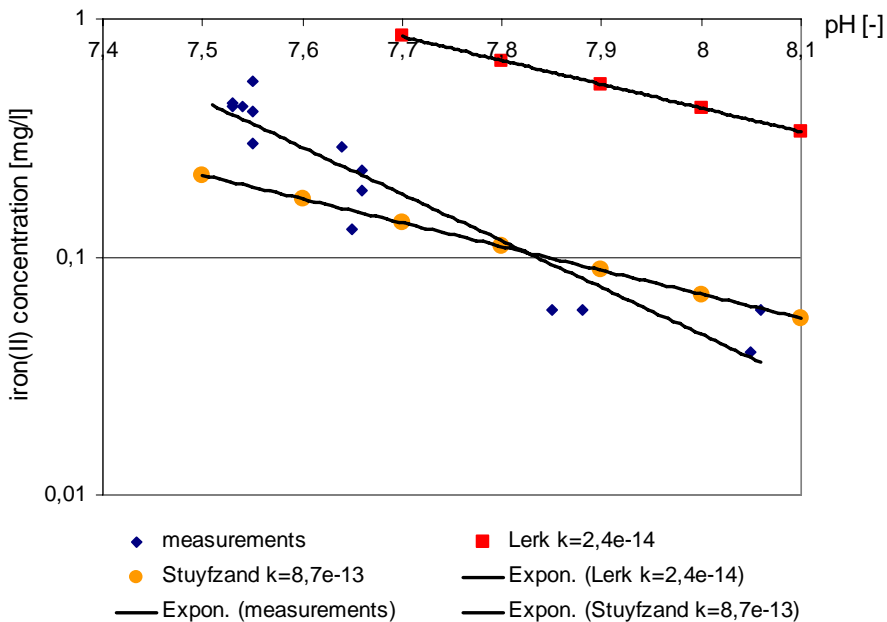


Figure 34: Iron(II) measurements at varying pH compared with theory.

Although the pH and the iron(II) removal increased some questions arose about the total removal of iron (Figure 32).

The caustic soda dosage clearly improved the iron(II) removal, but the total iron in the filter effluent is not changed by the dosage. While the ratio between iron(II) and iron(III) is considerably changed. After caustic soda dosage the majority of the iron in the filter effluent is iron(III), while in the reference the majority is iron(II).

The iron(III) concentration in the effluent is almost the same as the iron(III) concentration in the influent. One could conclude that iron(III) is not removed by the filtration step, but more realistic is that the iron(III) from the influent is removed and other iron(III) flocks are formed during filtration. The observation made during backwashing the columns, a dark brownish red colour leaving the filter, indicates proper flock filtration.

An explanation for the breakthrough of iron(III) might be found in a too high pH. Next to the oxidation also the flock formation depends on pH. Gregory (2006) describes the pH dependency of the hydrolysis reaction. He stated that a high pH can limit the collision of small pin flocks and therefore they are badly removed.

One hour after start-up the crushed limestone experiments show the same total iron concentration in the effluent as measured in the reference experiment. But the samples taken 4 hours after start-up show a decrease in the total iron concentration. Perhaps the filter material needs a longer ripening time than applied. The crushed limestone was fed with cascade effluent water for 16 hours before the experiment was started. A long duration experiment is necessary to evaluate the effect of ripening on the effluent iron concentrations.

The measured iron concentrations during part 2 were sometimes different than was expected:

- The total iron in the influent of columns 1+2 in which caustic soda is dosed: the measurement at t=4h gives a value of 0.67. This is probably not correct because the measured iron(II) concentration is higher, 0.81 mg/l and the total iron concentration in the influent (cascade effluent) is always about 1.40 mg/l during part 1 and part 2. ²

- Iron(II) influent 1+2 and 3+4, crushed limestone, t=1h is 0.21 mg/l and 0.81 mg/l respectively.

The iron(II) concentration in the column influent (cascade effluent) is always about 1.20 mg/l during part 1 and part 2. The crushed limestone filtration does not affect the column influent water, so no change in the ratio iron(II) iron(III) is expected.

- Iron(II) column 4, crushed limestone, t=1h and t=4h is 0.09 mg/l and 0.13 mg/l. This is unexpected as column 4 functioned as a reference. No change is applied compared to the experiments in part 1 and the other reference columns from part 2. This is the only column that showed a change in iron(II) concentration.

² 1.40 mg/l is also measured with the Applicon iron analysers, installed after this research.

4.6 Alternatives for Harderbroek

Based on the conclusion that the pH value should be raised, three alternatives to do this are discussed in the following paragraphs.

4.6.1 Tower aeration applied as a first treatment step

One of the alternatives to increase the pH is to move the tower aeration step and apply it on raw water. A more intensive aeration step will strip more carbon dioxide from the water, which results in a higher pH.

The surface area from the three installed aeration towers is 6.06 m². At the moment one tower can process a flow until 320 m³/h, which corresponds to a surface load of 53 m/h.

Both the tower aerator and the cascade step should remove the CO₂ present in the raw water. With a tower aerator, depending on the RQ and the packing material, an efficiency of 95% can be reached. The carbon dioxide concentration in the raw water is 4.5 mg/l or 0.102 mmol/l. After a CO₂ removal of 95%, the concentration CO₂ is decreased till 0.005 mmol/l. A decrease of the concentration CO₂ to almost zero will result in a pH of 8.3 (Figure 6, Paragraph 2.1.4).

The efficiency of a counter-current tower aerator can be described by:

$$K = \frac{1 - e^{(-k_2 \cdot t(1 - \frac{k_D}{RQ}))}}{1 - \frac{k_D}{RQ} \cdot e^{(-k_2 \cdot t(1 - \frac{k_D}{RQ}))}}$$

The calculation can be performed with use of the values for k₂. Van der Helm (1998) found for counter-current flow in packed aeration tower a k₂ value for methane: k₂ = 0.0424 s⁻¹

With use of the relation between D, k₂ (see Paragraph 2.2.1) the value for k₂ carbon dioxide can be calculated. A k₂ value of 0.044886 s⁻¹ is found when n is chosen to be 0.5.

The residence time in the packed tower at Harderbroek is 136 seconds. With an RQ of 18, the efficiency of the tower aeration step will be 99%:

$$K = \frac{1 - e^{(-0.0449 \cdot 136(1 - \frac{1.23}{18}))}}{1 - \frac{1.23}{18} \cdot e^{(-0.0449 \cdot 136(1 - \frac{1.23}{18}))}} = 0.996$$

The installed towers have enough capacity and a good efficiency. They can be used as first aeration step in the treatment. Only some adaptations in the hydraulic line of the treatment plant are necessary. The raw water pumps can probably pump up the water until the level of the aeration tower. But when the water flows down through the tower it needs to be pumped up unto the level of the first cascade step. This is an increase of 2m. From the cascade the water follows the current hydraulic line until the filter effluent. The filtrate

pumps that were used to transport the water towards the aeration tower can now be used to transport the water towards the clear water reservoir. The hydraulic line of pumping station Harderbroek is enclosed in Annex III.

4.6.2 *Caustic soda dosage*

For the implementation of caustic soda dosage basically only a pump and a stock vessel are necessary. The exact dosing per m³ water should be found with the pilot installation and optimised after installation in the full scale plant.

A drawback from this alternative is the phenomenon that goes often together with caustic soda dosage; the breakthrough of iron(III) hydroxide flocks. Due to the high pH after dosing the pin flocks formed by hydrolysis remain small. The flock formation phase hardly takes place. The small iron(III) hydroxide flocks are able to break through the filter. This phenomenon is probably already observed during the column experiments. In case Harderbroek is interested in caustic soda dosage more research into the flock formation and the filterability is necessary.

4.6.3 *Crushed limestone filtration*

Although the column experiments with crushed limestone did only show a small change in total iron removal, this technique is regarded as a promising alternative for Harderbroek. Van Dijk (1985) demonstrated that crushed limestone filtration is a process that merits renewed attention in neutralisation practice. He stated: "compared to other neutralisation processes, such as degasification and dosing of alkaline solutions, the process results in a better final water quality with respect to corrosion of distribution pipes. Furthermore, the process is robust, reliable and requires no process control. The chemical costs are relatively low. When applied in a plant that already has a filtering stage, the investment cost is also low." Furthermore he concluded that the process is well suited for the treatment of aggressive, highly ferrous groundwater, allowing a higher solids load than conventional sand filters at an improved removal of iron and CO₂.

An advantage of this technique is that there is no need for control. The process reaches its equilibrium by itself.

One drawback of crushed limestone filtration is the possibility that the particle load of the filter effluent water is increased. Small particles broken down from the filter media can be present in the filter effluent.

The hydraulic line scheme from pumping station Harderbroek, Annex III, shows a second filtration step, optionally in the future. The present filtration step can therefore be replaced by crushed limestone filtration. After the crushed limestone filtration step a second filtration step can be realised, were rapid sand filtration is applied.

The pH of the water is adjusted to approximately 8 by the crushed limestone filtration and tower aeration. The second filtration step will mainly have to deal with flock filtration. Besides, the surface load of this filter will be lower compared to the surface load of the present rapid sand filtration step. Already some particles and iron will be removed during the crushed limestone filtration. A smaller grain size can be applied on the second filter, resulting in

a better effluent quality with fewer particles. The second filtration step can function as a polishing filter. More research needs to be performed before conclusions can be drawn for the necessary contact time and the obtained effluent quality. It is recommended to perform pilot research on crushed limestone filtration.

5 Model

This chapter describes the model part of the thesis. In the method paragraph the applied differential equations are summarised and the model environment Stimela is introduced. The model structure is shown and the applied parameters are explained. In the paragraph model runs the model results for calibration are shown. This paragraph is followed by the discussion, in which the sensitivity of the parameters is investigated and simulations of alternative treatments are performed. The paragraph discussion finalises with a proposal for a measurement program which will lead to better calibration of the model.

5.1 Method

5.1.1 Summary applied differential equations

In chapter 2 the differential equations for the iron removal mechanisms and filtration were deduced. The following differential equations describe the different processes relevant for iron removal:

Flock formation

$$\frac{dFe^{3+}}{dt} = k \cdot [OH^-]^2 \cdot P_{O_2} \cdot [Fe^{2+}]^n$$

Particle removal

$$\frac{\partial \sigma}{\partial t} = -v \frac{\partial c}{\partial y}$$

$$-\frac{\partial c}{\partial y} = \lambda c$$

Adsorptive iron removal

$$q = K \cdot c_e^n$$

$$\frac{dc}{dt} = -v \frac{dc}{dx} - M(c - c_e)$$

5.1.2 Discretisation

In order to solve the differential equations of the model, the differential equations need to be discretised. The reactor is subdivided into n elements and per unit element i the different parameters are calculated per time step. For a rapid filter a discretisation in space looks like Figure 35:

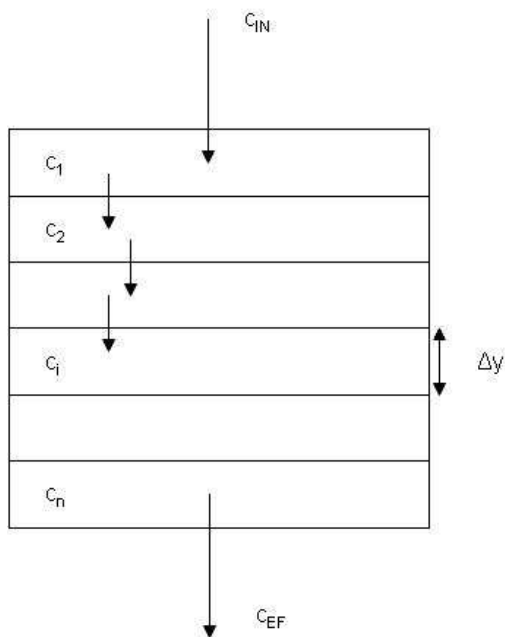


Figure 35: Discrete representation of a filter bed.

5.1.3 Stimela

The filtration process is described with mathematical equations in chapter 2. In the previous paragraph the differential equations are derived. By integrating the differential equations numerically the dynamic behaviour of the process can be followed.

The numerical integration is performed with the help of a numerical solver. For this thesis the model environment Stimela is used.

Description of Stimela

Stimela is an environment in which different drinking water treatment processes can be modelled. The Stimela models are developed in Matlab/Simulink™. Partial differential equations are numerically integrated with the consequence that variations in time and space can be followed. Because Matlab/Simulink™ is used, the models are easily accessible, the structure is open and flexible and all routines, toolboxes and visualisation techniques of Matlab/Simulink™ can be used (van der Helm and Rietveld, 2002).

A Stimela model consists of several blocks. It has an input block, one or more process blocks, control blocks and graphical output blocks.

In the input block the values for the raw water quality and the flow can be inserted. Within this thesis only one treatment step is used. The raw water quality parameters which generally form the input for a model are in this thesis the cascade effluent values. Cascade effluent water enters the filtration step.

The model can be run after inserting all parameters. For a run the integration method has to be chosen, as well as the step size and simulation time. The graphical output can be obtained by opening the output block. This output

block gives values for the effluent water quality parameters. Besides it gives information about the status of the filter, such as filter head loss.

File Set-up in Stimela

The model of a process in Stimela consists basically of 6 files (DHV, 1999). The initialisation file defines the number of input parameters, output parameters and the ordinary differential equations. The parameter file processes the parameters that are given in the process block, the heart of the model in the system file. The matlab code of the system file is included in Annex IV. In this file the ordinary differential equations (ODE's) are given in matrix notation after discretisation. Also the output parameters are defined in this file. The visualisation of the output from the numerical integration is accommodated in de graphical output file.

There are two remaining files, which determine the graphical interface for insertion of process parameters.

(Rietveld 2005)

5.1.4 Simplifications and assumptions

Simplifications can reduce the number of parameters. In the iron removal model the following can be assumed and simplified:

- In the supernatant water there is only the oxidation from iron(II) to iron(III) and flock formation, no removal.
- The oxidation is influenced by pH.
- The maximum adsorption capacity in the model is constant, while in practice the adsorption capacity reduces in time.
- The model used for adsorption of iron(II) is a film diffusion model (sharma).
- For removal of iron(III) flocks the lambda/sigma relation is linear, while in practice a convex shape is found (see Figure 12, paragraph 2.3.2) .
- The diameter of the filter grains is inserted as 1 mm. In reality there is a variation in diameter, between 0.8 and 1.25 mm.
- In the flock formation rate G value and residence time are not included.
- It is assumed that first oxidation takes place and afterwards hydrolysis and flock formation.

5.1.5 Model structure

The stimela model is built up out of two 'filters' (Figure 36). The first filter is actually a reservoir, representing the water phase. So the residence time in the cascade and the supernatant water are modelled in this reservoir. The grain size for this artificial filter is chosen very large and the porosity 100%.

The effluent of this filter can be used to calibrate the oxidation rate coefficient between iron(II) and iron(III). The iron(III) concentration in the cascade influent (raw water) is assumed to be zero, and all total iron (1.4 mg/l) is iron(II). After a residence time of 20 seconds in the cascade, the iron(II) concentration is 1.25 mg/l and the iron(III) concentration is 0.12 mg/l, as measured during the experiments as cascade effluent. This can give an estimation for the oxidation rate coefficient.

The second filter is the real filter bed. Therefore in this filter the supernatant water level is chosen zero, because the supernatant water is modelled in the first reservoir.

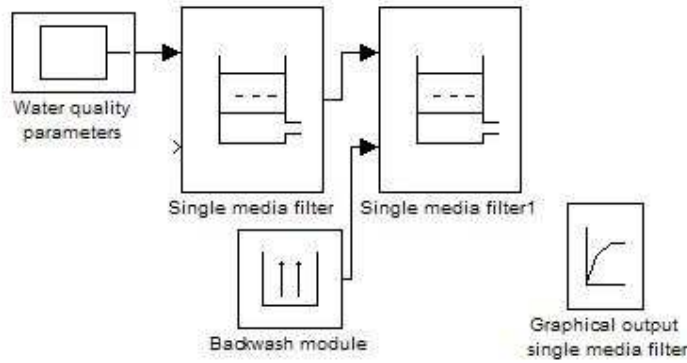


Figure 36: Build up of iron removal model in Stimela

5.1.6 Parameters

The parameters that need to be inserted in the model are split up in three groups of parameters;

- Water quality parameters
- Design parameters
- Calibration parameters

Water quality parameters

For an iron removal model of course the iron(II) and iron(III) influent values are required. The iron(II) removal depend on pH and P_{O_2} . The P_{O_2} is obtained from the oxygen concentration. With the conductivity (EGV) the ionic strength is calculated, resulting, together with the temperature, in a value for K1. From K1 and the bicarbonate concentration and pH the influent CO_2 concentration is calculated.

The changes in concentration of oxygen, bicarbonate and carbon dioxide are modelled with the basic differential equation. In addition these concentrations change by the oxidation reaction:

$$\frac{\partial c_i}{\partial t} + u \frac{\partial c_i}{\partial x} = 0$$

Where c_i can be concentration oxygen, concentration bicarbonate or concentration carbon dioxide.

$$\frac{dFe^{3+}}{dt} = k \cdot [OH^-]^2 \cdot P_{O_2} \cdot [Fe^{2+}]^n \quad [6.1]$$

Table 13 summarises the water quality parameters and their default values, obtained from the column experiments.

Table 13: Default values water quality parameters.

Water quality Parameter	Measured at Harderbroek	Unit
Flow	0.066	m ³ /h
Temperature	12.4	°C
Concentration iron(II)	1.25	mg/l
Concentration iron(III)	0.12	mg/l
Concentration O ₂	7.5	mg/l
Conductivity	15.7	mS/cm
pH	7.5	-
Concentration HCO ₃ ⁻	80	mg/l

Design parameters

Design parameters are determined by the installation. They are hard to change in practice. The parameters have a major influence on the actual state of the filter, such as pressure over the filter bed. The Lindquist diagram is used in the model to evaluate the state of the filter, although during the column experiments the state of the filter was barely recorded.

Tabel 14 summarises the design parameters used in the model and gives their default values for the column experiment installation.

For discretisation purposes 6 unit elements are chosen. The mass density of the grains is 2600 kg/m³ and 1 m³ of the filter exists for 60% of grains, resulting in a density of 1600 kg/m³.

Table 14: Default values design parameters.

Design Parameters	For used installation	Unit
Filter surface area	0.00636	m ²
Water level above filter	0	m
Filter bed height	0.30	m
Grain size	1.0	mm
Filter porosity	40	%
Maximum pore filling	75	%
Mass density flocks	3	kg/m ³
Mass density grains	1600	kg/m ³
Number of unit elements	6	-

Calibration parameters

Some parameters are not determined directly by the installation and are hard to measure in practice. By trial and error the values for the calibration parameters can be found, by which the modelled effluent simulates as good as possible the measured effluent. The less parameters are needed to be calibrated, the easier the process is and the higher the reliability of the obtained values.

When the solution for an optimisation problem needs to be found a starting vector close to the solution will give better results (Clemens 2001). Therefore appropriate starting values are searched in literature, see Table 9.

Some parameters need some extra explanation:

λ is calibrated in the model process. The relation between λ and λ_0 is proposed by researchers. In this model the relation proposed by Lerk (1965) is used. Lerk gives also an estimation for λ_0 .

$$\lambda_0 = \frac{k_1}{\eta v d^3}$$

In which

k_1	=	constant, $9 \cdot 10^{-18}$
d	=	grain diameter
v	=	filtration velocity
η	=	kinematic viscosity, $497 \cdot 10^{-6} / (T+42.5)^{1.5}$

For the situation at Harderbroek, with a filtration velocity of 10.4 m/h and a grain diameter of 0.001m, a filtration coefficient of 2.47 m^{-1} at $t=0$ is found.

For the oxidation rate coefficient a value for k was given by de Vet (2007), according to equation [6.1].

[6.1] is inserted in the model as:

$$\frac{dFe^{3+}}{dt} = k \cdot [H^+]^{-2} \cdot [O_2] \cdot [Fe^{2+}]^n \quad [6.2]$$

De Vet mentioned for k $4.17 \cdot 10^{11} \text{ m}^2/\text{s} \cdot \text{atm}$. This value corresponds with the k in equation [6.1] and is converted to a k corresponding with equation [6.2], calculated as $2.4 \cdot 10^{-14} \text{ m}^2/\text{s}$.

This parameter is calibrated with the first reservoir in the model, see Paragraph 5.2.1. A model run is performed with the values for the pumping station in practice, which means $Q = 220 \text{ m}^3/\text{h}$, iron(II) = 1.40 mg/l in the influent, iron(III) = 0 mg/l (the raw water) and the pH = 7.5. The effluent value for iron(III) should become 0.12 mg/l.

Adsorption is modelled as a combination of film diffusion and adsorption (Paragraph 2.4.2).

The value for Freundlich constant K was found by Sharma (2001) as $3.3 \cdot 10^{-4} \text{ g/m}^2 / (\text{g/m}^3)^n$ for a volume based calculation (g/m^3). Here a mass based calculation (g/kg) is applied, so the value is corrected with the density of the filter grains. The value used in the model is $3.4 \cdot 10^{-4} \cdot 1600^3 = 0.544$.

³ The density of the filter grind is 2600 kg/m^3 . But 1 m^3 of filter bed exists for 40% out of pores and for 60% out of filter material. The density for 1 m^3 filter material is 1600 kg/m^3 .

From the film diffusion theory in Paragraph 2.4.2 the parameters can be calculated for the Hardebroek situation. The diffusion coefficient D_x for iron(II) is $0.72e-9$ m²/s (CRC Handbook, 1996). The values for film diffusion are summarised in Table 15.

Table 15: Calculated values for diffusion theory.

Parameter	Value
Reynolds number	3.086
Schmidt number	1389
Sherwood number	30.40
Film diffusion coefficient	$2.19e-5$ m/s or $7.9e-2$ m/h.
Kinetic constant adsorption or transfer rate	0.0788 s ⁻¹ or 283.8 h ⁻¹

Table 16: Default values calibration parameters.

Calibration parameters	Value from literature	Reference
Clean bed filtration coeff	2.47	Lerk
Oxidation rate coeff	$2.4e-14$	De Vet
Freundlich constant n	0.43	Sharma
Freundlich constant K	0.544	Sharma
Kinetic adsorption constant	283.8 h ⁻¹	Sharma, van der Meer, van Schagen

The values for the calibration parameters found in literature will be used as a starting value in the calibration process. The simulation from the model is judged mainly on iron(II) and iron(III) effluent concentrations.

5.1.7 Modelling approach

In this stage of the research it is not possible to quantify the contribution of the different iron removal mechanisms to the total iron removal. The modelling part is therefore split up in three parts:

- Modelling the transformation from iron(II) in iron(III) and calibrating the oxidation rate coefficient (5.2.1);
- Modelling only the flock filtration iron removal and calibrating the clean bed filtration coefficient (5.2.2);
- Modelling the rapid sand filters from Hardebroek (5.2.3);
- Modelling adsorptive iron removal from theory (5.2.4).

The first two parts are based on the data obtained during the column experiments. The fourth part is based on measurements in the plant itself. By the lack of experimental data an adsorptive iron removal, model runs according to adsorptive iron removal are not incorporated in this research. The model runs performed make only use of flock filtration iron removal. In the developed model adsorptive iron removal is included. In the discussion a paragraph is included which proposes a measurement program in order to

calibrate the model in more detail and especially on adsorptive iron removal (Paragraph 5.3.4). The modelling part according to adsorptive iron removal performed in this study is only based on theory.

5.2 Model runs

5.2.1 Results for oxidation rate coefficient

The residence time in the cascade is approximately 10 seconds. The residence time in the dividing cutter is calculated as 20 seconds. The residence time in the reservoir was 30 seconds in order to simulate the situation. The raw water quality (Table 1) is used for the input parameters. The iron(II) in the influent is 1.4 mg/l and the iron(III) 0 mg/l. After the cascade the iron(III) concentration should be 0.12 mg/l and the iron(II) concentration 1.28 mg/l. The oxidation rate coefficient is varied until a proper simulation is obtained. The starting value for the oxidation rate coefficient was 2.4×10^{-14} . The results are potted in Figure 37 and summarised in Table 17. In Figure 37 the iron(II) and iron(III) concentrations are plotted over the filter bed height at $t = 20$ h. The measured iron(II) and iron(III) in the cascade effluent are plotted respectively as a square and a diamond. Finally a value for the oxidation rate coefficient was found as 3.85×10^{-14} .

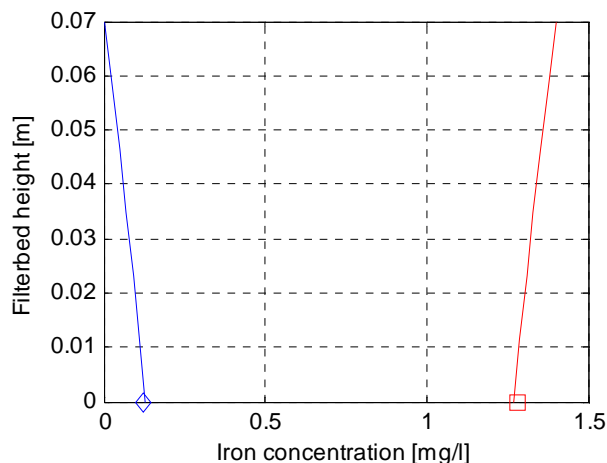


Figure 37: The modelled oxidation of iron(II) (red line, right) to iron(III) (blue line, left) in the reservoir over the height at $t = 20$ hours.

Table 17: Results for model run in order to calibrate the oxidation rate coefficient.

parameter	unit	Value
Iron(II) effluent	mg/l	1.28
Iron(III) effluent	mg/l	0.12
Residence time	sec	30
Oxidation rate coefficient	-	3.85×10^{-14}

5.2.2 Results for flock filtration iron removal

The water quality parameters are the data obtained during measurements in the cascade effluent. The iron(II) influent concentration is 1.28 mg/l and the iron(III) influent concentration 0.12 mg/l.

The reservoir represents the residence time in the tubing from the cascade to the columns. This residence time is two minutes. With a surface of 0.00636m² and a flow of 60 l/h the reservoir height should be 0.31 m.

After the columns the iron(II) concentration is 0.40 mg/l, the iron(III) concentration is 0.20 mg/l. The filtration coefficient is mainly determining the iron(III) concentration. Therefore the iron(III) effluent concentration is regarded more important compared to the iron(II) effluent concentration. A clean bed filtration coefficient of 4.3 m⁻¹ is found. The iron(III) concentration is plotted over the filter bed height at t = 4 hours in Figure 38. In addition the measured iron(III) concentration is plotted. Table 18 summarises the results for the calibration run.

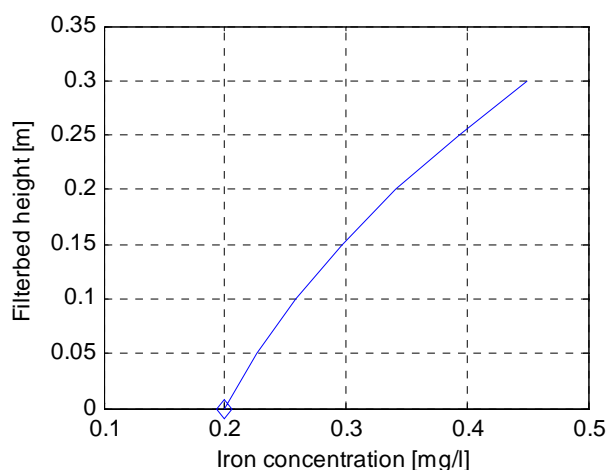


Figure 38: The modelled iron(III) concentration over the column height, including the measured iron(III) concentration in the column effluent.

Table 18: Results for model run in order to calibrate the clean bed filtration coefficient, pH = 7.5

parameter	unit	Measured value	Modelled value
Iron(III) effluent, t = 4h	mg/l	0.20	0.20
Clean bed filtration coefficient	m ⁻¹		4.3

Figure 39 and Table 19 show a model run with column experiments data and settings, the only adjusted parameter in this case was the bed height. The bed height in this run was 2 m. The pH is again 7.5 and the clean bed filtration coefficient 4.3. On this graph the plotted iron(III) concentration after 0.30 m of filter bed does not cross the measured iron(III) concentration after 0.30 m of filter bed. This is due to the iteration process of the model. From the column

experiments an iron(III) concentration of 0.033 mg/l can be expected. This is only the flock filtration iron removal.

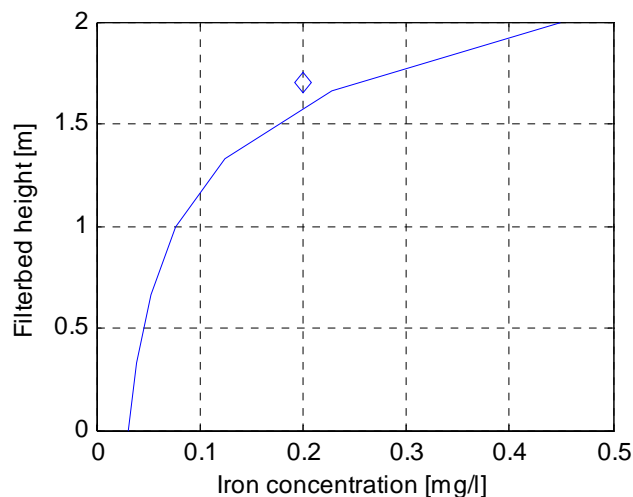


Figure 39: The modelled iron(III) concentration for a column height of 2 m, including the measured iron(III) concentration in the column effluent (after a bed of 0.30 m).

Table 19: Results for model run in order to simulate a filter bed height of 2 m.

parameter	unit	Modelled value
Iron(III) effluent, t = 4h	mg/l	0.033
Clean bed filtration coefficient	m ⁻¹	4.3

At Harderbroek some filters have a bed height of 2.0 m and some filters a bed height of 2.2 m. In order to see the influence of this variation in bed height on the iron(III) removal, a run with a bed height of 2.2 m is performed. The rest of the settings are still column settings.

Table 20: Results for model run in order to simulate a filter bed height of 2.2 m.

parameter	unit	Modelled value
Iron(III) effluent, t = 4h	mg/l	0.030
Clean bed filtration coefficient	m ⁻¹	4.3

5.2.3 Results for Harderbroek filters

The run is performed with only flock filtration iron removal, a pH of 7.5, an oxidation rate coefficient of 3.85e-14 and a clean bed filtration coefficient of 4.3. The residence time in the reservoir depend on the filter bed height. Filters 1 and 3 at Harderbroek have a filter bed height of 2.00 m and a supernatant water level of 0.20 m. The residence time in the reservoir is 110 seconds, representing the cascade (10 s), the dividing cutter (20 s) and the supernatant filter water (80 s). With a surface of 24 m² and a flow of 220 m³/h, the

reservoir height is 0.28 m. The results for this model run are plotted in Figure 40 and summarised in Table 21.

The residence time in the supernatant water for filters with a bed height of 2.20 m and a supernatant water level of 0.05 m is 20 s. The residence time in the reservoir for these filters is 50 seconds. With a surface of 24 m² and a flow of 220 m³/h, the reservoir height is 0.13 m. The results for this model run is plotted in Figure 41 and summarised in Table 22. From those two runs it can be concluded that the difference in residence time results in a difference in the iron(III) influent concentration. In Figure 40 the iron(III) influent concentration is 0.35 mg/l, while this concentration is 0.22 mg/l in Figure 41. The higher iron(III) influent concentration results in a slightly lower iron(III) effluent concentration, caused by a better filtration coefficient through the more deposits in the filter bed, although the iron(III) effluent concentrations are comparable (Table 21 and 22).

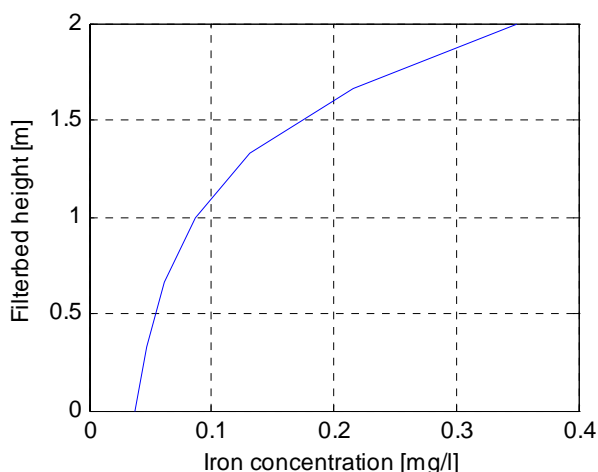


Figure 40: Modelled iron(III) concentration over the filter bed height for the Harderbroek filters with a bed height of 2.00 m, at t = 20 hours.

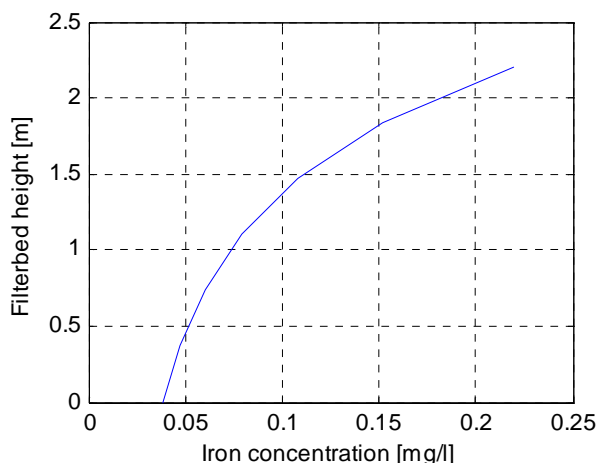


Figure 40: Modelled iron(III) concentration over the filter bed height for the Harderbroek filters with a bed height of 2.20 m, at t = 20 hours.

Table 21: Results for model run in order to simulate the Harderbroek filters with a filter bed height of 2m.

parameter	unit	Modelled value
Iron(III) effluent at t = 20 h	mg/l	0.037
Filter bed height	m	2.00
Residence time reservoir	s	110
Clean bed filtration coefficient	m ⁻¹	4.3

Table 22: Results for model run in order to simulate the Harderbroek filters with a filter bed height of 2.2 m.

parameter	unit	Modelled value
Iron(III) effluent at t = 20 h	mg/l	0.039
Filter bed height	m	2.20
Residence time reservoir	s	50
Clean bed filtration coefficient	m ⁻¹	4.3

Between those two runs a difference in iron(III) effluent concentration occurs. The question still remains what is causing this difference in the iron(III) effluent concentration. The difference in residence time or in filter bed height, or both? Therefore two extra model runs are performed. One with a residence time 110 s and a filter bed height of 2.20 m and one with a residence time of 46 s and a filter bed height of 2.00 m. In this way two situations can better be compared, although these combinations are not the real situations at Harderbroek.

Table 23: Results model run with exchanged filter bed height and residence time I.

parameter	unit	Modelled value
Iron(III) effluent t = 24h	mg/l	0.034
Filter bed height	m	2.20
Residence time reservoir	s	110
Clean bed filtration coefficient	m ⁻¹	4.3

Table 24: Results model run with exchanged filter bed height and residence time II.

parameter	unit	Modelled value
Iron(III) effluent	mg/l	0.042
Filter bed height	m	2.00
Residence time reservoir	s	50
Clean bed filtration coefficient	m ⁻¹	4.3

There are two couples of tables who have the same filter bed height and different residence time. In addition there also are two couples of tables with the same residence time, but different filter bed height. The difference in

iron(III) effluent concentration between a couple can give a clue about the influence of the varying parameter. This information is summarised in Table 25.

Table 25: Influence of filter bed height and residence time on iron(III) effluent concentration

Fixed parameter	Varying parameter	Table couple	Change in iron(III) concentration [mg/l]
Bed height	Residence time	24 and 21	-0.05
Bed height	Residence time	22 and 23	-0.05
Residence time	Bed height	21 and 23	-0.03
Residence time	Bed height	24 and 22	-0.03

From Table 25 it can be concluded that both, residence time and filter bed height, have an influence on the iron(III) removal. An increase in residence time from 50 s to 110 s seems to have a higher influence than an increase in filter bed height from 2.0 m to 2.20 m.

It is expected that in practice the difference by variation in filter bed height is less. The removal of iron(III) hydroxide flocks will mainly occur in the most upper layer of the filter bed. For the situation at Harderbroek the combination of a filter bed height of 2.00 m and a residence time of 110 seconds is regarded better than a filter bed height of 2.2 m. It must be noticed this is investigated for flock filtration iron removal only.

5.2.4 Results for adsorptive iron removal

Adsorption is modelled according to the film diffusion theory. First the iron(II) diffuses to a layer. From this layer the iron(II) can adsorb on the filter grain. This adsorption is modelled with the Freundlich isotherm (see Paragraph 2.1.6 and 2.4). The constants K and n for this isotherm are two of the calibration parameters. By the lack of information and data about adsorptive iron removal, these parameters were not included in the modelling part. But adsorptive iron removal is already included in the model itself. Paragraph 5.3.4 will suggest a measurement program in order to be able to calibrate the parameters for adsorption. In this stage the only application possible is to check the physical meaning of the two parameters. Isotherm constant K is the measure of adsorption capacity and constant n is the measure of adsorption intensity. With the purpose to check this physical meaning of the constants, model runs are performed, with the settings for the column experiments. In the runs only adsorptive iron removal is included, no oxidation and flock removal.

The first run is performed with the literature values for K and n (0.544 and 0.43). In the second and third run the value for K is varied and chosen as 1 and 0.1. In the fourth and fifth run the value of n is chosen as 1 and 0.1.

The shape of the breakthrough curves for the different runs are included in Annex V. From these breakthrough curves it can be concluded. That parameter K determines the distance between the different breakthrough curves. A larger distance between two curves indicates that more iron(II) is

adsorbed in one filter bed layer. The capacity of this layer is higher. Parameter n determined the shape of the breakthrough curve. A larger n will result in a flat S-curve, a smaller n in a steep S-curve. A steep S-curve indicates that the iron(II) breaks through the complete filter bed layer more fast and uniform, indicating a less intensive adsorption. The results for both constants comply with what is expected from theory.

5.3 Discussion

5.3.1 Reliability model results

The column experiments as carried out were not set up in order to calibrate a model. Too few parameters were varied in order to have sufficient data to calibrate all the parameters. The dataset obtained with the experiments is not complete enough to calibrate the model.

In this study the model is mainly used to become acquainted with the processes occurring in a filter bed, concerning iron removal.

5.3.2 Sensitivity of parameters

The sensitivity of the model for a specific parameter is interesting. Therefore a sensitivity analyses is performed. Again the model runs are split up and performed separately for different processes. At first the sensitivity is investigated for the oxidation rate coefficient, afterward for flock filtration. The sensitivity analysis for adsorption is not included. At first the calibration for adsorption was not successfully. A second reason is that it is disputable to vary K and n independently. Both constant are related to each other, ($q=KC^n$), and so together they are determining the total load q .

Oxidation rate coefficient

In Paragraph 5.2.1 the oxidation rate coefficient was calibrated. The found value was $3.85e-14$. To investigate the sensitivity, the oxidation rate is doubled and halved. In addition a run is performed with the k values proposed by Lerk and Stuyfzand. The model settings are the same as during the calibration process. Table 26 summarises the results.

Table 26: Results for sensitivity analyses for the oxidation rate coefficient.

Oxidation rate coefficient	Iron(II) [mg/l]	Iron(III) [mg/l]	Δ iron(II) [%]	Δ iron(III) [%]
$3.85e-14$ (calibrated)	1.28	0.12	100	100
$7.70e-14$ (doubled)	1.18	0.22	92	183
$1.42e-14$ (halved)	1.35	0.05	105	42
$2.40e-14$ (Lerk)	1.32	0.08	103	67
$8.70e-13$ (Stuyfzand)	0.57	0.83	45	692

Especially the iron(III) concentration is sensitive for a change in the oxidation rate coefficient. Although the absolute deviation in iron concentration is the same for iron(II) and iron(III), the relative deviation is larger for iron(III). The oxidation rate coefficient proposed by Lerk complies more with the modelled values as compared to the oxidation rate coefficient proposed by Stuyfzand. This is remarkable, because when the iron(II) concentrations in the

column effluent was compared with Lerks and Stuyfzands theory (Paragraph 4.5, Figure 34), Stuyfzand resulted in a better fit. The model calibration is performed with column influent measurements, the plot in Figure 34 are column effluent measurements.

Flock filtration

The calibrated value for the clean bed filtration coefficient is 4.3 m^{-1} . This value is doubled and halved in two more model runs. There is also a run performed with the clean bed filtration coefficient as proposed by Lerk. The settings used during these runs are the same as during the calibration process of the filtration coefficient, Paragraph 5.2.2.

Table 27: Results for sensitivity analyses for the filtration coefficient.

filtration coefficient	Iron(III) [mg/l]	Δ iron(III) [%]
4.3 (calibrated)	0.20	100
8.6 (doubled)	0.09	45
2.15 (halved)	0.32	160
2.47 (Lerk)	0.30	150

The model is sensitive for a change in the filtration coefficient. More experiments to determine the filtration coefficient are necessary for accurate results on the iron(III) effluent concentration.

5.3.3 Simulation of alternatives

Now the iron removal model is more or less calibrated the calibration parameters can be used to model the treatment plant itself. Alternatives for Harderbroek can be modelled and their influence on the iron removal can be investigated. The alternatives caustic soda dosage and crushed limestone filtration need more research and are not yet modelled. Both will change the formed iron(III) flocks and therefore the filtration coefficient. But the influence of a raise in pH can be seen from the model run.

After run with a change in pH and/or oxygen concentration a run is performed which simulates the application of the tower aeration as first treatment step.

Model runs with change in pH

The settings in the model are those for the treatment plant Harderbroek, as also used in Paragraph 5.2.3. The filter bed height is chosen as 2.0 m, with a residence time in the reservoir (water phase) of 110 seconds. Figure 42 shows the present iron(III) concentration over the reservoir height. Figure 43 shows the iron(III) concentration after a change in pH to 8.0 and a change in oxygen concentration to 8 mg/l. Table 21 shows the iron(III) concentration of the filter influent water and filter effluent water, for different pH and oxygen concentrations.

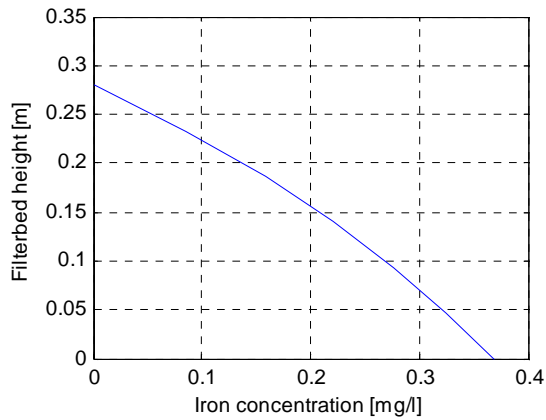


Figure 42: The modelled iron(III) concentration in the reservoir over the height at $t = 20$ hours, with a pH of 7.5 and an O_2 concentration of 7.5 mg/l.

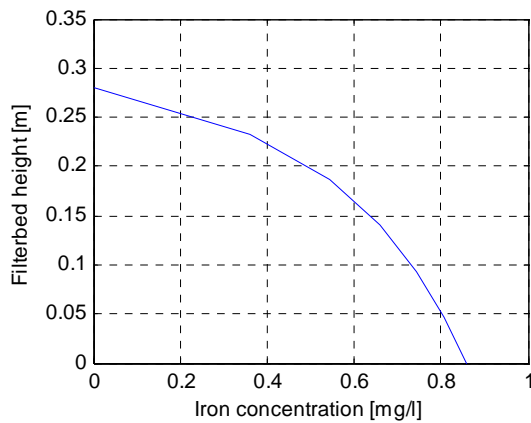


Figure 43: The modelled iron(III) concentration in the reservoir over the height at $t = 20$ hours, with a pH of 8.0 and an O_2 concentration of 8.0 mg/l.

Table 21: Results for model run in order to investigate the influence of the tower aeration as first treatment step.

pH	Oxygen concentration mg/l	Iron(III) concentration filter influent mg/l, at $t = 20$ h	Iron(III) concentration filter effluent mg/l, at $t = 20$ h
7.5	7.5	0.37	0.037
7.8	7.5	0.67	0.034
8.0	7.5	0.82	0.029
8.2	7.5	0.92	0.025
8.0	8	0.83	0.029
8.0	9	0.86	0.028
8.0	10	0.88	0.027

The increase in pH from 7.5 to 8.2 has a major effect on the iron(III) concentration in the filter influent. The oxidation of iron(II) in the water phase, simulated with the reservoir, gets more efficient with a higher pH. In

addition the iron(III) concentration in the filter effluent decreases by an increasing iron(III) concentration in the filter influent. This is due to the effect that the filtration coefficient increases by a higher deposits concentration in the filter bed.

The tower aeration will also increase the oxygen concentration of the water. This seems to have some influence.

Model run with aeration tower

For this run the settings are changed to be more representative for the aeration tower. For the origin of these settings see Paragraph 1.1 and 4.6.1. The applied flow is 320 m³/h. The dimensions for the reservoir are a surface of 6.06 m² and a height of 2 m, resulting in a residence time of 136 seconds. The pH attained with the aeration tower is expected to be 8.2, with an oxygen concentration of 9 mg/l.

Figure 44 shows the iron(III) concentration in the reservoir, which now simulated the aeration tower. Over the height of the tower the iron(III) concentration increases from 0 to almost 1 mg/l. Figure 45 shows the iron(III) concentration over the filter bed height, at t = 20 h. The influent concentration in the filter is the effluent concentration of the aeration tower, 1 mg/l. Over the filter bed height the iron(III) concentration decreases until 0.029 mg/l. The modelled tower aeration step obtains a higher oxidation efficiency and a good iron(III) removal by only flock filtration.

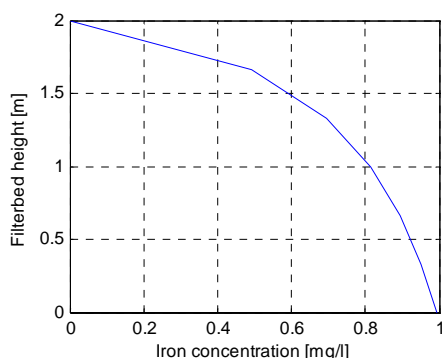


Figure 44: Modelled iron(III) concentration over the height in the aeration tower.

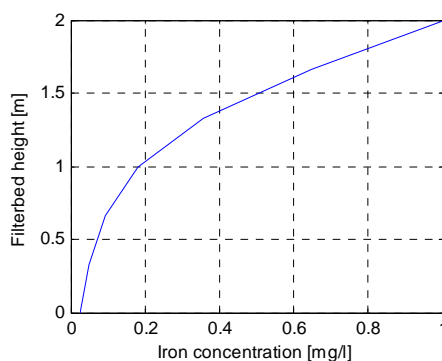


Figure 45: Modelled iron(III) concentration after tower aeration over the height in the filter bed.

5.3.4 Proposal measurement program

For this research the column experiments did not ally with the model. In order to be better able to calibrate the model, extended measurements are necessary. This paragraph proposes a measurement set-up for further calibration of the model. Distinction is made between measurements to determine the oxidation rate coefficient, the filtration coefficient for flock filtration iron removal and for adsorptive iron removal.

Oxidation rate coefficient

The oxidation efficiency depends on the pH, oxygen concentration, residence time and iron concentration, according to the equation:

$$\frac{dFe^{3+}}{dt} = k \cdot [H^+]^{-2} \cdot [O_2] \cdot [Fe^{2+}]^n$$

With a jar test apparatus those parameters can be varied and the concentration of iron(II) and iron(III) can be measured at the beginning of the experiments and on the end.

pH and residence time can easily be varied within the jar test apparatus. The oxygen concentration can be varied with a bubble aeration set-up. For this purpose an aquarium pump can be used, pumping small air bubbles in the jars. When all parameters are know, k can be calculated for different settings.

Flock filtration iron removal

The flock filtration iron removal mainly depends on the filtration coefficient. The filtration coefficient (λ) varies over the filter run time, depending on the amount of deposits in the pores (σ) of the filter bed. The relation between λ and σ should be found experimentally. Generally this λ - σ -relation has a shape according to Figure 46a. The concentration suspended solids in the filter effluent generally shows the opposite shape, Figure 46b.

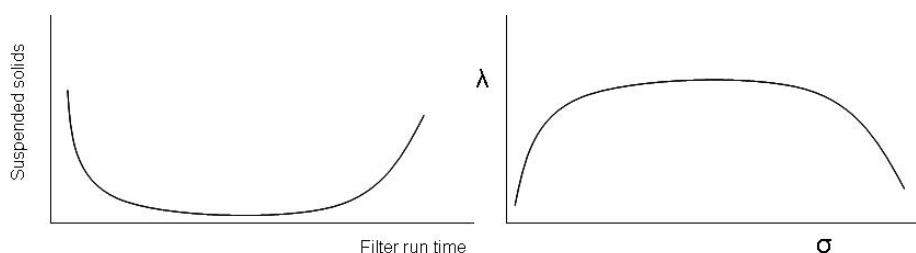


Figure 46: a) Filter effluent suspended solids concentration over the filter run time and b) the general λ - σ -relation.

Bai (1995) described two phases in this λ - σ -relation. In the first phase the filtration coefficient increases due to the increasing amount of pore deposits.

In the second phase the filtration coefficient is decreasing due to the still increasing amount of pore deposits. This two-phase linear approach can be build up out of measurements on the course of concentration, see Figure 47. The filter bed is split up in several layers. At the border between two layers the suspended solids concentration needs to be measured and λ can be calculated. By the removal of suspended solids the amount of pore deposits changes too. When besides the change in concentration also the filtration velocity in known, the change in pore deposits can be calculated.

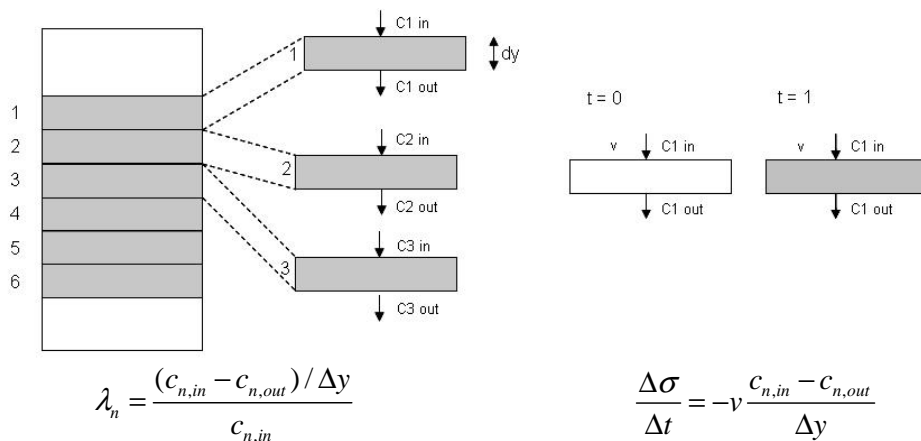


Figure 47: Determination of λ and σ by concentration measurements over the filter bed.

To determine λ and σ by measurements on concentration accurate measurements on water quality are required over the filter bed height. These measurements need to be performed several times over the filter run time, because the λ - σ -relation changes over the course of time, according to Figure 46. The measured λ and σ can be plotted in a several graph for each time step. The graph shows the two-phase linear λ - σ -relation, see Figure 48.

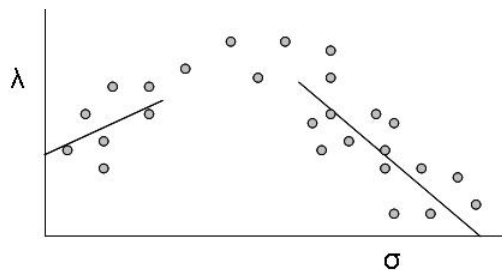


Figure 48: λ - σ -relation obtained from concentration measurements.

After determining the λ - σ -relation, optimisation of the filtration coefficient is of interest. Therefore different flocks need to be created and filtrated. For every flock a filtration coefficient can be determined according to the method

described above. The flock formation depends mainly on pH, G-value and residence time. With a jar test apparatus different flocks can be created on a laboratory scale. With the jar test apparatus all three mentioned parameters, pH, G-value and residence time can easily be varied. Afterwards the water with the flocks is filtrated over small columns and the influent and effluent suspended solids concentration can be measured. With this information the filtration coefficient accompanying the jar test setting can be determined.

Adsorptive iron removal

Sharma (2001) performed batch experiments on iron(II) adsorption. This set-up can also be used to determine the adsorption for Harderbroek. Sharma made use of a model groundwater, prepared by mixing iron(II) sulphate ($\text{FeSO}_4 \cdot 7\text{H}_2\text{O}$) stock solution (400 mg/l, pH < 2) with deoxygenated demineralised water. To determine the adsorption at Harderbroek, raw water can be used.

The set-up (Figure 49) should consist of a sealed vessel (with a volume of a few litres). The vessel should contain ports to allow solution feeding and sampling, oxygen, temperature and pH measurement, gas supply and mechanical stirring.

The vessel should be filled with a know amount of filter grind mass from Harderbroek and raw water. Nitrogen gas can be used to strip out the oxygen. During the experiment bubbling of nitrogen gas can be continued to control the oxygen concentration and pH. In addition the gas will provide a positive pressure against the inflow of air. The anoxic condition will keep all iron in iron(II) form. All 'loss' of iron concentration is due to adsorption. In addition, the adsorbed iron(II) can not oxidise and the adsorption sites will not be regenerated. All adsorption is due to adsorption on the filter grind itself and not due to adsorption on iron hydroxide.

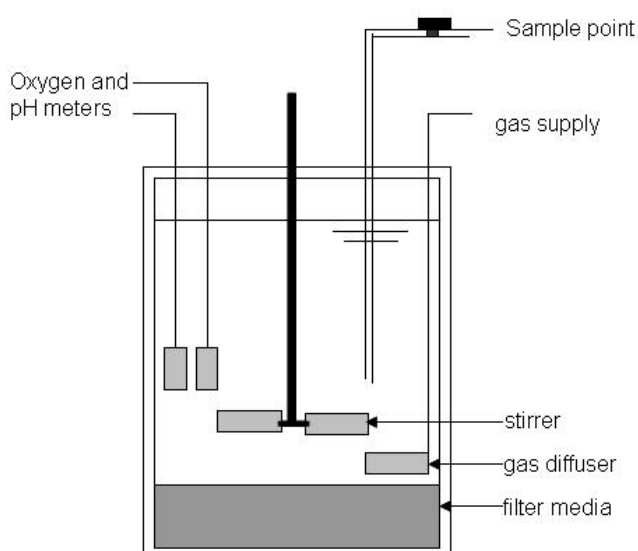


Figure 49: Experimental set-up for batch experiments on adsorption.

During the experiment the solution should be mixed with the mechanical stirrer. It is important to apply such a stirring velocity, that the filter material will remain settled on the bottom of the vessel, in order to avoid scouring of the surface coating.

After a few hours equilibrium with respect to iron(II) adsorption is reached (Sharma found an equilibrium time of 4 hours when 100 gram of coated sand was used and an equilibrium time of 6 hours by 50 gram of coated sand). The iron(II) concentration of the water can now be determined. The amount of iron(II) adsorbed onto the filter media can be calculated from the iron mass balance with the iron(II) concentration at $t = 0$. A blank experiment should be performed to determine the loss of iron(II), for example due to adsorption on the equipment.

The amount of iron(II) adsorbed per unit surface area of filter grain can be plotted against different equilibrium concentrations on a log-log graph. The Freundlich isotherm constants K and n can be calculated by linear regression. The Freundlich constant K can be determined from the intersection of the graph with the y-axis. The slope of the line is equal to the Freundlich constant n .

This procedure can be carried out by different pH values.

6 Conclusions and recommendations

In this chapter the conclusions from the three applied methods, the fingerprint, the column experiments and the model are summarised. Finally recommendations are given towards the operation of the treatment at Harderbroek and how to continue research.

6.1 Conclusions

To conclude on particle loads present after treatment, a volume graph gives additional information to the measured numbers of particles. A volume graph gives a clear view on the duration of a disturbance, caused by an operational event. Besides, finally in the distribution system, mass of iron is of most importance.

To evaluate the influence of a peak caused by operational events, the volume load during the peak is compared with the volume load during stable operation. The particle volume during the peak after a filter switch, which lasts for 30 min, was 2.4 ml. During this peak the average particle volume concentration was 19.4 ppb. During stable operation, lasting for 24 h, the average particle volume concentration was 2.6 ppb and the particle volume load was 15.7 ml. During this operational event in only 2 % of the time more than 15% of the particles break through the filter.

For a backwash event the load from the peak is compared to the load of the total filter run (32h). The load during the first 4h is 18.7 ml, while the load during the stable part of the filter run (28h) is slightly higher, 22.6 ml. The average particle volume concentration is 19.9 ppb during the first four hours and 3.4 ppb during stable operation. In 13% of the time, 45% of the particle volume load is added to the filter effluent.

Some measures to reduce the particle volume load are effective and relatively easy to implement. A reduction of the number of filter switches by two switches a day will result in a reduction of the particle volume load by this operational event of 21%. Recirculation of the first filtrate for four hours will eliminate the peak after a backwash and the particle volume load during one filter run will be reduced by 37%.

By a filter switch event the particles in the middle size ranges (2, 5 and 7 μm) are significantly influenced. After a backwash event mainly the bigger particles with good settling properties break through during the peak. These bigger particles with good settling properties are highly undesired in the distribution system.

A comparison between the cleaning frequency and particle volume load in the clear water for different treatment locations suggests a relation between those two. This suggests a reduction in particle volume load will reduce the necessary cleaning frequency of the distribution system.

Applying particle counters on individual filters can give information on the performance of the filter and information about variation of the performance over time. This information can be used to optimise the filtration and the treatment operation. A particle counter in the clear water can give

information about the performance of a treatment plant and information about the average particle load fed to the distribution system.

Particle count data can be used as a norm value. In that case companies should aim on an average particle volume concentration below 1 ppb. In addition they should aim to keep the 90%-percentile particle volume load below 2 ppb.

Part one of the column experiments showed mainly iron(II) in the aerated water. pH measurements gave reason to assume a slow oxidation rate. After NaOH dosage, the oxidation and the subsequent removal by filtration of iron(II) increased. For the flock filtration at Harderbroek the oxidation of iron(II) is the rate determining step, limited by the pH.

Alternatives for improving the iron removal at Harderbroek are caustic soda dosage or crushed limestone filtration. Both alternatives will result in a higher pH and therefore a better oxidation of iron. An alternative without dosing a chemical is to make tower aeration the first treatment step instead of the last step. When tower aeration is applied on raw water, the pH of the aerated water will be higher than currently is the case with only cascade aeration. It can be expected that fouling of the aeration tower can be controlled, because of the low particle load of the raw water.

The caustic soda dosage clearly improved the iron(II) removal, but the total iron in the filter effluent is not changed by the dosage. While on the other hand the ratio between iron(II) and iron(III) is changed. After caustic soda dosage the majority of iron in the filter effluent is iron(III), while in the reference the majority is iron(II).

In order to find a good process for oxidation improvement a extensive pilot research is necessary.

The present total iron removal is a combination of adsorptive iron removal and flock filtration iron removal. At the moment it is hard to determine which of those processes is dominant.

Besides adsorptive iron removal and flock filtration iron removal also biological iron removal can play a role. At the moment there is no information available about biological iron removal at Harderbroek. The biological iron removal was supposed to be not relevant, because of the assumed chemical oxidation of iron. Biological oxidation of iron(II) gets a change when the chemical oxidation is not fast enough. Since it is found out that the chemical oxidation is very slow at the moment, biological oxidation is realistic at Harderbroek.

The dataset obtained with the experiments is not complete enough to calibrate the iron removal model developed in Stimela. In this study the model is mainly used to study the flock filtration iron removal. In the iron removal model adsorptive iron removal is included, but with the obtained data set, no conclusions could be drawn according this removal mechanism.

An extensive measurement program is necessary to calibrate the model parameters and make a clear distinction between the contributions of the different iron removal mechanisms to the total iron removal.

The knowledge gathered at Harderbroek is probably applicable at more pumping stations in the Netherlands. In case of poor iron removal pH measurements in combination with determining the iron(II) and iron(III) concentration can give a clue about the oxidation rate.

6.2 Recommendations

6.2.1 Treatment at Harderbroek

The fingerprint research resulted in some clear recommendations for the treatment at Harderbroek. In order to reduce the peaks in particle volume concentration caused by operational events, Harderbroek should operate the treatment plant as smooth as possible.

In order to reduce the volume load after a backwash, recirculation of the first filtrate is recommended. The duration of the peak after a backwash was measured in this research as four hours. At the moment a first filtrate of 300 m³ is discharged to the infiltration pond. When also this water is recirculated, the recirculation time should be 5 hours with a flow rate of 240 m³/h.

In order to optimise the recirculation period and the recirculated water volume it is recommended to perform extended measurements (particle counts) on the filter effluent directly after a backwash.

6.2.2 Further research

The column experiments mainly show where the focus should be when executing further research. All experiments performed in this research are executed on small columns. Before any decision is taken it is advised to perform experiments on the pilot filter at Harderbroek. This filter is a more representative model of the treatment and results obtained with the pilot filter should be more reliable. Because crushed limestone filtration is seen as a promising alternative it should be tested on the pilot filter, especially because the contact time within the column experiments was too short. It should be investigated if a longer residence time will increase the pH effectively. In addition one should count the particles in the filter effluent. It could be possible that by dissolving the crushed limestone small calcium particles occur in the filter effluent. This phenomenon should be measured.

Caustic soda dosage seems to reduce the amount of iron(II). It is not completely sure from the column experiments if also the total iron concentration is decreased by the dosage. The removal of iron(III) hydroxide flocks after caustic soda dosage needs to be investigated in more detail on the pilot filter. It is possible that by the dosage only small iron(III) hydroxide flocks will be formed and breakthrough can occur.

In order to understand both treatment plants, Harderbroek and Fledite, an iron(II), iron(III) and pH fingerprint needs to be performed. The differences and similarities between Harderbroek and Fledite can lead to a lot of information.

In order to be able to quantify the contribution of biological iron removal, it is recommended to measure the presence of different bacteria's by DNA measurements. Especially the presence of the *Gallionella* bacterium is important to know.

For the distinction between the contribution of the different iron removal mechanisms and in order to be able to calibrate the model in more detail it is recommended to set up a measurement program according to the proposed program in Paragraph 5.3.4. By this way more quantitative statements can be put about the oxidation rate coefficient, the filtration coefficient and the adsorptive iron removal constants.

7 References

- Anderson, D.R., Row, D.D., and Sindelar, G.E. 1973. Iron and manganese studies of Nebraska water supplies. *Journal AWWA*, 65, 637-641.
- Appelo, C.A.J., Drijver, B., Hekkenberg, R. and de Jonge, M. 1999. Modelling in situ iron removal from groundwater. *Ground Water*, 37 (6), 811-817.
- Badjo, Y. and Mouchet, P. 1989. Appropriate technologies - example of a large biological iron removal plant in Togo. *Aqua*, 38 (3), 197-206.
- Bai, R. and Machie, R.I., 1995. Modelling the transition between deposition modes in deep bed filtration. *Water resources* 29, No 11, pp 2601 - 2604.
- van Beek, C.G.E.M. 1983. In situ iron removal - an evaluation of investigations. Report 78 (in Dutch), Nieuwegein, KIWA N.V., The Netherlands.
- Bourgine, F.P. et al 1994. Biological processes at Stains Hill water treatment plant, Kent. *Journal of IWEM*, 8 August 1994, 379-392.
- Braester, C. and Martinell, R. 1988 The Vyredox and Nitredox methods of in situ treatment of groundwater. In: *Water Science and Technology*, 20 (3), 149-163.
- Clemens, F.H.L.R. 2001. Hydrodynamic models in urban drainage: application and calibration. PhD dissertation, Delft University of Technologie / Witteveen en Bos, The Netherlands.
- Ceronio, A.D. and Haarhoff, J. 2002. Dealing with large particle counting data sets. *Water Science and Technology: Water Supply* Vol 2 No 5-6 pp 35-40.
- Ceronio, A.D. and Haarhoff, J. 2001. Standardisation of the Use of Particle Counting for Potable Water Treatment in South Africa. Department of Civil and Urban Engineering, Rand Afrikaans University. WRC Report No: TT 166/01.
- Cox, C.R. 1964. Operation and Control of water treatment processes. WHO, p209-218
- CRC Handbook of chemistry and Physics, 1996, 77th edn. CRC Press Inc.
- Czekalla, C., Mevius, W. and Hanert, H. 1985. Quantitative removal of iron and manganese by microorganisms in rapid sand filters (in situ investigations). *Water supply*, 3 (1), 111-123.
- Degremont 1991. *Water treatment handbook*. Vol. 1 and 2, Sixth edition, Degremont, France.

DHV Water BV, Stimela handleiding, 1999.

Frischherz, H., Zibuschka, F., Jung, H. and Zerobin, W. 1985. Biological elimination of iron and manganese. *Water Supply*, 3 (1), 125-136.

Ghosh, M.M., O'Connor, J.T. and Engelbrecht, R.S. 1967. Removal of iron from groundwater by filtration. *Journal AWWA*, 59 (7), 878-896.

Gregory, J. 2006. *Particles in water – properties and processes*. University College London. IWA publishing, Taylor and Francis.

Hatva, T. 1989. *Iron and Manganese in groundwater in Finland: Occurrence in glacial fluvial aquifers and removal by biofiltration*. National board of water and environment, Helsinki, Finland

Hauer, G.E. 1950. Iron and carbon dioxide removal. *Journal AWWA*, 42, 555-561.

Helm, A.W.C., 1998. *Modelling van intensieve gasuitwisselingsystemen* (In Dutch). Master thesis Delft University of Technology.

Helm, A.W.C. van der and Rietveld, L.C., 2002. *Modelling of drinking water treatment processes within the Stimela Environment*, *Water Science and Technology: Water Supply Vol2. No 1*, pp 87-93.

Jones, L. Atkins, P. *Chemistry – Molecules, Matter, and Change*. University of Northern Colorado and Oxford University. W.H. Freeman and Company New York 2000.

Kivit, C.F.T., 2004. *Origin and behavior of particles in drinking water networks*. Department of Watermanagement, Delft, Delft University of Technology.

Lerk, C.F. 1965 *Enkele aspecten van de ontijzering van grondwater* (in Dutch). PhD dissertation, Technical University Delft, The Netherlands.

Mayer, T.D. and Jarrell, W.M. 2000. Phosphorus sorption during iron(II) oxidation in the presence of dissolved silica. *Water Research Vol. 34, No. 16*, pp 3949-3956.

Van der Meer, W.G.J. 2003. *Mathematical modelling of NF and RO membrane filtration plants and modules*. (PhD dissertation) Delft University of Technology.

Van der Meulen, M., 2004. *Deeltjestellingen in een drinkwater distributienet* (in Dutch). Department of Watermanagement, Delft, Delft University of Technology.

- Mouchet, P. 1992. From conventional to biological removal of iron and manganese in France. *Journal AWWA*, 84 (4), 158-167.
- Moel, P.J., Verberk, J.Q.J.C., Dijk van, J.C. 2004. *Drinkwater – principes en praktijk* (in Dutch). Delft University of Technology / Sdu publiciers Den Haag.
- O'Connor, J.T. 1971. Iron and manganese. In: *Water quality and treatment – a handbook of public water supplies*. Chapter 11, p378-396; McGraw Hill Book Company, New York.
- Popel, H.J. 1993. *Aeration and gas transfer*, Delft University of Technology. Lecture notes.
- Raffin, M. and Teunissen, K. 2007. Fingerprint for groundwater treatment plant Harderbroek. BTO report nr 2007.015. Kiwa Water Research.
- Rietveld, L.C. 2005. *Improving operation of drinking water treatment through modelling*. PhD dissertation, Delft University of Technology, The Netherlands.
- Rott, U. 1973 *Untersuchungen zur Aufbereitung von Grundwasser mit hohem Gehalt an Eisen und Huminsäuren – Autokatalytische Enteuserung in Ein- und Mehrschichtfiltern* (in German). Ph.D Dissertation, Technical University of Hannover, Germany.
- Rott, U. 1985. Physical, chemical and biological aspects of the removal of iron and manganese underground. *Water supply*, 3 (2), 143-150.
- Salvato, J.A. 1992. *Environmental engineering and sanitation*. Fourth edition, John Wiley and Sons, Inc. New York.
- Van Schagen, K.M., Rietveld, L.C. and Babuska, R. 2007. Model based optimisation of pellet softening. To be submitted.
- Sharma, S.K., Mendis, B.S., Greetham, M.R. and Schippers, J.C. 2000. Modelling adsorptive iron removal in filters. IWA publishing, pp 604-608.
- Sharma, S.K. 2001a. *Adsorptive iron removal from groundwater*. PhD dissertation, Wageningen University / IHE Delft, The Netherlands.
- Sharma, S.K. 2001b. Comparison of physicochemical iron removal mechanisms in filters. In: *Journal of water supply: Research and Technology – aqua*. Pp 187 – 198.
- Snoeyink, V.L. and Jenkins, D. 1980. *Water Chemistry*. John Wiley and Son, United States of America.

Snoeyink, V.L., 1990. Adsorption of organic compounds. In: Water quality and treatment - A handbook of community water supplies. McGraw Hill Inc., Chapter 13, pp781-875.

Stevenson, D.G. 1997. Water treatment unit processes. World scientific publishing company.

Stuyfzand, P. 2007. Naar een effectievere diagnose, therapie en preventie van chemische put- en drainverstopping (in Dutch). H2O Vol 40, No 8, pp 44-47

Verberk, J.Q.J.C., Hamilton L.A., O'Halloran K.J. 2006a in : Water Science and Technology : water supply vol 6 No 4 pp35-43. Volume, mass, chemical composition and origin of particles in drinking water transportation pipelines.

Verberk, J.Q.J.C., O'Halloran, K.J., Hamilton, L.A., Vreeburg, J.H.G., van Dijk, J.C., 2006b (in text). Measuring particles in drinking water transportation systems with particle counters. Accepted in Journal of Water Supply: Research and Technology - AQUA.

Verberk, J.Q.J.C., Hamilton, L.A., Vreeburg, J.H.G., van Dijk, J.C., 2007a. Volume, mass chemical composition and origin of particles in drinking water transportation pipelines. Delft University of Technology. Submitted to Urban Water Journal.

Verberk, J.Q.J.C., Vreeburg, J.H.G., van Dijk, J.C., 2007b. Particles in drinking water distribution systems, Delft University of Technology, Conference proceedings for IWA Particle separation congress, Toulouse.

Verdel, J.D. Schotsman, R.M., Rietveld, L.C. Dijk J.C. van, 1998 Modelling of filtration of groundwater (in Dutch) H₂O (31, nr 16 pp26-30). Delft University of Technology, The Netherlands.

De Vet, 2007. Personal communication.

Wilson, E.J., Greankoplis, C.J., 1966. Liquid mass transfer at very low Reynolds numbers in packed beds. Ind. Eng. Chem. Fund. 5, 9-14.

Content Appendices

Annex I	Results column experiments part 1	IV
Annex II	Results column experiments part 2	VIII
Annex III	Hydraulic line scheme	X
Annex IV	Matlab code model	XII
Annex V	Model runs with adsorption isotherm constants	XVIII

I Results column experiments part 1

Results for iron

1.1

iron Fe 2+	time	column 1	column 2	column 3	column 4	influent
	11:00	0.36	0.43	0.43	0.49	1.13
	14:00	0.26	0.34	0.39	0.41	1.1
iron Fe 3 +	time	column 1	column 2	column 3	column 4	influent
	11:00	0.173	0.136	0.208	0.24	0.22
	14:00	0.172	0.203	0.208	0.249	0.24
total iron	time	column 1	column 2	column 3	column 4	influent
	11:00	0.533	0.566	0.638	0.73	1.35
	14:00	0.432	0.543	0.598	0.659	1.34

1.2

iron Fe 2+	time	column 1	column 2	column 3	column 4	influent
	11:00	0.14	0.16	0.22	0.23	1.03
	14:00	0.4	0.41	0.5	0.56	1.11
iron Fe 3 +	time	column 1	column 2	column 3	column 4	influent
	11:00	0.315	0.357	0.364	0.355	0.33
	14:00	0.116	0.217	0.214	0.231	0.23
total iron	time	column 1	column 2	column 3	column 4	influent
	11:00	0.455	0.517	0.584	0.585	1.36
	14:00	0.516	0.627	0.714	0.791	1.34

2.1

iron Fe 2+	time	column 1	column 2	column 3	column 4	influent
	11:00	0.38	0.36	0.55	0.51	1.19
	14:00	0.43	0.42	0.51	0.64	1.1
iron Fe 3 +	time	column 1	column 2	column 3	column 4	influent
	11:00	0.162	0.124	0.167	0.154	0.17
	14:00	0.208	0.148	0.242	0.173	0.26
total iron	time	column 1	column 2	column 3	column 4	influent
	11:00	0.542	0.484	0.717	0.664	1.36
	14:00	0.638	0.568	0.752	0.813	1.36

2.2

iron Fe 2+	time	column 1	column 2	column 3	column 4	influent
	11:00	0.21	0.14	0.22	0.33	1.07
	14:00	0.23	0.18	0.23	0.33	1.15
iron Fe 3 +	time	column 1	column 2	column 3	column 4	influent
	11:00	0.292	0.324	0.334	0.311	0.28
	14:00	0.161	0.125	0.127	0.121	0.18
total iron	time	column 1	column 2	column 3	column 4	influent
	11:00	0.502	0.464	0.554	0.641	1.35
	14:00	0.391	0.305	0.357	0.451	1.33

3.1

iron Fe 2+	time	column 1	column 2	column 3	column 4	influent
	11:00	0.14	0.25	0.39	0.51	1.19
	14:00	0.22	0.29	0.34	0.45	1.19
iron Fe 3 +	time	column 1	column 2	column 3	column 4	influent
	11:00	0.152	0.107	0.106	0.092	0.15
	14:00	0.109	0.094	0.107	0.102	0.14
total iron	time	column 1	column 2	column 3	column 4	influent
	11:00	0.292	0.357	0.496	0.602	1.34
	14:00	0.329	0.384	0.447	0.552	1.33

3.2

iron Fe 2+	time	column 1	column 2	column 3	column 4	influent
	11:00	0.33	0.37	0.46	0.48	1.17
	14:00	0.47	0.54	0.56	0.61	1.16
iron Fe 3 +	time	column 1	column 2	column 3	column 4	influent
	11:00	0.083	0.093	0.1	0.103	0.18
	14:00	0.066	0.075	0.097	0.116	0.19
total iron	time	column 1	column 2	column 3	column 4	influent
	11:00	0.413	0.463	0.56	0.583	1.35
	14:00	0.536	0.615	0.657	0.726	1.35

4.2

iron Fe 2+	time	column 1	column 2	column 3	column 4	influent
	11:00	0.23	0.25	0.44	0.4	1.07
	14:00	0.3	0.45	0.52	0.6	1.16
iron Fe 3 +	time	column 1	column 2	column 3	column 4	influent
	11:00	0.274	0.279	0.278	0.255	0.29
	14:00	0.175	0.153	0.138	0.14	0.2
total iron	time	column 1	column 2	column 3	column 4	influent
	11:00	0.504	0.529	0.718	0.655	1.36
	14:00	0.475	0.603	0.658	0.74	1.36

Results for turbidity

1.1	time	column 1	column 2	column 3	column 4	influent
	11:05					
	11:20	0.349	0.33	0.33	0.35	0.424
	11:45	0.382	0.468	0.428	0.384	0.38
	11:55	0.322	0.344	0.365	0.277	0.501
	12:30	0.312	0.296	0.295	0.315	0.415
	13:05	0.391	0.345	0.295	0.275	0.334
	13:15	0.285	0.293	0.318	0.324	0.44
	13:55	0.283	0.233	0.296	0.288	0.31

1.2	time	column 1	column 2	column 3	column 4	influent
	9:50	0.437	0.443	0.362	0.349	0.357
	10:00	0.315	0.316	0.293	0.321	0.39
	10:45	0.427	0.376	0.356	0.373	0.484
	11:30	0.367	0.357	0.45	0.528	0.432
	11:45	0.422	0.332	0.429	0.382	0.383
	11:55	0.427	0.347	0.334	0.388	0.572
	12:50	0.501	0.539	0.428	0.439	0.579
	13:45	0.371	0.356	0.302	0.329	0.394

2.1	time	column 1	column 2	column 3	column 4	influent
	10:05					
	10:30		0.434	0.532	0.484	0.555
	11:10	0.648	0.371	0.574	0.528	
	12:30	0.31	0.318	0.371	0.269	0.326
	13:10	0.306	0.243	0.277	0.254	0.578
	13:55	0.265	0.267	0.245	0.258	0.268

2.2	time	column 1	column 2	column 3	column 4	influent
	11:00	0.501	0.393	0.402	0.393	
	11:20	0.667	0.573	0.489	0.467	
	11:55	0.502	0.538	0.522	0.449	0.426
	12:15	0.429	0.465	0.373	0.384	
	13:10	0.438	0.371	0.33	0.328	0.476
	13:55	0.311	0.299	0.273	0.327	0.429

3.1	time	column 1	column 2	column 3	column 4	influent
	9:15	0.355	0.355	0.285	0.271	0.357
	10:00	0.256	0.238	0.223	0.201	0.233
	11:00	0.243	0.257	0.256	0.271	0.296
	12:00	0.189	0.204	0.206	0.197	0.255
	12:35	0.2	0.191	0.185	0.178	0.201
	13:10	0.191	0.188	0.186	0.184	0.2

3.2	time	column 1	column 2	column 3	column 4	influent
	9:10					
	9:15	0.362	0.286	0.224	0.23	
	9:50	0.244	0.193	0.201	0.189	0.234
	10:05	0.225	0.174	0.18	0.178	0.197
	11:10	0.163	0.179	0.172	0.184	0.18
	12:00	0.163	0.161	0.156	0.163	0.182
	12:30	0.213	0.204	0.196	0.191	0.271
	12:55	0.179	0.179	0.18	0.171	0.193

4.2	time	column 1	column 2	column 3	column 4	influent
	9:15					0.128
	9:25	0.129	0.117	0.116	0.119	0.128
	10:00	0.145	0.162	0.114	0.14	0.107
	10:15	0.108	0.101		0.079	0.107
	11:00	0.092	0.084	0.064	0.084	0.075
	11:10	0.089	0.062	0.066	0.085	0.091
	12:00	0.106	0.109	0.085	0.108	0.116
	13:05	0.089	0.089	0.072	0.084	0.105

II Results column experiments part 2

		pH	HCO ₃ ⁻ mg/l	EGV mS/m	Fe total mg/l	Fe 2 mg/l	Fe 3 mg/l	Ca mg/l
NaOH								
1 hour	influent							
	1+2	7.83	84	16.1	1.48	0.88	0.6	25.9
	influent							
	3+4	7.51	80	15.7	1.37	1.26	0.11	25.2
	column 1	7.85	83	16.1	0.646	0.06	0.586	24.5
	column 2	7.88	84	16.1	0.869	0.06	0.809	26.2
	column 3	7.55	80	15.7	0.533	0.41	0.123	25.6
column 4	7.55	80	15.7	0.686	0.55	0.136	27.1	
4 hours								
4 hours	influent							
	1+2	7.79	83	16	0.673	0.87	-0.197	25.8
	influent							
	3+4	7.51	80	15.6	1.39	1.24	0.15	24.3
	column 1	8.06	85	16.3	0.634	0.06	0.574	26
	column 2	8.05	85	16.2	0.718	0.04	0.678	25.7
	column 3	7.54	80	15.6	0.546	0.43	0.116	26
column 4	7.53	80	15.6	0.657	0.44	0.217	26.5	
Crushed limestone								
1 hour	influent							
	1+2	7.52	80	15.7	1.45	0.21	1.24	26.9
	influent							
	3+4	7.49	79	15.7	1.39	0.81	0.58	25.1
	column 1	7.65	84	16.2	0.57	0.13	0.44	27.6
	column 2	7.66	84	16.2	0.602	0.19	0.412	27.1
	column 3	7.55	80	15.7	0.643	0.3	0.343	25.8
column 4	7.51	80	15.7	0.673	0.09	0.583	25.9	
4 hours								
4 hours	influent							
	1+2	7.47	82	16	1.38	1.31	0.07	24.7
	influent							
	3+4	7.48	83	16	1.46	1.32	0.14	25.5
	column 1	7.66	88	16.6	0.244	0.23	0.014	26.7
	column 2	7.64	87	16.6	0.311	0.29	0.021	26.8
	column 3	7.53	83	16.1	0.34	0.43	-0.09	25.5
column 4	7.52	83	16.1	0.4	0.13	0.27	25.7	

IV Matlab code model

S-file

```
function [sys,x0,str,ts] = irofil_s(t,x,u,flag,B,x0,U,P),
% [sys,x0,str,ts] = irofil_s(t,x,u,flag,B,x0,U,P),
% Stimela S-Function
%
% t = time
% x = state vector, filled with continuous states (flag 1) or
% discrete states (flag 2)
% u = input vector
%
% P = proces parameters, filled with irofil_p.m and defined
in irofil_d.m
% B = Model size, filled with irofil_i.m,
% x0 = initial state, filled with irofil_i.m,
% U = Translationstructure for inout vector, filled in uit
Blok00_i.m.
% Fields are determined by 'st_varia'
%
% Stimela, 2004

% © Kim van Schagen,

% General purpose calculations
if any(abs(flag)==[1 2 3])

    %%%% MODEL-SPECIFIC =>
    %%%%%%%%%%%%%%%%%%%%%%%%%%%%%%%%%%%%%%%%%%%%%%%%%%%%%%%%%%%
    % optional: convert input vector to user names
    % eg. Temp = u(U.Temperature);
    % in the code it is also possible to use u(U.Temperature)
directly.
    NumCel = P.NumCel;
    Opp = P.Surf;
    Diam = P.Diam;
    nmax = P.nmax;
    rhoD = P.rhoD;
    rhoD = rhoD*1000; % g/m3
    rhoK = P.rhoK;
    FilPor0 = P.FilPor;
    Lwater = P.Lwater;
    Kf = P.Kf;
    nf = P.nf;
    M = P.M;
    %LaShift= P.LaShift;
    dy = P.dy;
    Lambda_Iron3 = P.Lambda_Iron3;
    Kfe = P.Kfe;
    %%%% <= MODEL-SPECIFIC
    %%%%%%%%%%%%%%%%%%%%%%%%%%%%%%%%%%%%%%%%%%%%%%%%%%%%%%%%%%%

    %%%% MODEL-SPECIFIC =>
    %%%%%%%%%%%%%%%%%%%%%%%%%%%%%%%%%%%%%%%%%%%%%%%%%%%%%%%%%%%
    % optional: calculated values used for al flags
    % eg. TempArea = u(U.Temperature)/P.Area;
```

```

Susp = u(U.Suspended_solids);%mg/l
Susp = Susp/1000;%kg/m3
Temp = u(U.Temperature);
Debiet = u(U.Flow);
Iron2 = u(U.Iron2);
Iron3 = u(U.Iron3);
Oxygen = u(U.Oxygen);
EGV = u(U.Conductivity);
pH = u(U.pH);
HCO3 = u(U.Bicarbonate);
%Hplus = 10^(-pH);

MatQ = spdiags([[ -
1*ones(NumCel,1)], [1*ones(NumCel,1)]] , [0,1], NumCel, NumCel+1);
I = 0.165/1000*EGV;
Fi = 10^(-((0.5*sqrt(I))/(1+sqrt(I))-0.2*I));
K1= (1/Fi)*10^(-356.3094-
0.06091964*(Temp+273.16)+21834.37/(Temp+273.16)+126.839*log10
(Temp+273.16)-1684915/((Temp+273.16)^2));
CO2 = 10^(-pH).*HCO3./K1*44/61;

vel = Debiet/(Opp*3600); %oppervlakte
filtratiesnelheid
[lambda0,I0] = d_filcof(Temp,vel,Diam,FilPor0);
% MatQ1 = d_filmat(dy,VelReal,vel,NumCel);
%Concentratie/accumulatie laag1
%%% <= MODEL-SPECIFIC
%%%%%%%%%%%%%%%%%%%%%%%%%%%%%%%%%%%%%%%%%%%%%%%%%%%%%%%%%%%%%%%%%%%%%%%%

end; % of any(abs(flag)==[1 2 3])

if flag == 1, % Continuous states derivative calculation

% default derivative =0;
sys = zeros(B.CStates,1);

%%% MODEL-SPECIFIC =>
%%%%%%%%%%%%%%%%%%%%%%%%%%%%%%%%%%%%%%%%%%%%%%%%%%%%%%%%%%%%%%%%%%%%%%%%
% fill sys with the derivatives of the continuous states
% eg. sys(1) = (u(U.Temperature)-x(1))/P.Volume;

FilPor(1:NumCel) = FilPor0 - (x(NumCel+1:2*NumCel)/rhoD);
FilPor=FilPor';
VelReal = vel/FilPor; %poriesnelheid
spoelen = u(U.Number+1);

if spoelen == 1
sys(1:2*NumCel)=- (1/90)*x(1:2*NumCel);
else
x(1+5*NumCel:6*NumCel);
phint=-
log10((x(1+5*NumCel:6*NumCel)/44)./(x(1+4*NumCel:5*NumCel)/61
));
pHcel=-log10(K1)+phint;%-
log10((x(1+5*NumCel:6*NumCel)/44)./(x(1+4*NumCel:5*NumCel)/61
))

% sys(1:2*NumCel) = MatQ1*[Iron3;x(1:NumCel)] -
VelReal*[lambda0*(1-

```

```

abs(x(NumCel+1:2*NumCel)/(nmax*rhoD*FilPor) -
LaShift));zeros(NumCel,1)].*x(1:2*NumCel);

    sys(1:NumCel) = -
(vel./(FilPor*dy)).*(MatQ*[Iron3;x(1:NumCel)])+
Kfe*(x(2*NumCel+1:3*NumCel)/56).^2).*x(3*NumCel+1:4*NumCel)
/32).*((10.^(-pHcel)).^(-2))-
(vel./(FilPor)).*([Lambda_Iron3*(1-
(x(NumCel+1:2*NumCel)./(nmax*rhoD*FilPor0)))]).*x(1:NumCel);

    %sys(1+NumCel:2*NumCel) = -
vel*MatQ*[Iron3;x(1:NumCel)]/dy;
    sys(1+NumCel:2*NumCel) = vel.*[Lambda_Iron3*(1-
(x(NumCel+1:2*NumCel)./(nmax*rhoD*FilPor0)))]).*x(1:NumCel);

    %sys(1+2*NumCel:3*NumCel) = -
(vel./(FilPor*dy)).*(MatQ*[Iron2;x(2*NumCel+1:3*NumCel)]) -
Kfe*(x(2*NumCel+1:3*NumCel)/56).^2).*x(3*NumCel+1:4*NumCel)
/32).*((10.^(-pHcel)).^(-2))-((1-
FilPor)./FilPor).*(rhoK*M).*(Kf*(sign(x(2*NumCel+1:3*NumCel))
.*(abs(x(2*NumCel+1:3*NumCel))).^nf)-x(6*NumCel+1:7*NumCel)));

    sys(1+2*NumCel:3*NumCel) = -
(vel./(FilPor*dy)).*(MatQ*[Iron2;x(2*NumCel+1:3*NumCel)]) -
Kfe*(x(2*NumCel+1:3*NumCel)/56).^2).*x(3*NumCel+1:4*NumCel)
/32).*((10.^(-pHcel)).^(-2))-((1-
FilPor)./FilPor).*(rhoK*M).*(x(2*NumCel+1:3*NumCel) -
((x(6*NumCel+1:7*NumCel)./Kf).^1/nf)));

    sys(1+3*NumCel:4*NumCel) = -
(vel./(FilPor*dy)).*(MatQ*[Oxygen;x(3*NumCel+1:4*NumCel)]) -
(32/224)*Kfe*(x(2*NumCel+1:3*NumCel)/56).^2).*x(3*NumCel+1:
4*NumCel)/32).*((10.^(-pHcel)).^(-2));

    sys(1+4*NumCel:5*NumCel) = -
(vel./(FilPor*dy)).*(MatQ*[HCO3;x(4*NumCel+1:5*NumCel)]) -
(8*61/224)*Kfe*(x(2*NumCel+1:3*NumCel)/56).^2).*x(3*NumCel+
1:4*NumCel)/32).*((10.^(-pHcel)).^(-2));

    sys(1+5*NumCel:6*NumCel) = -
(vel./(FilPor*dy)).*(MatQ*[CO2;x(5*NumCel+1:6*NumCel)]) + (8*44
/224)*Kfe*(x(2*NumCel+1:3*NumCel)/56).^2).*x(3*NumCel+1:4*N
umCel)/32).*((10.^(-pHcel)).^(-2));

    %sys(1+6*NumCel:7*NumCel) =
M*(Kf*(sign(x(2*NumCel+1:3*NumCel))).*(abs(x(2*NumCel+1:3*NumC
el))).^nf)-x(6*NumCel+1:7*NumCel)); %-
vel*MatQ*[Iron2;x(1:NumCel)]/dy;

    sys(1+6*NumCel:7*NumCel) = M*(x(2*NumCel+1:3*NumCel) -
(x(6*NumCel+1:7*NumCel)./Kf).^1/nf)); %-
vel*MatQ*[Iron2;x(1:NumCel)]/dy;
end

%sys(1:2*NumCel) = MatQ1*[coDOC;x(1:NumCel)] -
(1+FilPor)/FilPor*(rhoK*M)*[K*(sign(x(1:NumCel))).*(abs(x(1:Nu
mCel))).^n)-x(NumCel+1:2*NumCel)];zeros(NumCel,1)];

%sys(2*NumCel+1:3*NumCel) = (nX'|sys(2*NumCel+1:3*NumCel)>0).*s
ys(2*NumCel+1:3*NumCel);

```

```

%sys(6*NumCel+1:7*NumCel)=(nX'|sys(6*NumCel+1:7*NumCel)>0).*s
ys(6*NumCel+1:7*NumCel);
%%% <= MODEL-SPECIFIC
%%%%%%%%%%%%%%%%%%%%%%%%%%%%%%%%%%%%%%%%%%%%%%%%%%%%%%%%%%%%%%%%%%%%%%%%

elseif flag ==2, %discrete state determination

    % default next sample same states (length is B.DStates)
    sys = x(B.CStates+1:B.CStates+B.DStates);

    %%% MODEL-SPECIFIC =>
    %%%%%%%%%%%%%%%%%%%%%%%%%%%%%%%%%%%%%%%%%%%%%%%%%%%%%%%%%%%%%%%%%%%%%%%%%
    % fill sys with the state value on the next sample moment
    (determined by
    % B.SampleTime)
    % eg. sys(1) = (x(1)+u(U.Temperature))/P.Volume;

    %%% <= MODEL-SPECIFIC
    %%%%%%%%%%%%%%%%%%%%%%%%%%%%%%%%%%%%%%%%%%%%%%%%%%%%%%%%%%%%%%%%%%%%%%%%%

elseif flag ==3, % output data determination

    % default equal to the input with zeros for extra
    measurements
    sys = [u(1:U.Number); zeros(B.Measurements,1)];

    %%% MODEL-SPECIFIC =>
    %%%%%%%%%%%%%%%%%%%%%%%%%%%%%%%%%%%%%%%%%%%%%%%%%%%%%%%%%%%%%%%%%%%%%%%%%
    % Determine output for calculated values
    % eg. sys(U.Temperature) = x(1);
    % sys(U.Suspended_solids)=x(NumCel)*1000; %Concentratie
    zwevende stoffen [mg/l]
    sys(U.Iron3)=x(NumCel); %Concentratie driewaardig ijzer
    [mg/l]
    sys(U.Iron2)=x(3*NumCel); %Concentratie tweewaardig ijzer
    [mg/l]
    sys(U.Oxygen)=x(4*NumCel); %Concentratie zuurstof [mg/l]
    %sys(U.pH)=-log10(x(5*NumCel));

    % Determine extra measurements
    % eg. sys(U.Number+1) = x(1)/P.Opp;
    % sys(U.Number+1:U.Number+NumCel)= x(1:NumCel)*1000;
    %concentratie SS [mg/l]
    sys(U.Number+1:U.Number+NumCel)= x(1:NumCel); %concentratie
    Fe3 [mg/l]
    sys(U.Number+1+NumCel:U.Number+2*NumCel)=cumsum(dy-
    I0*dy*(FilPor0./(FilPor0-x(NumCel+1:2*NumCel)/rhoD)).^2);
    %weerstand tgv accumulatie laag1
    sys(U.Number+1+2*NumCel:U.Number+3*NumCel)=
    x(2*NumCel+1:3*NumCel); %concentratie Fe2 [mg/l]
    sys(U.Number+1+3*NumCel:U.Number+4*NumCel)=
    x(3*NumCel+1:4*NumCel); %concentratie O2 [mg/l]
    sys(U.Number+1+4*NumCel:U.Number+5*NumCel)=
    x(4*NumCel+1:5*NumCel); %concentratie HCO3 [mg/l]
    sys(U.Number+1+5*NumCel:U.Number+6*NumCel)=
    x(5*NumCel+1:6*NumCel); %concentratie CO2 [mg/l]
    %%% <= MODEL-SPECIFIC
    %%%%%%%%%%%%%%%%%%%%%%%%%%%%%%%%%%%%%%%%%%%%%%%%%%%%%%%%%%%%%%%%%%%%%%%%%

```

```

elseif flag == 0
    % initialize Model
    % [cs,ds,out,in,,direct]
    sys =
[B.CStates,B.DStates,U.Number+B.Measurements,U.Number+B.Setpo
ints, 0, B.Direct,1];
    ts = [B.SampleTime,0];
    str = 'irofil';
    x0=x0;
else
    % If flag is anything else, no need to return anything
    % since this is a continuous system
    sys = [];
end

```

```

function [lambda0F,I0F] = d_filcof(T,v,d,P0)

```

```

%%%%%%%%%%%%%%%%%%%%%%%%%%%%%%%%%%%%%%%%%%%%%%%%%%%%%%%%%%%%%%%%%%%%%%%%
% This function returns the factor coefficient
% for the filtration coefficient
%%%%%%%%%%%%%%%%%%%%%%%%%%%%%%%%%%%%%%%%%%%%%%%%%%%%%%%%%%%%%%%%%%%%%%%%

```

```

% Kinematic viscosity
nu=(497e-6)/((T+42.5)^1.5);

% Factor coefficient for head loss
I0F=(180*nu*(1-P0)^2*v)/(9.81*P0^3*d^2);

lambda0F=(9e-18)/(nu*v*d^3);%Lerk

```

```

function val = d_filmat(dy,vp,v,N)

```

```

% This function returns the main matrix Q for filtration

```

```

b      = -vp/dy;
c      = vp/dy;
e      = v/dy;
alpha = -vp/dy;
beta  = vp/dy;
v1=[ [c*ones(N,1);beta], [b*ones(N,1);0] ];
q1=spdiags(v1,[0,1],N,N+1);

v2=[ [e*ones(N,1);2*e], [-e*ones(N,1);0] ];
q2=spdiags(v2,[0,1],N,N+1);

```

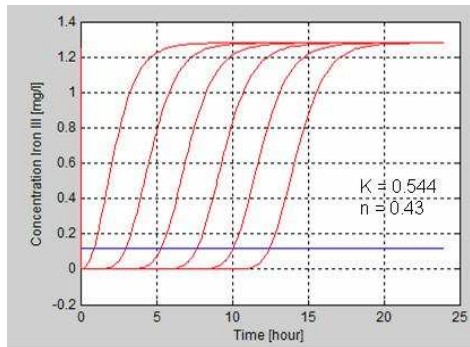
```

val = [q1;q2];

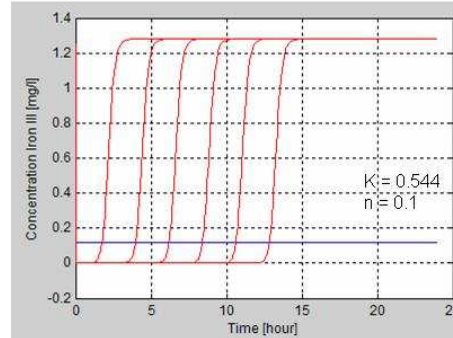
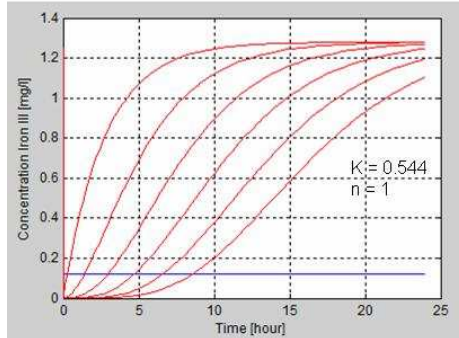
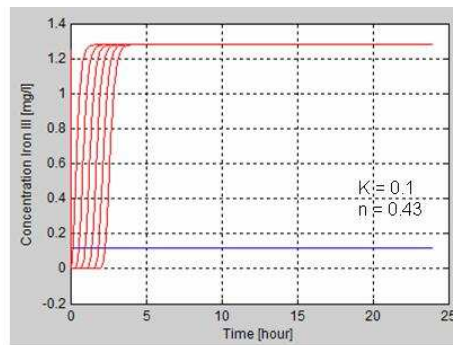
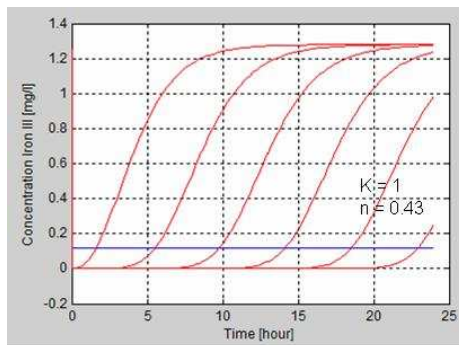
```


V Model runs with adsorption isotherm constants

The iron(II) concentrations in the effluent of each filter bed layer is plotted in the figures below. There are 6 filter bed layers modelled. The shape of the breakthrough curve changes by different values for the Freundlich isotherm constants.



Breakthrough curves with default K and n.



Breakthrough curves with $K=1$, $K=0.1$, $n=1$ and $n=0.1$.

